COLLEGE OF AGRICULTURE, ENGINEERING AND SCIENCE

UNIVERSITY OF KWAZULU-NATAL ™

INYUVESI YAKWAZULU-NATALI

RESEARCH, DEVELOPMENT AND TESTING OF BRAKE PAD MATERIALS FROM BIOMASS-BASED NANOCOMPOSITES

By

Oluwafemi Ezekiel, Ige

216075865

Dissertation submitted in fulfilment of the academic requirements for the degree of Doctor of Philosophy in Engineering (PhD)

Mechanical Engineering.

Supervisor: Professor Freddie L. Inambao

School of Engineering, Discipline of Mechanical Engineering,

Howard College, Durban.

22nd JULY 2021

Supervisor's Declaration

"As the candidate's supervisor I agree to the submission of this thesis".

Signed:

Name: Professor Freddie Inambao Signature: _____ Date: 22nd July 2021

Declaration 1: Plagiarism

I, Oluwafemi Ezekiel, Ige declare that:

1. The research reported in this thesis, except where otherwise indicated, is my original research.
2. This thesis has not been submitted for any degree or examination at any other university.
3. This thesis does not contain other persons' data, pictures, graphs or other information, unless specifically acknowledged as being sourced from other persons.
4. This thesis does not contain other persons' writing, unless specifically acknowledged as being sourced from other researchers. Where other written sources have been quoted, then:
    a. Their words have been re-written but the general information attributed to them has been referenced;
    b. Where their exact words have been used, then their writing has been placed in italics and inside quotation marks, and referenced.
5. This thesis does not contain text, graphics or tables copied and pasted from the Internet, unless specifically acknowledged, and the source being detailed in the thesis and in the references sections.

Signed _____ Date: 22nd July 2021

Oluwafemi Ezekiel, Ige

Student no.: 216075865

Declaration 2: Publications

This section presents publications that have been published.

ISI/SCOPUS/DoHET Accredited Journals

Publication 1:

O. E. Ige, F. L. Inambao, and G. A. Adewumi, "Biomass-Based Composite for Brake Pad: A Review," *International Journal of Mechanical Engineering and Technology* (IJMET), vol. 10, no. 3, pp. 920-943, 2019. **IAEME Publications**
http://www.iaeme.com/MasterAdmin/uploadfolder/IJMET_10_03_094/IJMET_10_03_094.pdf
(Published)

Publication 2:

O. E. Ige, F. L. Inambao, and G. A. Adewumi, "Effects of Fiber, Fillers and Binders on Automobile Brake Pad Performance: A Review," *International Journal of Mechanical Engineering and Technology* (IJMET), vol. 10, no. 6, pp. 135-150, 2019. **IAEME Publications**
http://www.iaeme.com/MasterAdmin/uploadfolder/IJMET_10_06_008/IJMET_10_06_008.pdf
(Published)

Publication 3:

O. E. Ige, F. L. Inambao, and G. A. Adewumi, "Synthesis of Natural Carbon Nanospheres From Palm Kernel Fiber," *International Journal of Mechanical Engineering and Technology* (IJMET), vol. 10, no. 12, pp. 625-641, 2019. **IAEME Publications**
http://www.iaeme.com/MasterAdmin/uploadfolder/IJMET_10_12_056/IJMET_10_12_056.pdf
(Published)

Publication 4:

O. E. Ige, F. L. Inambao, and G. A. Adewumi, "The Effect of Synthesis Temperature on Carbon Nanospheres from Palm Kernel Fiber," *International Journal of Engineering Research and Technology* (IJERT), vol. 13, no. 11, pp. 3099-3108, 2020. **International Research Publication House**
http://www.irphouse.com/ijert20/ijertv13n11_03.pdf
(Published)

Publication 5:

O. E. Ige, F. L. Inambao, and O. J. Gbadeyan, "Development and Study of Tribological Performance of Bio-Based Hybrid Nanocomposites for Brake Pad Application, *International Journal of Mechanical and Production Engineering Research and Development* (IJMPERD) ISSN (P): 2249–6890; ISSN (E): 2249–8001, Vol. 11, Issue 2, Apr 2021, 89–106. **Transstellar Journal Publications**

http://www.tjprc.org/view_paper.php?id=15005

(Published)

Publication 6:

O. E. Ige, F. L. Inambao, and O. J. Gbadeyan. "Thermo-mechanical analysis of bio-based hybrid nanocomposites for brake pad application," *International Journal of Mechanical and Production Engineering Research and Development* (IJMPERD). ISSN (Print): ISSN (P): 2249-6890; ISSN (E): 2249-8001. Vol. 11, Issue 2, Apr 2021, 155-170 **Transstellar Journal Publications**

http://www.tjprc.org/view_paper.php?id=15009

(Published)

In all the above publications, I, Oluwafemi Ezekiel, Ige was the main and corresponding author for all the publications, while Professor Freddie L. Inambao was my research supervisor. All other authors were collaborators who served in a supervisory capacity.

Dedication

This work is dedicated to God Almighty, my helper, who saw me through this program.

Acknowledgements

I want to express my sincere gratitude to my supervisor, Professor Freddie INAMBAO, who has been extremely helpful during the course of this research by providing advice, encouragement, and assistance. I am very grateful for the fee remission offered by the University of KwaZulu-Natal during my study. I would also like to thank Professor Neerish REVAPRASADU and his research group at the University of Zululand for the use of their laboratory to conduct my experiment. The technical support of Dr Gloria AKINRINDE, Dr Siphamandia MASIKANE, and Dr Oluwatoyin GBADEYAN for designing the research, for your insightful supervision, for your helpful comments, for your consistent encouragement and your assistances at laboratories during my studies are highly appreciated.

I thank Dr Emmanuel ONUH, Dr and Mrs Samuel ILUPEJU, Dr Tunji AKINRINDE, Dr Collins OBIORA, Dr Ayobami POPOOLA, Dr Kinsley UKOBA, Dr Omojola AWOGBEMI, Mr Adefemi OWOPUTI, Engr. Josiah PELEMO, Mr & Mrs Ife ADEGUNLOYE and all my colleagues at the Green Energy Solutions Group (GES) for their love, encouragement, support and for sharing information with me. My special thanks to Dr Richard Steele for his competent editing services during this research. I want to thank all the members of the Winners Chapel International, Durban, for their spiritual support and prayers. I want to thank all my friends and all the ANSU members at the University of KwaZulu-Natal for your love and support during my studies.

My deep appreciation goes to my parents Mr James & Mrs Elizabeth IGE, all my sisters Mrs Temilola IGE, Mrs Oluwakemi IGE, Mrs Funmilola SIYANBOLA and their husbands and children and my in-laws HRH RTD. COL Philip A. OKUBOTIN the AMADAOWEI II & Mrs Kehinde OKUBOTIN for your love, encouragement, your constant prayers and devotion daily. Finally, my sincere appreciation to my beloved wife, Mr. Temitope Ebierein IGE and my precious daughter Ogooluwa Faith IGE for your support, encouragement, sacrifice and motivation during my studies. I appreciate you both.

Abstract

Many variables affect braking systems in the automotive industry, including component geometry, brake materials, component interactions, and various operating conditions. The current research trend in the automotive industry is to use waste as raw material for nanocomposite materials in automobile applications. A novel bio-based hybrid nanocomposite (BHN) brake pad has been developed and investigated to serve as a functional replacement for metallic, ceramic, and hazardous asbestos-based brake pad materials. Carbon-based nanocomposites such as carbon nanospheres, carbon nanotubes, carbon nanosheets, and carbon nanofibers, etc., have attracted wide attention from researchers since their discovery. Carbon nanospheres (CNSs) are among the novel carbon nanostructures distinguished for their potential use in many areas, for instance lithium-ion batteries, electrodes in super capacitors, different parts of automobiles and adsorbents. In this study, CNSs were synthesized from palm kernel fiber (PKF) activated carbon using a simple physical activation method under CO_2. The BHN consisted of a matrix of carbon nanomaterials from PKF which acted as the filler material, epoxy resin which acted as the binder material, together at a nanoscale to produce brake pad. The temperature effect on synthesized nanomaterials was investigated using transmission electron microscopy (TEM), x-ray diffraction (XRD), scanning electron microscopy (SEM), energy dispersive x-ray spectroscopy (EDX), Fourier transform infrared microscopy (FTIR), and thermo-gravimetric analysis (TGA). The SEM results showed the highest purity, and the largest number of CNSs were formed at a synthesis temperature of 1000 °C.

The tribological properties of BHN brake pads were studied and compared with conventional (CON) brake pad material. The BHN brake pads exhibited low wear rate compared to the CON brake pads, while the coefficient of friction (COF) of the BHN brake pad samples (0.3 to 0.5) were within the SAE J661 CODE standard. The results showed that the brake pad performance differed with each pad formulation. The BHN brake pad material had excellent performance in most of the analyses when compared to the CON brake pad material. The mechanical properties of the BHN brake pad such as compressive strength, compressive modulus, hardness and impact strength were tested. The nanocomposite material showed a higher impact strength and compressive strength compared to the (CON) brake pads. The hardness of the material of the two brake pads was statistically akin. Furthermore, the performance of oil and water absorption, thermal stability as well as degradation of the BHN brake pad were determined. The results showed that the BHN brake pad material had low oil absorption rate and low moisture water absorption rate. The BHN brake pad showed thermal stability within the range 300 °C to 400 °C, which are within the standard temperature range.

Result from SEM analysis carried out on the worn surfaces of the BHN brake pads reveals a tougher structure than SEM of the worn surfaces of the CON brake pads. Dynamic mechanical analysis (DMA)

results showed that at a temperature between 55 °C and 105 °C, the $Tan\ \delta$ magnitude of BHN was higher due to the loss modulus supremacy over the storage modulus. In addition, in the temperature range 105 °C to 190 °C, the storage modulus and the loss modulus was as low as that of the CON, and the BHN $Tan\ \delta$ magnitude reduced. Excellent mechanical and tribological properties of BHN brake pad was achieved at 0.3 % CNS.

Table of Contents

Nomenclature

T	Temperature (°C)
P_{WA}	Percentage of water absorption
W_0	Initial weight of water sample
W_1	Final weight of water sample
P_{OA}	Percentage of oil absorption
WO_0	Oil sample initial weight
WO_1	Oil sample final weight
κ	Specific wear rate
V	The volume change (m^3)
χ	Total sliding distance (m)
μ	Friction coefficient
M	Torque induced in the specimen due to friction (in N-mm)
r	The disc radius (mm)
N	Normal load acting on the specimen (N)
$l_\circ$	Original gauge length (mm)
A°	Original cross-sectional area of the sample in the gauge length (mm^2)
F^*	Maximum load applied before crushing (N)
σ_e	Compressive strength
l^*	Specimen length after crushing (mm)
σ_1, σ_2	Corresponding stress at the specific strain (MPa)
ε_1,ε_2	Corresponding stress at the specific stress (MPa)
E	Compressive modulus (MPa)
E’	Storage modulus
E”	Loss modulus
$Tan\ \delta$	Tan-delta

Acronyms / Abbreviations

ASTM	American Society for Testing and Materials
BHN	Bio-Based Hybrid Nanocomposite
C	Carbon
CO_2	Carbon dioxide
CF	Carbon Fiber
CNPs	Carbon Nanoparticles
CNS	Carbon Nano-Sphere
CNT	Carbon Nanotube
CVD	Chemical Vapour Deposition
COF	Coefficient of Friction
CONTR	Control
CON	Conventional
DMA	Dynamic Mechanical Analysis
DSC	Differential Scanning Calorimetry
EDX	Energy Dispersive X-Ray Spectrometer
FESEM	Field Emission Scanning Electron Microscopy
FTIR	Fourier Transform Infrared Spectroscopy
GNs	Graphite Nanoparticles
HRTEM	High-Resolution Transmission Electron Microscopy
Fe	Iron
MWCNT	Multi-Walled Carbon Nanotube
NAO	Non-Asbestos Organic
O	Oxygen
PKF	Palm Kernel Fiber
K	Potassium
SEM	Scanning Electron Microscopy
SAED	Selected Area Electron Diffraction
SI	Silicon
SWCNT	Single-Walled Carbon Nanotube
SAE	Society of Automobile Engineers
TGA	Thermo-Gravimetric Analysis
TEM	Transmission Electron Microscopy
XRD	X-Ray Diffraction

CHAPTER 1: INTRODUCTION

1.1 General introduction

Braking systems are the most critical safety components, especially for slowing down or stopping vehicles such as modern passenger cars [1]. Brake pads are used to control the working speed of different types of machinery such as cars, boats, aircraft, motorcycles, trains, and automobile vehicles [2]. The development of functioning brake pads and discs, which are among the main components of braking systems disc type, has been the subject of much research since their invention so as to improve their braking performance. Brake pad composition continues to change to meet technological growth and environmental requirements. Researchers and engineers have concentrated on selecting materials for brake pads from the friction material perspective and in relation to their tribological properties. Choosing a suitable brake pad for commuting has created numerous challenges, regardless of the braking systems' quality and performance. These challenges include but are not limited to high braking force, maintaining a constant friction coefficient, low absorption, dissipating heat energy over a short time, and improving wear resistance, all of which make the braking requirements for brake pad material more complicated. Other aspects of the braking experience which brake pad manufacturers have to bear in mind include pneumatic pressure, thermal stresses and mechanical fade on both the wheel and on the surface of the brake pad. Development of brake pads with properties that can improve the braking performance in the automobile industry have become a necessity [3-7]. Some research groups have responded to the environmental challenges by researching alternatives to asbestos brake pads which include constituents such as copper (Cu), tin (Sn) and whiskers which are harmful to humans [8-11].

Due to the health issues associated with using asbestos brake pad material, the whole world has focused on producing bio-based materials with the same mechanical and thermal properties, which is the most important interest of the current research [2, 12-15]. A braking system must offer vibration-free performance, stable friction, low noise, and low wear rate. For that reason, it is not easy to develop cost-effective brake pads with satisfactory performance. Each component makes an essential contribution to the thermo-mechanical properties of a brake pad [16, 17]. Studies have affirmed that brake pad material must offer good thermal stability to avoid an increase in wear at higher temperatures [17]. Besides, the brake pad must have low thermal expansion as well as capacity to absorb the heat that dissipates from the friction surfaces within seconds [18].

Although significant improvements have been made in developing brake pad materials for automobiles, but problems such as heat dissipation and noise pollution still exist. Multi-phase composites typically contain more than ten components. During the braking operations, these components work together to

achieve different performances [19]. Extensive research has been widely discussed and is available for reference in the literature regarding the role of other fibers [20, 21], fillers [22], binders [23], and modifiers [24, 25] in the formulation of brake pads.

Carbon nanospheres (CNSs) similar to the type used in this study are produced using the chemical vapor deposition method (CVD) and used as a filler to improve the performance properties such as mechanical and tribological properties as well as thermal stability of material [26-29]. In this study, epoxy resin was one of the main components used as a binder to uphold the structural wholeness of the material in the brake pad mixture under thermal and mechanical stress. Epoxy resin is a basic component that holds together and combines all components of the brake pad. Graphite nanoparticles with a density of 1.8 g/cm^3, a size of < 100 nm and 99.5 % purity from hydrophobic natural graphite were used as a friction modifier. Graphite is generally employed as an internal lubricator because it improves thermal stability and is used to check the friction and wear of the brake pads [30-32]. Stainless steel nanoparticles with a density of 7.86 g/cm^3, a size of 70 nm and 99.9% purity were used as reinforcement to improve the properties such as mechanical, tribological, and thermal stability of the BHN brake pad. These materials were intended to improve the performance of the brake pad friction materials [17, 20, 33-37]. The role of nanoparticles in friction composite formulations is to effectively control the performance of fade and recovery of the brake pad [38-40].

According to Nagesh et al. [41], a brake pad is a mixed material consisting of various constituents that improve the brake performance under various conditions such as high or low temperatures. These components improve brake pad durability, increase pad strength and rigidity, and reduce brake pad noise during their operation. Similarly, they should be environmentally friendly. Ikpambese et al. [14], Lawrence and Paul [42], and Kim et al. [43] emphasize that the combination ratios, the nature of the materials, the mixing methods, and the manufacturing techniques of these materials determine the properties of the final product (brake pad sets). Kumar et al., [44] varied four different bio-composite materials for brake pad application using compression molding machine by analysing the wear rate and frictional behaviour of the new composites. The bio-composite materials were discovered to be well-suited with each other. Vivek et al., [45] used bio-based material (Palm fiber) as reinforcement for absorbent brake pad production. They evaluated the effect of palm fiber on mechanical, physical, and tribological properties of the newly brake pad composite by varying the pressure and speed in a pin on disc tribometer. The result showed that the palm fiber composite friction stability is high at high pressure, and thus reduces fluctuation for continuous sliding. This means all these factors must well-controlled and considered when producing brake pads. Brake pads are required to meet all the engineering and environmental requirements [43]. The engineering requirements include mechanical, tribological, and thermal properties. Motor vehicle companies discovered that it is easier to adjust the brake pad than change the braking system [46].

1.2 History and overview of brake pads

Brake history goes back to the late 19th century when automobile braking (rail) systems were used consisting of wood and leather components. Brake pads are an essential component of the vehicle braking system. Brake pads help to smooth deceleration and keep the vehicle at a stop when it is parked. Brake-efficiency depends on the quality of brake pads used and excellent composition [43]. Good brake pads must be reliable, safe, and effective. Therefore, the material or combination of brake pad materials must have good engineering and environmental qualities. In 1953 the United States introduced phenolic resin as a new binder for the patent area of the brake shoe [47]. Regarding the development of resins, there is a continuous record of lignin in brake pads applications since 1977. Jacko and Gager [48] developed patents that used different kraft lignins and lignosulfonates as a fractional substitute for phenolic resin, indicating that lignosulfonates have better thermal stability than Kraft lignin.

The selection of materials is one of the necessary procedures for the production of brake pads. Maleque et al. [49] observed that selection and combination of materials for the ideal brake pad is not a simple job but a systematic process involving various decision-making stages. Nicholson et al. [50] stated that the selection of brake pad material depends not only on the material function but also on the available material, material costs, and material handling. Jang and Kim [51] and Kennedy et al. [52] stated that material selection is primarily based on the suitable properties needed for brake pad performance. The material or mixture of materials used for brake pads must have particular properties before they can be used for brake pad applications. These include thermal stability, mechanical strength, stable friction coefficient, short braking distance and low wear rate. Lawrence and Paul [4] stated that brake pad material composition is in three categories: metallic, semi-metallic and non-asbestos organic (NAO) materials. Many studies have been done on the nanocomposites as well as several types of fibers such as glass, ceramic, metallic and mixtures of carbon fiber for production of brake pad applications [17, 41, 53-60]. The fibers mentioned above are widely used as fillers or reinforcements material to produce NAO brake pads [4, 54].

However, NAO brake pad materials exposed to a high-temperature environment commonly encounter an incident called fade [56, 61-63], where the average low-temperature friction coefficient decreases in the short term. For safety reasons, automotive brake pad materials must be light and withstand high temperatures and absorb adequate friction energy [56]. There is a great need for better thermal resistance due to the thermal degradation characteristics in organic material. Authors have considered carbon nanotubes (CNTs) and carbon nanospheres (CNSs) as being suitable for brake pad applications due to their low density and high thermal resistance. This study used palm kernel fiber (PKF) activated carbon

to grow CNSs through a simple physical activation method under a CO_2 to produce brake pad material instead of using commercial CNSs which are difficult to disperse and are very expensive.

As established by many researchers [5, 14, 18], various studies have been carried out on materials or constituent combinations to produce brake pads and determine their strength. All the reinforcement materials are carbon-based, but they have different functions. In this study, the CNSs were used to improve the mechanical and tribological properties as well as the thermal conductivity of the BHN brake pad. The graphite nanoparticles acted as an internal lubricant to control the wear and the friction coefficient of the brake pad. The bio-based hybrid nanocomposite for the BHN brake pads was developed by selecting raw materials, then weighing, mixing, compacting and sintering of the materials. In the mixing process, graphite nanoparticles were added to minimize fracturing. In this study, PKF CNSs were used as a filler material. The method used in the production of this newly developed bio-based hybrid nanocomposite brake pad was the powder metallurgy technique due to its ability to obtain uniform part and reduce faded. Testing of hardness, wear, absorption, compression strength, impact, thermal conductivity, and friction coefficient was used to determine the fitness of the materials for brake pad application. The testing of material properties helps with the selection of a suitable combination of materials and improves the study consistency.

1.3 Problem statement

Historically, asbestos has been used in brake pads as the primary material, though it started to be avoided because of its carcinogenic nature and high cost, so asbestos substitutes emerged [64]. After banning of asbestos, many metallic and semi-metallic materials have been used [65-68]. Presently, the most important area of research is the use of natural fiber as the primary component in production of brake pads [67, 69, 70]. Due to biodegradability and cost efficiency, synthetic fibers have been replaced with natural fibers. Many natural fibers have been used as the main component in brake pad applications and different results have been obtained. Thus, to prevent health issues and minimize production costs, new asbestos-free brake pads need to be produced locally from natural fiber. For that reason, it is essential to research the exact formula and mixture ratio of the additives to formulate a functioning brake pad material with superior or equivalent properties to existing brake pad materials commonly used by local vehicles.

1.4 Research motivation

Biobased CNSs are becoming a more favorable alternative to synthetic carbon nanotubes because they are thermally stable and form smaller agglomerates. In monitoring the morphology and yield of CNTs, the precursor material used is essential. For example, precursors rich in carbon, hydrocarbons, graphite

powder, and petroleum pitch have been used already, and there is ongoing research in this field. However, due to environmental risks and possible toxicity, it is essential to manufacture nanomaterials from green sources that are not harmful to humans and the environment, and this is the motivation behind this study.

The motivations for this research work were:

i. Lack of literature on carbon nanomaterials synthesised from palm kernel fiber.
ii. Limited past literature on the development of biobased hybrid nanocomposite brake pads using PKF activated carbon.
iii. Lack of prior studies on the thermo-mechanical properties of bio-based hybrid nanocomposite brake pads from PKF.

1.5 Statement of purpose

The safety and toxicity problem is becoming more prevalent as nanoparticle applications increase since they have been recorded as damaging humans and wildlife as they can enter the body through breathing, digestion, and skin contact [71, 72]. In recent times, concern for environmentally friendly and renewability of materials has grown, giving rise to the study of bio-based precursors in the synthesis of carbon nanomaterials. The results show that biomass nanocomposites have excellent potential for nanotechnology because they can be derived from agricultural waste. Besides improving environmental sustainability, bio-based nanocomposites also improve rural economic development as well as the national energy security [73]. In 2014, the South African Department of Science and Technology launched the national bio-economy strategy. The document stated that bio-based materials should be developed from non-fossil resources, for instance, biomass [74].

Therefore, the purpose of this research was to synthesize carbon nanocomposite from a PKF bio-based precursor using it as a filler to produce brake pads.

1.6 Aim of the study

This research aimed to develop an efficient brake pad material from PKF bio-based hybrid nanocomposite material and investigate these brake pads' functional properties compared with conventional brake pads.

1.7 Objectives of the study

a. To Convert PKF agricultural waste to carbon nanomaterial.

b. To synthesize and characterize carbon nanomaterials from PKF activated carbon.

c. To develop a brake pad consisting of nanocomposites material synthesized from agro-waste, steel nanoparticles, and graphite nanoparticles.

d. To determine the mechanical and tribological properties such as wear rate, coefficient of friction, microstructure analysis, hardness, impact strength, and compressive strength of bio-based hybrid nanocomposite (BHN) brake pad material compared with conventional brake pad material.

e. To determine the BHN brake pad thermal properties, such as dynamic mechanical analysis (DMA) and thermogravimetric analysis (TGA) compared with those of conventional (control) brake pads.

1.8 Research hypothesis

Bio-based nanocomposite can be synthesized from PKF through ethanol vapor treatment. The morphology and size of the synthesized bio-based hybrid nanocomposite depend on the temperature of the synthesis. The newly developed BHN brake pad friction material is a suitable replacement for current brake pads because it provides better durability, improved braking performance, and eco-friendliness.

1.9 Synthesis techniques of carbon nanospheres

The materials included CNSs synthesized from PKFs, steel nanoparticles, graphite nanoparticles, and epoxy resin as a binder. To synthesize the nanomaterials, the PKFs were collected, cleaned, and sun-dried to remove the moisture content. The PKFs were then inserted in a horizontal tube furnace where carbonization took place at 600 °C for two hours. The carbonized PKF was physically activated at temperature 850 °C for one hour using CO_2 gas to improve the carbonized material's pore structure, followed by treatment in methanol vapor for 60 minutes in the presence of argon gas to produce CNSs.

1.10 Thesis layout

The thesis consists of the outcomes of research published in peer-reviewed journals for awarding of a doctoral degree as required by the University of KwaZulu-Natal. Six publications were produced for the thesis and the thesis is divided into seven chapters.

Chapter 1 is the study introduction, problem statement, research motivation and statement of purpose. It also presents the aim, objectives, research hypothesis and highlights major contributions of the study.

Chapter 2 is in two parts. Part 1 provides a critical review of the most suitable eco-friendly and optimal brake pad composites and provides a broad review on biomass-based composites from agro-waste such as natural fibers.

Chapter 3 is a comprehensive review on the effects of fiber, fillers and binders on automobile brake pad performance and provides a review of the influence of different binders such as phenolic resin, and epoxy resin.

Chapter 4 discusses the general time and economical methods of preparing CNSs from palm kernel fiber bio-based materials. Carbon nanospheres were successfully synthesized from PKF activated carbon through ethanol vapor treatment at 700 °C to 1000 °C at 150 °C intervals.

Chapter 5 examines the effect of synthesis temperature on CNSs from PKF activated carbon.

Chapter 6 presents the results of tribological study of brake pad applications developed from bio-based hybrid nanocomposites compared with conventional brake pads.

Chapter 7 focuses on the thermo-mechanical analysis of prepared brake pad applications from bio-based hybrid nanocomposites compared with control brake pads.

Chapter 8 presents the conclusions drawn from the study, and recommendations for future work.

Reference

[1] A. Belhocine and N. M. Ghazaly, "Effects of material properties on generation of brake squeal noise using finite element method," *Latin American Journal of Solids and Structures,* vol. 12, no. 8, pp. 1432-1447, 2015.

[2] J. Abutu, S. Lawal, M. Ndaliman, R. Lafia-Araga, O. Adedipe, and I. Choudhury, "Production and characterization of brake pad developed from coconut shell reinforcement material using central composite design," *SN Applied Sciences,* vol. 1, no. 1, p. 82, 2019.

[3] M. Afolabi, O. Abubakre, S. Lawal, and A. Raji, "Experimental investigation of palm kernel shell and cow bone reinforced polymer composites for brake pad production," *International Journal of Chemistry and Materials Research,* vol. 3, no. 2, pp. 27-40, 2015.

[4] I. Lawrence and U. Paul, "Critical evaluation/reassessment of (abfm) automotive brake friction materials," *Standard Research Journal,* 2013.

[5] M. Kumar, B. K. Satapathy, A. Patnaik, D. K. Kolluri, and B. S. Tomar, "Hybrid composite friction materials reinforced with combination of potassium titanate whiskers and aramid fibre: assessment of fade and recovery performance," *Tribology International,* vol. 44, no. 4, pp. 359-367, 2011.

[6] P. J. Blau, "Compositions, functions, and testing of friction brake materials and their additives," Oak Ridge National Lab., TN (US), 2001.

[7] K. Liew and U. Nirmal, "Frictional performance evaluation of newly designed brake pad materials," *Materials & Design,* vol. 48, pp. 25-33, 2013.

[8] N. Aranganathan and J. Bijwe, "Development of copper-free eco-friendly brake-friction material using novel ingredients," *Wear,* vol. 352, pp. 79-91, 2016.

[9] P. W. Lee and P. Filip, "Friction and wear of Cu-free and Sb-free environmental friendly automotive brake materials," *Wear,* vol. 302, no. 1-2, pp. 1404-1413, 2013.

[10] R. Yun, P. Filip, and Y. Lu, "Performance and evaluation of eco-friendly brake friction materials," *Tribology International,* vol. 43, no. 11, 2010.

[11] R. Yun, Y. Lu, and P. Filip, "Application of extension evaluation method in development of novel eco-friendly brake materials," *SAE International Journal of Materials and Manufacturing,* vol. 2, no. 2, pp. 1-7, 2010.

[12] S. S. Bernard, M. J. Ahmed, J. Dasaprakash, M. S. Nitin, S. Vivek, and G. Kannan, "Friction and Wear Properties of Bio-Based Abrasive in a High-Friction Composite Material," in *Advances in Manufacturing Technology*: Springer, 2019, pp. 577-585.

[13] J. Andersons, M. Kirpluks, P. Cabulis, K. Kalnins, and U. Cabulis, "Bio-based rigid high-density polyurethane foams as a structural thermal break material," *Construction and Building Materials,* vol. 260, p. 120471, 2020.

[14] K. Ikpambese, D. Gundu, and L. Tuleun, "Evaluation of palm kernel fibers (PKFs) for production of asbestos-free automotive brake pads," *Journal of King Saud University-Engineering Sciences,* vol. 28, no. 1, pp. 110-118, 2016.

[15] O. E Ige, F. L Inambao, and G. A Adewumi, "Biomass-Based Composites for Brake Pads: A Review," *International Journal of Mechanical Engineering and Technology,* vol. 10, no. 3, 2019.

[16] S. S. Bernard and L. Jayakumari, "Effect of the properties of natural resin binder in a high friction composite material," *Polímeros,* vol. 24, no. 2, pp. 149-152, 2014.

[17] J. Bijwe, N. Majumdar, and B. Satapathy, "Influence of modified phenolic resins on the fade and recovery behavior of friction materials," *Wear,* vol. 259, no. 7-12, pp. 1068-1078, 2005.

[18] M. Eriksson, F. Bergman, and S. Jacobson, "On the nature of tribological contact in automotive brakes," *Wear,* vol. 252, no. 1-2, pp. 26-36, 2002.

[19] D. Chan and G. Stachowiak, "Review of automotive brake friction materials," *Proceedings of the Institution of Mechanical Engineers, Part D: Journal of Automobile Engineering,* vol. 218, no. 9, pp. 953-966, 2004.

[20] B. Satapathy and J. Bijwe, "Performance of friction materials based on variation in nature of organic fibres: Part I. Fade and recovery behaviour," *Wear,* vol. 257, no. 5-6, pp. 573-584, 2004.
[21] M. Kumar and J. Bijwe, "Optimized selection of metallic fillers for best combination of performance properties of friction materials: A comprehensive study," *Wear,* vol. 303, no. 1-2, pp. 569-583, 2013.
[22] S. Kim, M. Cho, R. Basch, J. Fash, and H. Jang, "Tribological Properties of Polymer Composites Containing Barite (BaSO 4) or Potassium Titanate (K 2 O· 6 (TiO 2))," *Tribology Letters,* vol. 17, no. 3, pp. 655-661, 2004.
[23] U. Hong, S. Jung, K. Cho, M. Cho, S. Kim, and H. Jang, "Wear mechanism of multiphase friction materials with different phenolic resin matrices," *Wear,* vol. 266, no. 7-8, pp. 739-744, 2009.
[24] V. Tomášek, G. Kratošová, R. Yun, Y. Fan, and Y. Lu, "Effects of alumina in nonmetallic brake friction materials on friction performance," *Journal of materials science,* vol. 44, no. 1, pp. 266-273, 2009.
[25] L. Gudmand-Høyer, A. Bach, G. T. Nielsen, and P. Morgen, "Tribological properties of automotive disc brakes with solid lubricants," *Wear,* vol. 232, no. 2, pp. 168-175, 1999.
[26] K. Yang, M. Gu, Y. Guo, X. Pan, and G. Mu, "Effects of carbon nanotube functionalization on the mechanical and thermal properties of epoxy composites," *Carbon,* vol. 47, no. 7, pp. 1723-1737, 2009/06/01/ 2009, doi: https://doi.org/10.1016/j.carbon.2009.02.029.
[27] S.-Y. Yang *et al.*, "Synergetic effects of graphene platelets and carbon nanotubes on the mechanical and thermal properties of epoxy composites," *Carbon,* vol. 49, no. 3, pp. 793-803, 2011/03/01/ 2011, doi: https://doi.org/10.1016/j.carbon.2010.10.014.
[28] F. H. Gojny and K. Schulte, "Functionalisation effect on the thermo-mechanical behaviour of multi-wall carbon nanotube/epoxy-composites," *Composites Science and Technology,* vol. 64, no. 15, pp. 2303-2308, 2004.
[29] F. Gojny, M. Wichmann, U. Köpke, B. Fiedler, and K. Schulte, "Carbon nanotube-reinforced epoxy-composites: enhanced stiffness and fracture toughness at low nanotube content," *Composites science and technology,* vol. 64, no. 15, pp. 2363-2371, 2004.
[30] K. Takahashi, M. Yoshida, Y. Hagiwara, K. Kondoh, Y. Takano, and Y. Yamashita, "Titanium and/or titanium alloy sintered friction material," ed: Google Patents, 1999.
[31] A. Yasmin, J.-J. Luo, and I. M. Daniel, "Processing of expanded graphite reinforced polymer nanocomposites," *Composites Science and Technology,* vol. 66, no. 9, pp. 1182-1189, 2006.
[32] R. Sengupta, M. Bhattacharya, S. Bandyopadhyay, and A. K. Bhowmick, "A review on the mechanical and electrical properties of graphite and modified graphite reinforced polymer composites," *Progress in polymer science,* vol. 36, no. 5, pp. 638-670, 2011.
[33] A. Patnaik, M. Kumar, B. K. Satapathy, and B. S. Tomar, "Performance sensitivity of hybrid phenolic composites in friction braking: effect of ceramic and aramid fibre combination," *Wear,* vol. 269, no. 11-12, pp. 891-899, 2010.
[34] N. Dadkar, B. S. Tomar, B. K. Satapathy, and A. Patnaik, "Performance assessment of hybrid composite friction materials based on flyash–rock fibre combination," *Materials & Design,* vol. 31, no. 2, pp. 723-731, 2010.
[35] B. Satapathy and J. Bijwe, "Fade and recovery behavior of non-asbestos organic (NAO) composite friction materials based on combinations of rock fibers and organic fibers," *Journal of reinforced plastics and composites,* vol. 24, no. 6, pp. 563-577, 2005.
[36] K. H. Cho, M. H. Cho, S. J. Kim, and H. Jang, "Tribological properties of potassium titanate in the brake friction material; morphological effects," *Tribology letters,* vol. 32, no. 1, pp. 59-66, 2008.
[37] M. H. Cho, J. Ju, S. J. Kim, and H. Jang, "Tribological properties of solid lubricants (graphite, Sb2S3, MoS2) for automotive brake friction materials," *Wear,* vol. 260, no. 7-8, pp. 855-860, 2006.

[38] T. Singh, A. Patnaik, B. Satapathy, and M. Kumar, "Composites: Mechanics, Computations, Applications," *An International Journal,* vol. 3, no. 3, pp. 189-214, 2012.
[39] T. Singh, A. Patnaik, B. K. Satapathy, M. Kumar, and B. S. Tomar, "Effect of nanoclay reinforcement on the friction braking performance of hybrid phenolic friction composites," *Journal of materials engineering and performance,* vol. 22, no. 3, pp. 796-805, 2013.
[40] T. Singh, A. Patnaik, and B. K. Satapathy, "Thermo-mechanical characterization of nano filled and fiber reinforced brake friction materials," in *AIP conference proceedings*, 2013, vol. 1536, no. 1: American Institute of Physics, pp. 259-260.
[41] S. Nagesh, C. Siddaraju, S. Prakash, and M. Ramesh, "Characterization of brake pads by variation in composition of friction materials," *Procedia Materials Science,* vol. 5, pp. 295-302, 2014.
[42] I. Lawrence and U. Paul, "Critical evaluation/reassessment of (abfm) automotive brake friction materials," *Stand. Sci. Res. Essays,* vol. 1, no. 11, pp. 275-288, 2013.
[43] S. W. Kim, S. J. Lee, B. K. Park, and S. K. Rhee, "A comprehensive study of humidity effects on friction, pad wear, disc wear, DTV, brake noise and physical properties of pads," SAE Technical Paper, 0148-7191, 2011.
[44] P. M. Kumar, S. Bachina Harish, And K. Rajesh, "Development and Study of Tribological Properties of Biocomposite For Brake Pad Application," *International Journal of Mechanical and Production Engineering Research and Development (IJMPERD),* vol. 7, no. 6, pp. 263-270, 2017.
[45] S. Vivek, J. LS, and J. A. Md, "Tribological and mechanical properties of biobased reinforcement in a friction composite material," *Matéria (Rio de Janeiro),* vol. 25, no. 3, 2020, doi: https://doi.org/10.1590/S1517-707620200003.1085.
[46] H. Jang, J. Lee, and J. Fash, "Compositional effects of the brake friction material on creep groan phenomena," *Wear,* vol. 251, no. 1-12, pp. 1477-1483, 2001.
[47] J. S. G. Tilden, "Method of making and bonding brake friction material to a brake shoe," ed: Google Patents, 1953.
[48] M. G. Jacko and R. F. Gager, "Lignin modified friction material," ed: Google Patents, 1980.
[49] M. Maleque[1], S. Dyuti, and M. Rahman, "Material selection method in design of automotive brake disc," in *Proceedings of the world congress on engineering*, 2010, vol. 3.
[50] G. Nicholson, "Facts about Friction: 100 years of Brake Linings & Clutch Facings," *Geodoran America, Winchester, VA,* 1995.
[51] H. Jang and S. J. Kim, "The effects of antimony trisulfide (Sb2S3) and zirconium silicate (ZrSiO4) in the automotive brake friction material on friction characteristics," *Wear,* vol. 239, no. 2, pp. 229-236, 2000/04/01/ 2000, doi: https://doi.org/10.1016/S0043-1648(00)00314-8.
[52] F. Kennedy, A. Balbahadur, and D. Lashmore, "The friction and wear of Cu-based silicon carbide particulate metaal matrix composites for brake applications," *Wear,* vol. 203, pp. 715-721, 1997.
[53] S. J. Kim and H. Jang, "Friction and wear of friction materials containing two different phenolic resins reinforced with aramid pulp," *Tribology international,* vol. 33, no. 7, pp. 477-484, 2000.
[54] H. Hwang, S. Jung, K. Cho, Y. Kim, and H. Jang, "Tribological performance of brake friction materials containing carbon nanotubes," *Wear,* vol. 268, no. 3-4, pp. 519-525, 2010.
[55] H. Jang, K. Ko, S. Kim, R. Basch, and J. Fash, "The effect of metal fibers on the friction performance of automotive brake friction materials," *Wear,* vol. 256, no. 3-4, pp. 406-414, 2004.
[56] K.-J. Lee *et al.*, "Tribological and mechanical behavior of carbon nanotube containing brake lining materials prepared through sol–gel catalyst dispersion and CVD process," *Journal of alloys and compounds,* vol. 483, no. 1-2, pp. 389-393, 2009.
[57] M. H. Cho, S. J. Kim, D. Kim, and H. Jang, "Effects of ingredients on tribological characteristics of a brake lining: an experimental case study," *Wear,* vol. 258, no. 11-12, pp. 1682-1687, 2005.

[58] G. Yi and F. Yan, "Mechanical and tribological properties of phenolic resin-based friction composites filled with several inorganic fillers," *Wear,* vol. 262, no. 1-2, pp. 121-129, 2007.
[59] O. J. Gbadeyan, "Low friction hybrid nanocomposite material for brake pad application," 2017.
[60] O. J. Gbadeyan, K. Kanny, and T. Mohan, "Influence of the multi-walled carbon nanotube and short carbon fibre composition on tribological properties of epoxy composites," *Tribology-Materials, Surfaces & Interfaces,* vol. 11, no. 2, pp. 59-65, 2017.
[61] A. E. Anderson, *Friction and wear of automotive brakes*. ASM International, 1992.
[62] J. Bijwe, "Composites as friction materials: Recent developments in non-asbestos fiber reinforced friction materials—a review," *Polymer composites,* vol. 18, no. 3, pp. 378-396, 1997.
[63] P. Tsang, M. Jacko, and S. Rhee, "Comparison of chase and inertial brake dynamometer testing of automotive friction materials," *Wear,* vol. 103, no. 3, pp. 217-232, 1985.
[64] U. Idris, V. Aigbodion, I. Abubakar, and C. Nwoye, "Eco-friendly asbestos free brake-pad: Using banana peels," *Journal of King Saud University-Engineering Sciences,* vol. 27, no. 2, pp. 185-192, 2015.
[65] T. Singh, A. Tiwari, A. Patnaik, R. Chauhan, and S. Ali, "Influence of wollastonite shape and amount on tribo-performance of non-asbestos organic brake friction composites," *Wear,* vol. 386, pp. 157-164, 2017.
[66] I. Sugözü, "Investigation of using rice husk dust and ulexite in automotive brake pads," *Materials Testing,* vol. 57, no. 10, pp. 877-882, 2015.
[67] V. Mahale, J. Bijwe, and S. Sinha, "Influence of nano-potassium titanate particles on the performance of NAO brake-pads," *Wear,* vol. 376, pp. 727-737, 2017.
[68] D. L. Singaravelu, R. Vijay, and M. Rahul, "Influence of crab shell on tribological characterization of eco-friendly products based non asbestos brake friction materials," SAE Technical Paper, 0148-7191, 2015.
[69] V. Thiyagarajan, K. Kalaichelvan, R. Vijay, and D. L. Singaravelu, "Influence of thermal conductivity and thermal stability on the fade and recovery characteristics of non-asbestos semi-metallic disc brake pad," *Journal of the Brazilian Society of Mechanical Sciences and Engineering,* vol. 38, no. 4, pp. 1207-1219, 2016.
[70] R. Vijay, D. Lenin Singaravelu, and P. Filip, "Influence of molybdenum disulfide particle size on friction and wear characteristics of non-asbestos-based copper-free brake friction composites," *Surface Review and Letters,* vol. 27, no. 01, p. 1950085, 2020.
[71] M. Sajid *et al.*, "Impact of nanoparticles on human and environment: review of toxicity factors, exposures, control strategies, and future prospects," *Environmental Science and Pollution Research,* vol. 22, no. 6, pp. 4122-4143, 2015.
[72] B. Nowack and T. D. Bucheli, "Occurrence, behavior and effects of nanoparticles in the environment," *Environmental pollution,* vol. 150, no. 1, pp. 5-22, 2007.
[73] S. P. Singh, E. P. Ekanem, T. Wakefield Jr, and S. Comer, "Emerging importance of bio-based products and bio-energy in the US economy: information dissemination and training of students," *International Food and Agribusiness Management Review,* vol. 5, no. 1030-2016-82598, 2003.
[74] (2013). *The bio-economy strategy*. [Online] Available: https://www.dst.gov.za/images/ska/Bioeconomy%20Strategy.pdf
[75] I. M. Dagwa and A. Ibhadode, "Some physical and mechanical properties of asbestos–free experimental brake pad," *Journal of Raw Materials Research,* vol. 3, no. 2, 2015.

CHAPTER 2: REVIEW OF BIOMASS-BASED COMPOSITES FOR BRAKE PADS

To cite this article: O. E. Ige, F. L. Inambao, and G. A. Adewumi, "Biomass-Based Composite for Brake Pad: A Review," *International Journal of Mechanical Engineering and Technology,* vol. 10, no. 3, pp. 920-943, 2019.

International Journal of Mechanical Engineering and Technology (IJMET)
Volume 10, Issue 03, March 2019, pp. 920–943, Article ID: IJMET_10_03_094
Available online at http://www.iaeme.com/ijmet/issues.asp?JType=IJMET&VType=10&IType=3
ISSN Print: 0976-6340 and ISSN Online: 0976-6359

BIOMASS-BASED COMPOSITES FOR BRAKE PADS: A REVIEW

Oluwafemi E. Ige, Freddie L. Inambao and Gloria A. Adewumi
Department of Mechanical Engineering
School of Engineering, University of KwaZulu-Natal, Durban, South Africa

ABSTRACT

There is a growing need to develop automobile brake pad materials from sustainable sources. The study of substitute brake pad materials from sustainable sources is an area that requires immediate attention. This is because previous materials used (such as asbestos) are known to have carcinogenic effects. Several studies have investigated alternative materials to asbestos for brake pads. This review paper presents some of the most appropriate environmentally friendly and optimal composites for brake pads. Biomass-based composites from agricultural waste such as natural fibers waste are reviewed. This paper also surveyed the use of substitute materials as filler and binder, such as epoxy resin, phenolic resins, and other adhesives.

Key words: Brake pad, fillers, Natural fiber composite, Agricultural waste, Material properties.

Cite this Article: Oluwafemi E. Ige, Freddie L. Inambao and Gloria A. Adewumi, Biomass-Based Composites for Brake Pads: A Review, *International Journal of Mechanical Engineering and Technology* 10(3), 2019, pp. 920–943.
http://www.iaeme.com/IJMET/issues.asp?JType=IJMET&VType=10&IType=3

1. INTRODUCTION

In the past few years several studies have been conducted on the development of non-asbestos brake pads. Uses of palm kernel shell, palm kernel fiber and other biomass precursors have been investigated [1]. The present trend in research for asbestos-free brake pads is to use industrial or agricultural waste (agro-waste) as a raw material source for composite development [2] [3] [4]. Recently, international efforts to address environmental issues and the need to protect the environment has drawn research focus to the use of natural fibers in several applications, including brake pads. Typically, brake pads contain asbestos embedded in a polymer matrix with several other ingredients. Due to its carcinogenic effects on human health and its other harmful properties, the use of asbestos is increasingly being avoided, and therefore new non-asbestos materials and brake pads have been developed [5-8].

The brake pad is one of the most important components of an automobile braking system, as its helps in the conversion of a vehicle's kinetic energy to heat energy. The types of automotive brake pads that are in the market are characterized by metallic materials, semi-metallic materials or non-asbestos organic (NAO) materials [9]. According to Idris et al. [10],

a brake pad is a steel back-plate with a friction material bound to the surface facing disk. The effectiveness and performance of brake pads are absolutely dependent on the frictional material used in the process of its manufacture [11]. In recent years, extensive research has focused on environmentally friendly brake pad composites that use natural fiber from agro-waste as a replacement for asbestos fibers [12].

For more than a decade, natural fibers have been used as reinforcing materials [13]. In addition, composite materials have evolved into a cost-effective and potentially eco-friendly substitute for synthetic fiber reinforced composites for use in various parts of an automobile. The availability, comfort and low cost of natural fibers in industrial use have attracted many researchers to study their suitability in meeting the basic specifications of well-reinforced polymer composites for tribological and other applications [14].

Over the years, the production of composite materials worldwide has grown significantly, which means many industries and technology sectors now use the newly formulated polymer composites materials which have successfully replaced traditional composite materials [15]. The investigation of new materials, especially agro-waste, has led to the development of new and low-cost options for the development of brake pads which are commercially viable and environmentally acceptable, including all the properties required.

In addition, studies which investigated the properties of selected agro-waste are reviewed in regard to their application as filler and binder.

2. AGRICULTURAL WASTE

Fibers derived from agro-waste have economic significance and cultural impact throughout the world [16]. Such fibers also have great potential as composite materials because of their high strength, low cost, eco-friendly nature, availability, and sustainability [17, 18]. Fibers derived from agricultural waste have many properties with potential for industrial application, which have led to a great deal of research on how to channel them to useful materials while taking human health and environmental safety into consideration. Agricultural waste, also referred to as biomass, is a potential renewable energy source with several applications which in building materials and multipurpose materials for automobile applications. The use of organic waste and residual materials in polymer composites represents an eco-friendly and significantly high-value substitute [19]. Table 1 shows some agricultural products which have potential as natural fiber resources and their countries of origin

Table 1. Biomass and their countries of origin: Agricultural products as potential natural fiber resources

	Brazil	**China**	**India**	**Indonesia**	**Malaysia**	**Philippine**	**Thailand**	**USA**	**Vietnam**
Banana	6.90	10.55	24.87	6.19	0.335	9.23	1.65	0.008	1.56
Coconut	2.82	0.250	11.93	18.30	0.605	15.35	1.01	NA	1.31
Pineapple	2.48	1.00	1.46	1.78	0.334	2.40	2.65	0.180	0.540
Sugarcane	0.739	125.54	341.20	33.70	0.830	31.87	100.10	27.91	20.08
Rice	11.76	203.29	159.20	71.28	2.63	18.44	38.79	8.63	44.04
Oil palm fruit	1.34	0.670	NA	120.00	100.00	0.473	12.81	NA	NA
Jute	26.71	0.17	1.98	0.007	0.002	0.002	0.06	NA	0.02
Kenaf	14.20	0.08	0.12	4.35	0.01	NA	1.30	NA	8.20
Flax	0.71	0.47	0.22	NA	NA	0.002	0.01	0.004	NA
Sisal	0.25	0.15	0.21	0.03	NA	NA	0.003	NA	0.01
Abaca	1.20	0.65	NA	0.05	NA	0.08	NA	NA	0.01
Kapok	NA	0.06	NA	0.03	0.008	NA	0.07	NA	0.003

Agricultural waste as shown in Figure 1 can be found in many plants, for example oil palm tree, corn stalks, bagasse, bamboo, coir (coconut shell), sugarcane pineapple, banana, rice husk, rice straw and plants (stem, leaf, seed, fruit, stem, grass, reed) [17]. Only 10 % of the potential of these natural fibers are being harnessed and used as alternative raw materials in industry, where the most common applications include bio-composites, bio-medical, automotive parts, and others [20]. The most important fiber waste produced by agricultural activities are cellulose fibers (CF) which have the potential to enhance materials because of their easy availability, lightweight, renewable, degradable, low abrasive properties, and low cost [17, 18, 20]. Cellulose fibers (CF) occurs in combination with other materials for instance lignin, hemicelluloses and pectin [21]. Agro-waste is the most abundant form of natural fiber and has been used in many areas of modern industry These materials vary in relation to conditions of growth and harvesting [22].

Figure 1. Agricultural waste

2.1. Properties of Agricultural Biomass

For more than two decades the characteristics of biomass have been investigated. However, the properties of natural fibers have not been enumerated consistently because of the different fibers utilized, different moisture conditions introduced, and different testing methods. Researchers agree that the properties of agricultural biomass are decided by many variables such as its structure, chemical composition, cell dimensions, microfibril angle, physical properties and mechanical properties. These properties vary widely among plant species and even in the same plant [23]. It is necessary to understand the properties of the fibers in order to elaborate on the use of natural fibers for composites so as to improve their performance.

2.1.1. Chemical Properties

According to Kumar et al. [24], agricultural biomass is mainly made of cellulose, hemicellulose, and lignin, as well as small amounts of pectin, protein, and ash. Cellulose is a semi-crystalline polysaccharide composed of D-anhydroglucose and glycosidic bonds. It offers strength, stiffness and structural stability to the fiber, helping to maintain the structure of the plant, and serves as a determining factor in its mechanical properties. Hemicellulose is a branched and fully amorphous polymer. Lignin is a complex hydrocarbon polymer with aliphatic and aromatic components. Lignin is linked with hemicellulose in agricultural plant cells and plays

a role in the natural decay resistance of agro-biomass materials [25]. Table 2 shows the variability in cell wall composition in biomass. The chemical properties of agro-biomass as shown in Table 4 indicates that the polymer content is highly variable, depending on the plant species. The composition, structure and biomass properties depend on the age of the plant, conditions of the soil and other environmental factors which include humidity, stress, and temperature [26]. The polymer chemistry of these fibers affect their characteristics, functionalities and properties [27].

Table 2. Agricultural biomass chemical properties

Composition (%)					
Type of biomass	**Cellulose**	**Extractive**	**Hemicellulose**	**Lignin**	**Reference**
Sisal	43.85-56.63	2	21.12-24.53	7.21-9.20	[28]
Oil palm	44.20-49.60	4	18.30-33.54	17.30-26.51	[26, 29]
Kapok	65.63-69.87		6.66-10.49	5.46-5.63	[30, 31]
Bamboo	73	3	12	10	[26]
Corn stalks	38.33-40.31	5	25.21-32.22	7.32-21.45	[28, 32]
Banana	60.25-65.21	-	48.20-59.2	5.55-10.35	[33, 34]
Abaca	69.23-70.64		21.22-21.97	5.15-5.87	[35]
Sugarcane (Bagasse)	55.60-57.40	10	23.90-24.50	24.35-26.30	[28, 36, 37]
Pineapple	70.55-82.31		18.73-21.90	5.35-12.33	[38]
Flax	69.22-71.65	6	18.31-18.69	3.05-2.56	[28, 35]
Kenaf	37.50-63.00	6.4	15.10-21.40	18.00-24.30	[35, 39, 40]
Jute	69.21-72.35	4	12.55-13.65	12.67-13.21	[28, 35]
Rice straw	28.42-48.33	17	23.22-28.45	12.65-16.72	[32, 41]
Coconut (coir)	36.62-43.21		0.15-0.25	41.23-45.33	[42]

2.1.2. Physical and Mechanical Properties

The physical and mechanical properties of fiber are highly dependent on the growing conditions, chemical composition, extraction methods and its ratio Cristaldi et al. [43] and Huang et al [44]. Table 5 presents a summary of the mechanical and physical properties of different biomasses.

2.1.2.1. Physical Properties

The properties of biomass fibers are strongly affected by their individual material, which play an important role in the consideration of such materials in multidisciplinary applications. Biomass fiber properties associated with important variables include fiber structure, microfibril angle, cell dimension and defects [45]. John and Thomas [46] stated that origin, source, species, and fiber maturity are determined by the size of a single cell in a biomass fiber. The properties of an end product, such as tensile strength, tear strength, drainage, adhesion and stress distribution, are highly dependent on the structural properties of the fiber, particularly fiber length, fiber width and cell wall thickness [47, 48]. In addition, the lumen structure affects the bulk density of fibers, which affects the thermal conductivity and acoustic factors of the fiber end product [49].

2.1.2.2. Mechanical Properties

The processing of natural fibers can occur in various ways to produce reinforcing elements with different mechanical properties. The mechanical properties of natural fibers are affected by many factors, for example, whether fiber bundles or ultimate fibers are being tested. The mechanical properties of the types of fibers from different sources are clearly illustrated (Table 3) while large variation in the mechanical properties of biomass has become a key concern

when it comes to commercial use. The large changes in tensile properties during plant growth are also a disadvantage for all-natural products, which is affected by species, fiber structure and environmental conditions.

Table 3. Physical and mechanical properties of certain agricultural waste fibers

Types of fiber	Density gm^{-3}	Tensile strength (MPa)	Young's modulus (GPa)	Elongation at break (%)	References
Banana	0.65-1.36	51.6-55.2	3.00-3.78	1.21-3.55	[50] [51] [52]
Oil palm	0.7-1.55	227.5-278.4	2.7-3.2	2.13-5.00	[47]
Bagasse	0.31-1.25	257.3-290.5	15-18	6.20-8.2	[37, 53]
Corn stalks	0.21-0.38	33.40-34.80	4.10-4.50	1.90-2.30	[54]
Jute	1.3-1.45	300-700	20-50	1.69-1.83	[55] [56] [57]
Pineapple	1.25-1.60	166-175	5.51-6.76	2.78-3.34	[50]
Coconut (coir)	0.67-1.15	173.5-175.0	4.0-6.0	27.21-32.32	[50] [52]
Rice straw	0.86-0.87	435-450	24.67-26.33	2.11-2.25	[58] [59]
Sisal	1.45-1.5	300-500	10-30	4.10-4.3	[55] [56] [57]
Kapok	0.68-1.47	80.3-111.5	4.56-5.12	1.20-1.75	[60, 61]
Abaca	1.42-1.65	879-980	38-45	9-11	[55]
Flax	1.27-1.55	500-900	50-70	2.70-3.6	[57] [62]
Kenaf	0.15-0.55	295-955	23.1-27.1	1.56-1.78	[63, 64]
Bamboo	0.6–1.1	360.5–590.3	22.2–54.2	4.0–7.0	[65]

The physical and mechanical properties of biomass fibers are very important and allied to the structure of the biomass fibers. Biomass fibers are largely natural organic fibers that exhibit high variability in different properties. This raises different questions in characterizing the quality of the physical and mechanical properties of the fiber. The most important physical property is density, while the mechanical properties of a single fiber are measured by using modulus and tensile strength values. It is very important to reference the development of biomass fibers as a biomaterial and the manufacture of polymer composites [66, 67]. In conclusion, it can be seen from the literature that biomass fibers have good potential as filler/enhancement material in polymer composites. Table 3 gives a comparison of the physical and mechanical properties of selected biomass fibers.

3. ALTERNATIVE FILLER MATERIALS FOR BRAKE PADS

In the production of brake pads there are three types of filler components used, namely, binders, friction modifiers, and reinforcements. The binder is a thermos resin used to bind all other components together to form a thermal stability matrix. The fillers are used to reduce the cost of pads. Reinforcements materials to improve the mechanical strength of the material include mineral fiber, carbon fiber, glass fiber, steel fiber, natural fiber, and ceramic fiber [13]. The friction modifiers are solid lubricants such as graphite and metal sulfides used to control stable friction and wear properties primarily at high temperatures. The objectives for using alternative materials for brake pad are to reduce the use of potentially destructive components in the brake pad material formulation while maintaining friction properties and reducing the pad wear rate. According to Lee and Filip [68], reducing the wear of material will likely reduce the negative environmental impact.

There are several characteristics and criteria that must be considered when selecting composite materials for brake pads. According to Lee and Filip [68] and Matějka et al. [69], the ability of the material to resist brake fade at higher temperatures must be considered when selecting brake pad materials. Lee [70] stated that the material must show good thermal stability and ability to recover quickly from high temperatures or moisture. According to Matějka et al.

[69], the material must exhibit an appropriate value of friction coefficient and good wear resistance.

3.1. Natural Fibers

Natural fibers are fibers derived from natural resources, and can be classified into three categories: plant, animal and mineral fibers [26]. According to Bledzki [71], stems, bark, seeds, and leaves can be used as natural fiber materials.

3.1.1. Maize husks

Ademoh and Olabisi [72], developed a new composite brake pad used maize husks (Figure 2) as a filler material and epoxy resin as a binder. They analyzed the mechanical, physical and tribological properties of the produced brake pad. It was observed that reducing the filler content of the produced composite brake pad increased the hardness, wear rate, tensile strength, compressive strength, and thermal conductivity, while density, the coefficient of friction, water and oil absorption increased with increased maize husk filler content as shown in Figure 3.

Figure 2. Maize husks

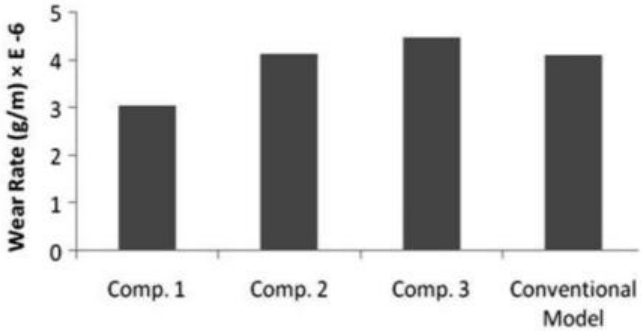

Figure 3. Wear rate analysis of the samples [72]

Studies have shown that reducing the filler content will increase the hardness, wear rate, tensile strength, compressive strength and thermal conductivity of the composite brake pad, while the density and friction coefficient increase with filler wt.%. as shown in Fig 4.

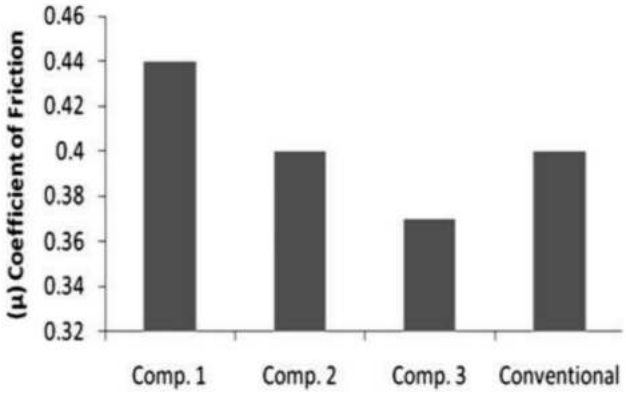

Figure 4. Coefficient of friction analysis of the samples [72]

The properties of the newly developed brake pad from maize husk were compared with asbestos-based brake pad as shown in Table 4. The results showed that the composite brake pad developed is environmentally friendly and is a suitable alternative to asbestos and many agro-biomass friction materials in the automotive brake pad.

Wisdom and Abraham [73] developed an asbestos-free brake pad using corn husks as an alternative filler with a view to replacing asbestos-based brake pads. The corn husks were milled and sieved into sieve grades of 100 μm and 200 μm. The different proportions of the selected corn husk fibers and silicon carbide were mixed together with a fixed ratio of other ingredient such as graphite, steel dust and phenolic resin (phenol formaldehyde) as a binder to produce a brake pad using compressional molding.

The properties such as compressive strength hardness, density, wear rate, flame resistance and porosity of the new brake pad were determined. The results showed that the samples from the 100 μm sieve grade of corn husk fiber gave the best properties. The hardness, compressive strength, density and porosity of the developed samples were observed to decrease with increase in sieve size of the corn husk, while the wear rate and percentage charred increased as the sieve size of the corn husk increased. The results obtained from the developed brake pad were compared with a commercial brake pad and were found to be in close agreement, indicating that corn husks can be used as an alternative filler material in the production of asbestos-based brake pads.

Table 4. Summary of the properties of the brake pads developed from maize husks (MH) compared with asbestos-based brake pads [72]

Properties	Asbestos-based	Maize husks-based
Wear rate (mg/m)	3.800	2.146
Tensile strength (MPa)	7.00	20.22
Hardness	101.0	127.8
Compressive strength (MPa)	110.0	103
Friction coefficient	0.30 – 0.40	0.37 – 0.40
Thermal conductivity (W/mK)	0.539	0.251 – 0.372
Specific gravity (g/cm3)	1.890	0.853
Thickness swells in SAE oil (%)	0.30	0.58
Thickness swell in water (%)	0.9	0.91

3.1.2. Sugar cane fiber (bagasse)

Aigbodion et al. [74] developed a new asbestos-free brake pad using bagasse (Figure 5) as a filler material, with phenolic resin (phenol formaldehyde) as a binder with a view to using it as a substitute for asbestos in brake pads because it is carcinogenic. They also investigated its mechanical, physical and tribological properties, which included hardness, microstructure analysis, density, compressive strength, flame resistance, water, and oil absorption.

Figure 5. Sugar cane fiber (Bagasse) [75]

The microstructure results showed that the resin distribution in the bagasse was uniform. Their results showed that the finer the sieve particle size, the better the properties of the new brake pad. The hardness, compressive strength, and density of the samples produced decreased when the sieve grade increased, whereas the oil soak, percentage charred, water soak and wear rate increased as sieve grade increased. The results show that bagasse can be effectively used as an asbestos substitute in the manufacture of brake pads by using bagasse of 100 µm sieve grade with 70 % and 30 % composition of resin.

3.1.3. Banana

Idris et al. [10] developed a non-asbestos brake pad using banana peel waste (Figure 6) as a filler with phenolic resin (phenol formaldehyde) as a binder. The work varied the resin content from 5 wt% to 30 wt% with an interval of 5 wt%. This work investigated and tested for mechanical, physical, wear, and morphological properties of the new brake pad. The samples containing non-carbonized banana peels (BUNCp) with 25 wt% and carbonized (BCp) sample with 30 wt% gave the best properties in all the samples.

Figure 6. Banana peel [10]

The results of the study (Table 5) showed that hardness, compressive strength, and specific gravity of the samples were increased with increase in wt% of additional resin. The result also showed that water absorption decreased as the wt.% resin increased.

Table 5. Summary of carbonized and non-carbonized based brake pad results compared with asbestos-based brake pads [10]

Properties	Commercial brake pad (asbestos-based)	Laboratory formulation (banana peels uncarbonized at 25% resin)	Laboratory formulation (banana peels carbonized at 30% resin)
Friction coefficient	0.3-0.4	0.40	0.35
Specific gravity (g/cm^3)	1.89	1.26	1.20
Hardness values (HRB)	101	98.8	71.6
Compressive strength (N/mm^2)	110	95.6	61.20
Wear rate (mg/m)	3.80	4.15	4.67
Thickness swell in water (%)	0.9	3.21	3.0
Thickness swell in SEA Oil (%)	0.3	1.15	1.12
Flame resistance (%)	Charred ash 9%	Charred ash 12%	Charred ash 24.67%

From Table 5 it is evident that the carbonized and non-carbonized based brake pads are in good agreement with commercial brake pads. Therefore, these formulations can be used to produce asbestos-free brake pads based on the expected dimensions of the brake pads as per the study (Peugeot 504 brake pad prototype with a length of 77 mm, friction depth of 12 mm and width of 65 mm). The prototype produced from banana peel particles showed that the formulation can be used in the production of automotive brake pads without adding any binder to the formulation. The result of this research revealed that banana peel particles can be used as a substitute for asbestos in the manufacturing of brake pads.

3.1.4. Rice husk dust

Shahril Anuar Bahari et al. [76] investigated the hardness and impact resistance properties of an automotive brake pad produced with rice husk dust (RHD) (Figure 7) as an alternative filler material. The dust was obtained with different sizes of mesh (80 mesh and 100 mesh) with other materials at different percentages of composition (10 % and 30 %). Phenol formaldehyde was used as a binder. Regarding the brake pad composed with fine mesh size, the results showed that a decrease in the percentage of rice husk dust showed an increase in the coefficient of friction, and a decrease in the percentage of rice husk dust in the mixture also decreased the wear rates, therefore rice husk dust increased the frictional performance. Thus, the smaller particle size of rice husk dust performed better as a filler material within a higher percentage of the composition. This study has shown that a high percentage of rice husk dust has a good result on hardness and impact resistance properties.

Figure 7. Rice husk

3.1.5. Pineapple

Felix and Prasanth [77] developed an asbestos-free brake pad using pineapple leaf fiber (PALF) as a filler material. Epoxy resin was used as a binder because it has good mechanical properties. They varied the samples with different percentages of pineapple leaf fiber and examined the compressive strength impact, hardness, flexural, density, and wear. Their results showed that with the increase in the percentage of PALF content, the compressive strength, hardness and wear decreased. Compressive strength, hardness, and wear of different samples decreased with an increase in the percentage of PALF, whereas the water absorption rate increased as the percentage of pineapple leaf fiber increased.

3.1.6. Coconut fiber

Bahari et al. [78] used dried coconut husks (Figure 8) as a filler material and phenolic resin (phenol formaldehyde) as a binder. They determined the friction coefficient and characteristics of the heat resistance of the developed brake pads with size 80 mesh and 100 mesh, as well as the percentage (10 % and 30 %) of coconut husk particles. The results showed that the brake pads with 100 mesh and 10 % coconut husk particles composition had the highest coefficient of friction. In terms of heat resistance, the composition of the brake pad with 100 mesh and 30 % of coconut husk dust showed the highest decomposition temperature which increased the thermal stability due to the high proportion of the coconut husk particles in the composition. The results also showed that the asbestos-free brake pad from coconut husk particles had better heat resistance than commercial brake pads.

Figure 8. Coconut fiber [79]

Maleque et al. [79] used coconut fibers as filler material with phenolic resin as a binder, and reinforced aluminum composites, for the application of automotive brake pads. Four different combinations of coconut fiber content such as BP1, BP2, BP3 and BP4 varied from 0, 5, 10 and 15 volume friction using a metallurgy technique for the development of a new composite material. They examined density, porosity, microstructural analysis, hardness and mechanical properties using a densometer, scanning electron microscopy (SEM), hardness tester and universal testing machine. The properties of the coconut fiber composites improved from the sample with 5 % (BP2) and 10 % (BP3) when they achieved lower porosity, higher density, and higher compressive strength. The compressive strength indicates that the 10 % coconut fiber had the best strength to bear the load applications and the best ability to carry the compressive force. The microstructure showed a uniform distribution of resin and coconut fiber in the matrix. The results showed that 5 % and 10 % had better physical and mechanical properties than other formulations.

3.1.7. Palm kernel fiber

Ikpambese et al. [80] investigated the properties of asbestos-free automobile brake pad filler material produced from palm kernel fiber (PKF) (Figure 9) together with epoxy resin as a binder. They added 100 µm of PKFs in varying percentages with aluminum oxide (Al_2O_3), calcium carbonate ($CaCO_3$) and epoxy polymers and other ingredients to produce the composite. They investigated mechanical properties, physical properties, tribological properties, and microstructure analysis. The composition of 40 % of epoxy resin, 10 % of palm waste, 6 % of aluminum oxide (Al_2O_3), 29 % of graphite and 15 % of calcium carbonate ($CaCO_3$) had better properties than other compositions tested. The results show that the properties of the developed brake pad such as the coefficient of friction, temperature, wear rate, stopping time and noise level, moisture content, specific gravity hardness, surface roughness, porosity, water, and oil absorption rate were stabled with speed increased. Furthermore, the values obtained from the PKF parameters were within the standard requirements for commercial brake pad performance. The researchers' results showed that PKF can be used as a substitute filler material for asbestos brake pads, with epoxy resin as a binder.

Figure 9. Palm kernel fiber [80]

Achebe et al. [3] developed a non-asbestos brake pad material using palm kernel fiber (PKF) as an alternative filler base material in conjunction with epoxy resin as a binder. They investigated the physical and mechanical properties of the three sets of composition made using standard materials, procedures, and equipment to determine their suitability and possible performance. The results of their studied showed that sample C with 40 % PKF content with hardness 178 MPa, compressive strength 96.2 MPa, abrasion resistance 1.67 mg/m) specific gravity 1.8 g/cm3, water absorption 1.86% and oil absorption 0.89% had the best performance

rating. The sample C result was used to produce the brake pad. The results obtained were compared with other studies using common brake pads made from other material including asbestos; the result showed that hardness, wear resistance and specific gravity of the composite brake pad increased as the filler content increased, while water and oil absorption decreased as the filler content increased. This showed that palm kernel fiber is a possible alternative material for asbestos as a filler material in the production of automotive brake pads.

3.1.8. Palm slag

Ruzaidi et al. [81] used palm slag as a filler for the production of brake pads with phenolic resin as a binder. They examined properties which include hardness, compressive strength, and wear behavior of the new composite. The results showed that in the composite formulation used to produce the brake pads, palm slag has great potential to replace existing fillers.

Ruzaidi et al. [82] used palm slag (agro-waste) as filler material together with calcium carbonate (C_aCO_3) and dolomite in the brake pad material to increase the performance-to-cost ratio. Phenolic resins were used as a binder with other friction additives. They also investigated thermal properties, compressive strength, and wear behavior. The results showed that the thermal stability of the palm slag material showed a higher performance in the range of 50 °C to 1000 °C compared to the other two fillers. This showed that palm slag can be used as a substitute to the present fillers in composite formulations used to fabricate brake pads.

3.1.9. Lemon peel powder

Ramanathan et al. [83] developed and evaluated an asbestos-free brake pad using lemon peel powder as a filler material and epoxy resin as a binder. They varied the percentage of lemon peel powder, aluminum oxide, and iron oxide composition and made two samples by employing hand molding techniques. They investigated the wear rate, hardness, density, water and oil absorption of the samples produced. The results showed that the first sample with the composition of epoxy resin (40 %), Al2O3 (12.5 %), iron oxide (12.5 %), graphite (1 5%), calcium hydroxide (10 %) and lemon peel powder (10 %) had better properties than the second sample. Lemon peel powder can be used effectively as an alternative filler material for asbestos in brake pad production.

3.2. Shell waste

3.2.1. Cocoa bean shell

Olabisi et al. [84] developed an asbestos-free brake pad using pulverized cocoa bean shell (CBS) as (Figure 10) as filler and epoxy resin as a binder. The mechanical, physical, and tribological properties of the non-asbestos brake pad sample were investigated. The results showed that reducing the pulverized cocoa bean shell filler content of the brake pad increased the wear rate, tensile strength, compressive strength, at the same time as hardness, density and thermal conductivity varied differently. The friction coefficient increased with the increase in the filler wt.%. After an investigation, the outcomes of their work showed that CBS, which is an agro-waste material, can be used as a substitute for asbestos in friction lining and in the production of automotive brake pad material.

Figure 10. Cocoa beans

3.2.2. Coconut shell

Darlington et al. [6] produced an asbestos-free brake pad using coconut shell powder and palm kernel shell from locally sourced raw materials and other additives with polyester resin as a binder. They produced three different samples of brake pads in their study by varying mass compositions of coconut shell powder and palm kernel shell. The results showed that newly developed samples had a density between 2.55 g/cm3 and 2.78 g/cm3 while the commercial brake pad density was 3.36 g/cm3; the wear rate was between 0.2007 g/min and 0.2733 g/min and the commercial brake pad wear rate was 0.1873 g/min; the water absorption was between 0.0399% and 0.0522 % while the commercial pad was 0.0327 %; and, the hardness was between 3.00 and 3.41 while the commercial brake pads was 2.53. The results show that the developed brake pad cannot meet the properties of commercial brake pads due to its high density and high wear rate, but it can be used as a substitute for commercial products due to its environmentally friendly compared to the asbestos brake pad that is carcinogenic nature.

Figure 11. Coconut shell

Bashar et al. [85] produced asbestos-free brake pads using coconut shells (Figure 11) as a filler with epoxy resin as a binder matrix and other ingredients. A series of tests, including tensile, compression, hardness, impact, wear, and corrosion, were performed to determine the composition and optimum performance compared to the widely used commercial Honda brake pad (Enuco) model in Nigeria. Their results showed that a higher percentage of ground coconut shell powder gave lower breaking strength, hardness, compressive strength, and impact strength, indicating that increased coconut powder increased the brittleness of pads.

3.2.3. Palm kernel shell

Fono-Tamo [86] developed a non-asbestos brake pad used palm kernel shell (PKS) (Figure 12) as friction filler material by following the standard manufacture procedures for commercial brake pads. He evaluated the mechanical, physical, thermal and the wear characteristics of the PKS-based brake pads compared with the values of the asbestos brake pads. The properties of the PKS-based brake pad completely fulfilled the NIS 323 standard.

Ibhadode and Dagwa [8] developed asbestos-free friction lining materials using an agro-waste material based on PKS as a filler material and with phenolic resin as a binder and other components. The mechanical and physical properties of the asbestos-free pads were investigated. Among the agro-waste shells that were studied, the PKS demonstrated more favorable properties than others. The performance of the newly developed brake pad, under static and dynamic conditions, was found to be satisfactorily when compared with the asbestos-based commercial brake pad. However, more pad wear on PKS at a high vehicle speed beyond 80 km/hour was evident (Figure 13). Nevertheless, the results indicated that the palm kernel shell may be a possible alternative for friction lining material.

Figure 12. Palm kernel shells [4]

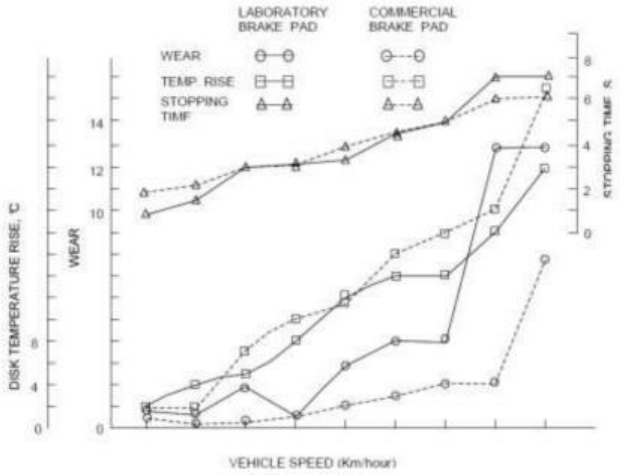

Figure 13. Comparison of laboratory and commercial brake pads under static testing [8]

Mayowa et al. [4] investigated the properties of newly developed brake pad friction material using PKS and cow bone particles as alternative brake pad formulations. The different sizes of the sieved graded palm kernel shell and cow bone were added into 60 % of epoxy resin and 10 % of hardener along with 30 % of different grade sizes at 120 µm, 100 µm and grading below 100 respectively to produce brake pad friction material. Table 8 shows the results.

Table 6. Properties of palm kernel shell and cow bone composite investigated [4]

Properties	Palm Kernel Shell (PKS)	Cow Bone
Hardness	55.7 HRB	46.0 HRB
Oil absorption	2.23 %	4.16 %
Water absorption	5.05 %	5.53 %
Density	1.2 g/cm^3	1.5 g/cm^3
Impact	1.0 J	1.5 J
Wear rate	9.57E-7 g/cm	1.44E-6 g/cm
Tensile strength	23 J/mm^2	21 J/mm^2
Coefficient of friction	0.735	0.677

The study reported that as the particle size increased, the density decreased. The result from the impact test indicated that the impact strength of the higher sieved size samples was relatively increased when compared to the finer particle size sample, and cow bone composite absorbed more water than PKS composite. From the thermogravimetric analysis (TGA) results, it was observed that as the percentage weight loss increased, the temperature also increased from 200° to 500° as the sieved size of the particle increased. All the properties investigated were within the standard requirements for brake pad production.

Samuel et al. [87] used different particle sizes of PKS to develop an asbestos-free brake pad with an idea to replace the use of asbestos-based brake pads. The PKS was sieved into grades of 100 µm, 350 µm, 710 µm and 1mm. The sieved PKS was utilized in asbestos-free brake pad production with a ratio of 35 % to 55 % PKS, 20 % resin, 10 % graphite, 15 % steel, and 0% 20 % SiC by using compression molding. They investigated properties such as hardness, density, microstructure, compressive strength, flame resistance, water, and oil absorption. The result of their study showed that the 100 µm samples of PKS offered better properties than other samples. The microstructure analysis showed that the resin in PKS was regular. Their results showed that the finer the size of the sieve particle the better the properties of the brake pad. When their result was compared with the asbestos-based commercial brake pad, the results are promising. Therefore, PKSa can be effectively used as an asbestos substitute in the production of an asbestos-free brake pad.

Fono-Tamo and Koya [88] developed asbestos-free automobile brake pad materials used factory standard procedures from PKS and more importantly its mechanical properties. The mechanical characteristics of the developed materials were evaluated. The results of developed brake pad showed hardness of 32.34 and shear strength of 40.95 MPa. At the same time, the coefficient of friction was investigated, and the result showed that the pad retained a coefficient of friction of 0.43.

Mgbemena et al. [89] developed an asbestos-free friction lining material for automobile brake pads using pulverized PKS as base filler material and spent workshop metallic cutting fillings as abrasives. Phenolic resin and alkyd resin were used as a binder material in this work. The properties of the newly developed samples of friction lining material were investigated. The thermal and friction surfaces of the samples were characterized using Simultaneous Thermal Analyzer and Optical Stereomicroscopy (ZEISS) respectively, compared to commercially available ones in the market produced by original equipment manufacturers

(OEM). It was established that pulverized PKS-based brake friction lining displayed high wear rate of 0.24 µm and high char content as compared to OEM brake lining materials with a wear rate of 0.16 µm. Also, PKS based brake friction lining demonstrated better thermal stability when it was compared to the OEM materials.

3.2.4. Cashew nut shell

Adeyemi et al. [90] produced asbestos-free automotive brake pads from a composite made of mixed agro-waste materials namely, cocoa beans shells (CBS), maize husks (MH) and palm kernel shells (PKS). The binder used was an epoxy resin. They investigated the physical, mechanical and tribological properties of the new composite. The properties of the mixed agro-waste based brake pad sample were compared with those made of single filler materials such as cocoa beans shell (CBS) based sample pads and maize husks (MH) based sample pads. The result of the analysis showed that as matrix wt.% formulation increased, the friction coefficient, abrasion resistance, and water soak decreased, while the tensile strength and compressive strength increased. However, the density, hardness, thermal conductivity, and oil soak varied inconsistently. The results showed that mixed agro-waste (CBS+MH+PKS) particles can be used effectively as an alternative filler material for asbestos brake pad friction materials.

3.3. Animal Waste

3.3.1. Periwinkle shell

Aku et al. [91] used spectroscopic and wear analysis to investigate the characterization of the periwinkle shell (Figure 14) as asbestos-free brake pad material. The experiment was carried out by using X-ray diffractometer (XRD), thermogravimetric analysis (TGA/DTA), Fourier-transform infrared spectrometry (FTIR), and X-ray fluorescent spectrometry (XRF). They investigated the density, hardness values and wear rate of the periwinkle shell. Their results were compared with asbestos commonly used in the production of brake pads. The results confirmed that periwinkle shell can be used as an alternative material for brake pad production.

Yakubu et al. [92] developed a brake pad using periwinkle shell particles (PSP) as a filler to replace asbestos and investigated thermoset resin as a binder. They varied the PSP size from 710 µm-125 µm and analyzed the wear test, surface morphology, and thermal analysis of the samples. Their results showed that the periwinkle shell particles (PSP) size decreased from 710 µm-125 µm which showed a good interfacial bonding. The wear rate of the brake pad increased as the load and the particle size of the periwinkle shell increased. The coefficient of friction of the developed brake pad was in the same range as the automobile brake pad standard. The PSP had a higher temperature of maximal decomposition than asbestos which showed that PSP can withstand higher temperatures than asbestos. The results of this research work showed that PSP can be successfully used as an alternate filler material instead of asbestos in brake pad production.

Yawas et al. [93] produced brake pads from periwinkle shells as a filler material with phenolic resin as a binder. Five sets of brake pads were produced by using compressive molding with a different sieve size of periwinkle shells (710 µm to 125 µm) with 35 % resin. They evaluated mechanical, physical and tribological properties of the periwinkle shells-based brake pad and compared the values with asbestos brake pads. In their work, they determined the properties and morphology of developing a PSP asbestos-free brake pad and its material was characterized. The results of their research showed that the compressive strength, hardness, and density of the newly developed brake pad samples increased when the particle size of periwinkle shell decreased from 710 µm to 125 µm, whereas the water soak, oil soak and wear rate decreased when the periwinkle shell particle size decreased. The research results indicated that periwinkle shells can be used as a replacement filler material for asbestos in brake pad manufacture.

Figure 14. Periwinkle shell

3.3.2. Snail shell

Abhulimen and Orumwense [94] developed an asbestos-free automotive brake pad with a view to replacing the use of asbestos, snail shell was used as a reinforcement material, while rubber seed husk was used as frictional filler material and epoxy resin as a binder. The pulverized snail shells were sieved into grades of 125 µm, 250 µm, 355 µm, 500 µm, and 710 µm. The composite brake pad was developed in the ratio of 65 v% snail shell, 10 v% rubber seed husk and 25 v% resin by using compression molding. They investigated the characterization of the snail shell through XRD, XRF, differential thermal analysis (DTA), and TGA. They then investigated the properties of the developed brake pad such as density, compressive strength coefficient of friction, hardness, abrasion resistance, and porosity. The microstructure showed equal distribution of the resin in the snail shell, and the results showed that the 125 µm grade of sieved snail shell revealed the best properties. When the results were compared with common asbestos-based brake pads they found that the effect of the developed brake pad was more favorable than the asbestos brake pad. This outcome of the work confirmed that snail shells and rubber seed husk can be used to produce alternative brake pads.

4. RESULTS AND CONCLUSION

This paper studied different agricultural wastes as an alternative to asbestos brake pads. The results show that the performance of the waste materials was almost the same as the asbestos brake pads but without any of the health issues and environmental impact. Brake pad production from biomass materials to substitute asbestos brake pad materials has become the center of research in laboratories, and many studies and investigations are ongoing, although the results from these studies have not yet been translated into commercial applications. Similarly, it is necessary to utilize the combinations of biomass materials at different ratios to further study their effects on the physical, mechanical and tribological properties of brake pad production using these various mixtures. The mechanical and physical properties of the composites are affected by the filler content. In general, studies so far have found that as the composite filler content of the material decreases the properties such as thermal conductivity, hardness, compressive strength and tensile strength of the composite brake pad increase, while the density, water, and oil absorption of the brake pad increases when the filler content of the composite increases.

The studies by Ikpambese et al. [80] and Ibhadode and Dagwa [8] reported that an increase in speed of a vehicle results in an increase in contact pressure between the brake pads and rotor, consequently increasing the wear rate. Table 3 shows the characteristics of the environmentally friendly brake pads manufactured from PKS and PKF. From these studies, it is evident that

brake pads using palm kernel fiber (PKF) had a higher wear rate, while the brake pads using palm kernel shell (PKS) had a low friction coefficient.

The mechanical, physical and tribological properties of these brake pads developed from agro-waste biomass materials had certain advantages compared to commercial brake pads. The results obtained from this laboratory work tackles the existing gap in the production of the environmental-friendly and cheap brake pads. Agricultural waste may be effectively used as an alternative component in the production of brake pads when properly used in conjunction with other additives to accommodate the good performance of the brake pads. Then again, concerning their low thermal stability, they should always be considered carefully. In conclusion, an exciting point of these materials is that biomass demonstrates good mechanical properties. Increased use of biomass composites product is expected to have a certain ripple effect in the agricultural sector.

In brake pad applications, the wear resistance improved with the addition of natural fibers as a filler to the friction formulation. Normal load and speed have a significant effect on the wear rate of the brake pad composite. The finer the size of the sieve, the better its properties. The small particle size of natural fibers had a positive result on the composite wear rate. The coefficient of friction result was within the recommended standard for brake pad formulation. Physical and chemical treatments can be used to overcome poor wettability as well as a natural fiber with higher moisture absorption.

Agricultural waste has been used as prospect reinforcement materials for a wide range of applications including brake pad production. The good thing about these materials is that they are waste biomass and present good mechanical properties.

REFERENCES

[1] E. Ishidi, I. Adamu, E. Kolawale, K. Sunmonu, and M. Yakubu, "Morphology and Thermal Properties of Alkaline Treated Palm Kernel Nut Shell–HDPE Composites," *Journal of Emerging Trends in Engineering and Applied Sciences (JETEAS),* vol. 2, pp. 346-350, 2011.

[2] Z. Leman, S. Sapuan, A. Saifol, M. Maleque, and M. Ahmad, "Moisture absorption behavior of sugar palm fiber reinforced epoxy composites," *Materials & Design,* vol. 29, pp. 1666-1670, 2008.

[3] C. Achebe, J. Chukwuneke, F. Anene, and C. Ewulonu, "A retrofit for asbestos-based brake pad employing palm kernel fiber as the base filler material," *Proceedings of the Institution of Mechanical Engineers, Part L: Journal of Materials: Design and Applications,* p. 1464420718796050, 2018.

[4] M. Afolabi, O. Abubakre, S. Lawal, and A. Raji, "Experimental investigation of palm kernel shell and cow bone reinforced polymer composites for brake pad production," *International Journal of Chemistry and Materials Research,* vol. 3, pp. 27-40, 2015.

[5] R. U. Rao and G. Babji, "A Review paper on alternate materials for Asbestos brake pads and its characterization," *International Research Journal of Engineering and Technology,* vol. 2, pp. 556-562, 2015.

[6] D. Egeonu and C. O. P. Okolo, "Production of Eco-Friendly Brake Pad Using Raw Materials Sourced Locally In Nsukka."

[7] F. Onyeneke, J. Anaele, and C. Ugwuegbu, "Production of Motor Vehicle Brake Pad Using Local Materials (Perriwinkle and Coconut Shell)," *The International Journal Of Engineering And Science (IJES) in,* 2014.

[8] A. O. A. Ibhadode and I. M. Dagwa, "Development of asbestos-free friction lining material from palm kernel shell," *J. Braz. Soc. Mech. Sci. Eng.,* vol. 1, pp. 1-2, 2008.

[9] Z. Fu, B. Suo, R. Yun, Y. Lu, H. Wang, S. Qi, *et al.*, "Development of eco-friendly brake friction composites containing flax fibers," *Journal of Reinforced Plastics and Composites,* vol. 31, pp. 681-689, 2012.

[10] U. Idris, V. Aigbodion, I. Abubakar, and C. Nwoye, "Eco-friendly asbestos free brake-pad: Using banana peels," *Journal of King Saud University-Engineering Sciences,* vol. 27, pp. 185-192, 2015.

[11] S. Nagesh, C. Siddaraju, S. Prakash, and M. Ramesh, "Characterization of brake pads by variation in composition of friction materials," *Procedia Materials Science,* vol. 5, pp. 295-302, 2014.

[12] P. K. Bajpai, I. Singh, and J. Madaan, "Tribological behavior of natural fiber reinforced PLA composites," *Wear,* vol. 297, pp. 829-840, 2013/01/15/ 2013.

[13] P. L. Menezes, P. K. Rohatgi, and M. R. Lovell, "Studies on the tribological behavior of natural fiber reinforced polymer composite," in *Green Tribology*, ed: Springer, 2012, pp. 329-345.

[14] F. M. Al-Oqla, S. M. Sapuan, M. R. Ishak, and A. A. Nuraini, "A Model for Evaluating and Determining the Most Appropriate Polymer Matrix Type for Natural Fiber Composites," *International Journal of Polymer Analysis and Characterization,* vol. 20, pp. 191-205, 2015/04/03 2015.

[15] M. Carus, A. Eder, L. Dammer, H. Korte, L. Scholz, R. Essel, *et al.*, "Wood-Plastic Composites (WPC) and Natural Fibre Composites (NFC)," *Nova-Institute: Hürth, Germany,* p. 16, 2015.

[16] A. Shalwan and B. F. Yousif, "In State of Art: Mechanical and tribological behaviour of polymeric composites based on natural fibres," *Materials & Design,* vol. 48, pp. 14-24, 2013/06/01/ 2013.

[17] M. Jawaid and H. A. Khalil, "Effect of layering pattern on the dynamic mechanical properties and thermal degradation of oil palm-jute fibers reinforced epoxy hybrid composite," *BioResources,* vol. 6, pp. 2309-2322, 2011.

[18] S. Kalia, B. Kaith, and I. Kaur, "Pretreatments of natural fibers and their application as reinforcing material in polymer composites—a review," *Polymer Engineering & Science,* vol. 49, pp. 1253-1272, 2009.

[19] T. Väisänen, A. Haapala, R. Lappalainen, and L. Tomppo, "Utilization of agricultural and forest industry waste and residues in natural fiber-polymer composites: A review," *Waste Management,* vol. 54, pp. 62-73, 2016.

[20] S. Kalia, A. Dufresne, B. M. Cherian, B. Kaith, L. Avérous, J. Njuguna, *et al.*, "Cellulose-based bio-and nanocomposites: a review," *International Journal of Polymer Science,* vol. 2011, 2011.

[21] X. Li, L. G. Tabil, and S. Panigrahi, "Chemical treatments of natural fiber for use in natural fiber-reinforced composites: a review," *Journal of Polymers and the Environment,* vol. 15, pp. 25-33, 2007.

[22] K. Pickering, *Properties and performance of natural-fibre composites*: Elsevier, 2008.

[23] M. J. John and R. D. Anandjiwala, "Recent developments in chemical modification and characterization of natural fiber- reinforced composites," *Polymer composites,* vol. 29, pp. 187-207, 2008.

[24] P. Kumar, D. M. Barrett, M. J. Delwiche, and P. Stroeve, "Methods for pretreatment of lignocellulosic biomass for efficient hydrolysis and biofuel production," *Industrial & engineering chemistry research,* vol. 48, pp. 3713-3729, 2009.

[25] S. K. Majhi, S. K. Nayak, S. Mohanty, and L. Unnikrishnan, "Mechanical and fracture behavior of banana fiber reinforced Polylactic acid biocomposites," *International Journal of Plastics Technology,* vol. 14, pp. 57-75, 2010.

[26] M. Jawaid and H. A. Khalil, "Cellulosic/synthetic fibre reinforced polymer hybrid composites: A review," *Carbohydrate polymers,* vol. 86, pp. 1-18, 2011.

[27] T. Gorshkova, N. Brutch, B. Chabbert, M. Deyholos, T. Hayashi, S. Lev-Yadun*, et al.*, "Plant fiber formation: state of the art, recent and expected progress, and open questions," *Critical Reviews in Plant Sciences,* vol. 31, pp. 201-228, 2012.

[28] H. A. Khalil, A. Bhat, and A. I. Yusra, "Green composites from sustainable cellulose nanofibrils: A review," *Carbohydrate Polymers,* vol. 87, pp. 963-979, 2012.

[29] H. A. Khalil, S. Hanida, C. Kang, and N. N. Fuaad, "Agro-hybrid composite: the effects on mechanical and physical properties of oil palm fiber (EFB)/glass hybrid reinforced polyester composites," *Journal of Reinforced Plastics and Composites,* vol. 26, pp. 203-218, 2007.

[30] K. Anigo, B. Dauda, A. Sallau, and I. Chindo, "Chemical composition of kapok (Ceibapentandra) seed and physicochemical properties of its oil," *Nigerian Journal of Basic and Applied Sciences,* vol. 21, pp. 105-108, 2013.

[31] S. Chaiarrekij, A. Apirakchaiskul, K. Suvarnakich, and S. Kiatkamjornwong, "Kapok I: characteristcs of Kapok fiber as a potential pulp source for papermaking," *BioResources,* vol. 7, pp. 0475-0488, 2011.

[32] N. Reddy and Y. Yang, "Biofibers from agricultural byproducts for industrial applications," *TRENDS in Biotechnology,* vol. 23, pp. 22-27, 2005.

[33] J. Guimarães, E. Frollini, C. Da Silva, F. Wypych, and K. Satyanarayana, "Characterization of banana, sugarcane bagasse and sponge gourd fibers of Brazil," *Industrial Crops and Products,* vol. 30, pp. 407-415, 2009.

[34] P. Preethi and G. Balakrishna Murthy, "Physical and chemical properties of banana fibre extracted from commercial banana cultivars grown in Tamilnadu State," *Agrotechnol S11,* vol. 8, 2013.

[35] A. Leão, S. M. Sartor, and J. C. Caraschi, "Natural fibers based composites–technical and social issues," *Molecular Crystals and Liquid Crystals,* vol. 448, pp. 161/[763]-177/[779], 2006.

[36] B. Wahlang, K. Nath, U. Ravindra, R. Chandu, and K. Vijayalaxmi, "Processing and utilization of sugarcane bagasse for functional food formulations," in *Proceedings of the International Conference and Exhibition on Food Processing and Technology*, 2012, pp. 106-112.

[37] A. Hemmasi, A. Samariha, A. Tabei, M. Nemati, and A. Khakifirooz, "Study of morphological and chemical composition of fibers from Iranian sugarcane bagasse," *American-Eurasian J. Agric. & Environ. Sci,* vol. 11, pp. 478-481, 2011.

[38] M. E. S. Pardo, M. E. R. Cassellis, R. M. Escobedo, and E. J. García, "Chemical characterisation of the industrial residues of the pineapple (Ananas comosus)," *Journal of Agricultural Chemistry and Environment,* vol. 3, p. 53, 2014.

[39] H. A. Khalil, A. I. Yusra, A. Bhat, and M. Jawaid, "Cell wall ultrastructure, anatomy, lignin distribution, and chemical composition of Malaysian cultivated kenaf fiber," *Industrial Crops and Products,* vol. 31, pp. 113-121, 2010.

[40] M. Thiruchitrambalam, A. Alavudeen, and N. Venkateshwaran, "Review on kenaf fiber composites," *Rev. Adv. Mater. Sci,* vol. 32, pp. 106-111, 2012.

[41] X. Zhao, L. Zhang, and D. Liu, "Biomass recalcitrance. Part I: the chemical compositions and physical structures affecting the enzymatic hydrolysis of lignocellulose," *Biofuels, Bioproducts and Biorefining,* vol. 6, pp. 465-482, 2012.

[42] K. G. Satyanarayana, G. G. Arizaga, and F. Wypych, "Biodegradable composites based on lignocellulosic fibers—An overview," *Progress in polymer science,* vol. 34, pp. 982-1021, 2009.

[43] G. Cicala, G. Cristaldi, G. Recca, and A. Latteri, "Composites based on natural fibre fabrics," in *Woven fabric engineering*, ed: InTech, 2010.

[44] H. Yan-hui, F. Ben-hua, Y. Yan, and Z. Rong-jun, "Plant age effect on mechanical properties of moso bamboo (Phyllostachys heterocycla var. pubescens) single fibers," *Wood and Fiber Science,* vol. 44, pp. 196-201, 2012.

[45] H. A. Khalil, M. Jawaid, A. Hassan, M. Paridah, and A. Zaidon, "Oil palm biomass fibres and recent advancement in oil palm biomass fibres based hybrid biocomposites," in *Composites and their applications*, ed: InTech, 2012.

[46] M. J. John and S. Thomas, "Biofibres and biocomposites," *Carbohydrate polymers,* vol. 71, pp. 343-364, 2008.

[47] H. Abdul Khalil, M. Siti Alwani, R. Ridzuan, H. Kamarudin, and A. Khairul, "Chemical composition, morphological characteristics, and cell wall structure of Malaysian oil palm fibers," *Polymer-Plastics Technology and Engineering,* vol. 47, pp. 273-280, 2008.

[48] C. Ververis, K. Georghiou, N. Christodoulakis, P. Santas, and R. Santas, "Fiber dimensions, lignin and cellulose content of various plant materials and their suitability for paper production," *Industrial crops and products,* vol. 19, pp. 245-254, 2004.

[49] K. Liu, H. Takagi, R. Osugi, and Z. Yang, "Effect of lumen size on the effective transverse thermal conductivity of unidirectional natural fiber composites," *Composites Science and Technology,* vol. 72, pp. 633-639, 2012.

[50] M. S. Alwani, H. A. Khalil, N. Islam, O. Sulaiman, A. Zaidon, and R. Dungani, "Microstructural study, tensile properties, and scanning electron microscopy fractography failure analysis of various agricultural residue fibers," *Journal of Natural Fibers,* vol. 12, pp. 154-168, 2015.

[51] M. Sumaila, I. Amber, and M. Bawa, "Effect of fiber length on the physical and mechanical properties of ramdom oriented, nonwoven short banana (musabalbisiana) fiber/epoxy composite," *Cellulose,* vol. 62, p. 64, 2013.

[52] M. Sakthivel and S. Ramesh, "Mechanical properties of natural fiber (banana, coir, sisal) polymer composites," *Science park,* vol. 1, pp. 1-6, 2013.

[53] C. Driemeier, W. D. Santos, and M. S. Buckeridge, "Cellulose crystals in fibrovascular bundles of sugarcane culms: orientation, size, distortion, and variability," *Cellulose,* vol. 19, pp. 1507-1515, 2012.

[54] M. Rodriguez, A. Rodriguez, J. Bayer, F. Vilaseca, J. Girones, and P. Mutje, "Determination Of Corn Stalk Fibers'strength Through Modeling Of The Mechanical Properties Of Its Composites," *BioResources,* vol. 5, pp. 2535-2546, 2010.

[55] K. Vijayalakshmi, C. Y. Neeraja, A. Kavitha, and J. Hayavadana, "Abaca fibre," *Transactions on Engineering and Sciences,* vol. 2, pp. 16-19, 2014.

[56] C. Alves, M. Freitas, A. Silva, S. Luz, and D. Alves, "Sustainable design procedure: the role of composite materials to combine mechanical and environmental features for agricultural machines," *Materials & Design,* vol. 30, pp. 4060-4068, 2009.

[57] U. Bongarde and V. Shinde, "Review on natural fiber reinforcement polymer composites," *International Journal of Engineering Science and Innovative Technology,* vol. 3, pp. 431-436, 2014.

[58] M. Bouasker, N. Belayachi, D. Hoxha, and M. Al-Mukhtar, "Physical characterization of natural straw fibers as aggregates for construction materials applications," *Materials,* vol. 7, pp. 3034-3048, 2014.

[59] N. Reddy and Y. Yang, "Properties of high-quality long natural cellulose fibers from rice straw," *Journal of agricultural and food chemistry,* vol. 54, pp. 8077-8081, 2006.

[60] L. Mwaikambo and M. Ansell, "The determination of porosity and cellulose content of plant fibers by density methods," *Journal of materials science letters,* vol. 20, pp. 2095-2096, 2001.

[61] S. Chaiarrekij, A. Apirakchaiskul, K. Suvarnakich, and S. Kiatkamjornwong, "Characteristcs of Kapok fiber as a potential pulp source for papermaking," *BioResources,* vol. 7, pp. 0475-0488, 2011.

[62] M. Soiela, A. Ilves, A. Viikna, and E. Erberg, "Properties of flax fiber-reinforced polyethylene films," *Cheminë technologija,* vol. 36, pp. 38-45, 2005.

[63] S. S. Munawar, K. Umemura, and S. Kawai, "Characterization of the morphological, physical, and mechanical properties of seven nonwood plant fiber bundles," *Journal of Wood Science,* vol. 53, pp. 108-113, 2007.

[64] M. Paridah and A. Khalina, "Effects of soda retting on the tensile strength of kenaf (Hibiscus cannobnius L.) bast fibres," *Project Report Kenaf EPU,* vol. 21, 2009.

[65] A. Rathod and A. Kolhatkar, "Analysis of physical characteristics of bamboo fabrics," *International Journal of Research in Engineering and Technology,* vol. 3, pp. 21-25, 2014.

[66] J. Biagiotti, S. Fiori, L. Torre, M. López- Manchado, and J. M. Kenny, "Mechanical properties of polypropylene matrix composites reinforced with natural fibers: a statistical approach," *Polymer composites,* vol. 25, pp. 26-36, 2004.

[67] D. Puglia, J. Biagiotti, and J. Kenny, "A review on natural fibre-based composites—Part II: Application of natural reinforcements in composite materials for automotive industry," *Journal of Natural Fibers,* vol. 1, pp. 23-65, 2005.

[68] P. W. Lee and P. Filip, "Friction and wear of Cu-free and Sb-free environmental friendly automotive brake materials," *Wear,* vol. 302, pp. 1404-1413, 2013/04/01/ 2013.

[69] V. Matějka, Z. Fu, J. Kukutschová, S. Qi, S. Jiang, X. Zhang, *et al.*, "Jute fibers and powderized hazelnut shells as natural fillers in non-asbestos organic non-metallic friction composites," *Materials & Design,* vol. 51, pp. 847-853, 2013.

[70] P. W. Lee, *Design and optimization of low-copper and copper-free automotive brake friction materials*: Southern Illinois University at Carbondale, 2013.

[71] A. Bledzki, P. Franciszczak, Z. Osman, and M. Elbadawi, "Polypropylene biocomposites reinforced with softwood, abaca, jute, and kenaf fibers," *Industrial Crops and Products,* vol. 70, pp. 91-99, 2015.

[72] N. A. Ademoh and A. I. Olabisi, "Development and evaluation of maize husks (asbestos-free) based brake pad," *Development,* vol. 5, 2015.

[73] W. ASOTAH and A. ADELEKE, "Development of asbestos free brake pads using corn husks," *Leonardo Electronic Journal of Practices and Technologies,* pp. 129-144, 2017.

[74] V. Aigbodion, U. Akadike, S. Hassan, F. Asuke, and J. Agunsoye, "Development of asbestos-free brake pad using bagasse," *Tribology in industry,* vol. 32, pp. 12-17, 2010.

[75] S. K. Acharya, P. Mishra, and S. K. Mehar, "Effect of surface treatment on the mechanical properties of bagasse fiber reinforced polymer composite," *BioResources,* vol. 6, pp. 3155-3165, 2011.

[76] S. A. Bahari, K. H. Isa, M. A. Kassim, Z. Mohamed, and E. A. Othman, "Investigation on hardness and impact resistance of automotive brake pad composed with rice husk dust," in *AIP Conference Proceedings 2nd*, 2012, pp. 155-161.

[77] V. F. Swamidoss and Prasanth, "Fabrication And Characterization Of Brake Pad Using Pineapple Leaf Fiber (Palf)," *International Journal Of Research In Computer Applications And Robotics,* vol. 3, p. 5, March 2015.

[78] S. A. Bahari, M. S. Chik, M. A. Kassim, C. M. Som Said, M. I. Misnon, Z. Mohamed, *et al.*, "Frictional and heat resistance characteristics of coconut husk particle filled automotive brake pad," in *American Institute of Physics Conference Series*, 2012, pp. 162-168.

[79] M. Maleque, A. Atiqah, R. Talib, and H. Zahurin, "New natural fibre reinforced aluminium composite for automotive brake pad," *International journal of mechanical and materials engineering,* vol. 7, pp. 166-170, 2012.

[80] K. Ikpambese, D. Gundu, and L. Tuleun, "Evaluation of palm kernel fibers (PKFs) for production of asbestos-free automotive brake pads," *Journal of King Saud University-Engineering Sciences,* vol. 28, pp. 110-118, 2016.

[81] C. M. R. Ghazali, H. Kamarudin, S. B. Jamaludin, and M. Abdullah, "Comparative study on thermal, compressive, and wear properties of palm slag brake pad composite with other fillers," in *Advanced Materials Research*, 2011, pp. 1636-1641.

[82] C. M. R. Ghazali, H. Kamarudin, J. Shamsul, M. Abdullah, and A. Rafiza, "Mechanical properties and wear behavior of brake pads produced from palm slag," in *Advanced Materials Research*, 2012, pp. 26-30.

[83] K. Ramanathan, P. Saravanakumar, S. Ramkumar, P. P. kumar, and S. R. Surender, "Development of Asbestos-Free Brake Pads: Using Lemon Peel Powder," *International Journal of Innovative Research in Science, Engineering and Technology,* vol. 6, p. 7, March 2017.

[84] A. I. Olabisi, A. N. Adam, and O. M. Okechukwu, "Development and assessment of composite brake pad using pulverized cocoa beans shells filler," *International Journal of Materials Science and Applications,* vol. 5, pp. 66-78, 2016.

[85] D.-A. Bashar, P. B. MADAKSON, and J. MANJI, "Material selection and production of a cold-worked composite brake pad," *World Journal of Engineering and Pure & Applied Sciences,* vol. 2, p. 92, 2012.

[86] Fono-Tamo and R. Sephyrin, "Agro-Waste Based Friction Material for Automotive Application," 2014.

[87] Z. Elakhame, O. Alhassan, and A. Samuel, "Development and production of brake pads from palm kernel shell composites," *International Journal of Scientific & Engineering Research,* vol. 5, pp. 735-744, 2014.

[88] R. Fono-Tamo and O. Koya, "Evaluation of mechanical characteristics of friction lining from agricultural waste," *International Journal of Advancements in Research & Technology,* vol. 2, pp. 1-5, 2013.

[89] C. O. Mgbemena, C. E. Mgbemena, and M. O. Okwu, "Thermal stability of pulverized palm kernel shell (PKS) based friction lining material locally developed from spent waste."

[90] I. O. Adeyemi, "Development of Asbestos-Free Automotive Brake Pad Using Ternary Agro-Waste Fillers," *Development,* vol. 3, 2016.

[91] S. Aku, D. Yawas, P. Madakson, and S. Amaren, "Characterization of periwinkle shell as asbestos-free brake pad materials," *The Pacific Journal of Science and Technology,* vol. 13, pp. 57-63, 2012.

[92] A. S. Yakubu, S. Amaren, and Y. D. Saleh, "Evaluation of the wear and thermal properties of asbestos free brake pad using periwinkles shell particles," *Usak University Journal of Material Sciences,* vol. 2, pp. 99-108, 2013.

[93] D. Yawas, S. Aku, and S. Amaren, "Morphology and properties of periwinkle shell asbestos-free brake pad," *Journal of King Saud University-Engineering Sciences,* vol. 28, pp. 103-109, 2016.

[94] E. Abhulimen and F. Orumwense, "Characterization and Development of Asbestos Free Brake Pad, using Snail Shell and Rubber Seed Husk," *African Journal of Engineering Research,* vol. 5, pp. 24-34, 2017.

CHAPTER 3: EFFECTS OF FIBER, FILLERS AND BINDERS ON AUTOMOBILE BRAKE PAD PERFORMANCE

To cite this article: O. E. Ige, F. L. Inambao, and G. A. Adewumi, "Effects of Fiber, Fillers and Binders on Automobile Brake Pad Performance: A Review," *International Journal of Mechanical Engineering and Technology,* vol. 10, no. 6, pp. 135-150, 2019.

International Journal of Mechanical Engineering and Technology (IJMET)
Volume 10, Issue 06, June 2019, pp. 135-150, Article ID: IJMET_10_06_008
Available online at http://www.iaeme.com/ijmet/issues.asp?JType=IJMET&VType=10&IType=6
ISSN Print: 0976-6340 and ISSN Online: 0976-6359

EFFECTS OF FIBER, FILLERS AND BINDERS ON AUTOMOBILE BRAKE PAD PERFORMANCE: A REVIEW

Oluwafemi E. Ige*, Freddie L. Inambao and Gloria A. Adewumi
Department of Mechanical Engineering
School of Engineering, University of KwaZulu-Natal, Durban, South Africa
*Corresponding Author

ABSTRACT

Natural waste has been used to produce fillers and fibers, including palm kernel shell and fiber, groundnut shell, maize husk, rice straw and husk, jute, coconut shell, cotton, and cellulose. This review work seeks to explore research using combinations of fillers and fibers at different ratios with a view to further studying their effects on brake pad properties using various mixtures for the production. The influence of different binders such as phenolic resin, epoxy resin and others were also investigated.

Composite materials from fiber and fillers have been seen to improve composite mechanical properties, reduce costs and increase impact strength. The choice of fiber, filler, binder, particle size and composition play important responsibility in the composite of the brake pad performance. In order to obtain better physical properties, palm kernel fiber and coconut fiber brake pads were studied and the composition percentage was optimized.

Key words: Asbestos, binder, fiber, filler, epoxy, phenolic

Cite this Article: Oluwafemi E. Ige, Freddie L. Inambao and Gloria A. Adewumi, Effects of Fiber, Fillers and Binders on Automobile Brake Pad Performance: A Review. *International Journal of Mechanical Engineering and Technology* 10(6), 2019, pp. 135-150.
http://www.iaeme.com/IJMET/issues.asp?JType=IJMET&VType=10&IType=6

1. INTRODUCTION

In recent decades the production of composite materials has grown significantly worldwide, which means many industries and technology sectors are using polymer composite materials to successfully replace traditional composite materials [1]. The investigation of new materials, especially agricultural waste as a filler material, is providing new and low-cost materials for development of brake pads which are commercially viable and environmentally acceptable and which have all the required properties. Brake pads are used to control the speed of a vehicle via the braking system [2]. Friction materials in braking application systems are

considered as the most important sections in a vehicle performance. The brake pad material must be able to sustain a higher and uniform coefficient of friction alongside the brake disc.

In the last two decades, asbestos materials have been employed in brake pad production. Recently, uses of asbestos materials have been prevented due to their carcinogenic properties and their danger to human health. This has led to the necessity of finding suitable alternative materials to make non-carcinogenic brake pads [3]. A lot of research has been conducted to develop brake pads using different agricultural residues or wastes. Because of current regulations, research on eco-friendly brake friction materials is very important. The objectives for using alternative filler materials for brake pads are to moderate the potentially destructive components used in the brake pad material formulation whereas reducing the brake pad wear rate and maintaining friction properties.

According to Lee and Filip [4], reducing the wear rate of a material also reduces the environmental impact. Saffar and Shojaei [5] stated that over 100 components are used in automotive friction materials. Most commercial automotive brake pad friction materials contain multiple components [6-8] and divided into four groups: fibers, fillers, binders, and friction modifiers. Fibers provide mechanical strength in the composition. Friction modifiers influences the brake pads frictional properties and contain a mixture of abrasive as well as lubricants.

Filler materials are mainly used for brake pad production to improve brake manufacturability and reduce production costs and as functional modifiers. A small amount of filler is usually added to improve or optimize performance of bake pad material. Harder particles, for instance Al_2O_3 is added to increase the COF (μ) which is the force of friction caused by the scraping the surface of the material and the disc [9].

Binders hold all the components together in the brake pad application, thereby reducing the component shear rate [10]. Binder contribute to the brake pad friction and wear rate [11]. The binder offers mechanical unity to the friction materials by firmly combining the other three components in order to improve the composites properties. In the past fifty years, phenolic resins (unmodified or modified) have been employed as binders in the preparation of the friction materials due to their good thermal and mechanical properties in addition to lower costs [12].

In this review paper the effects of different natural fibers, fillers and binders such as phenolic and epoxy resin on the performance of non-asbestos brake pad material are studied and compared with asbestos brake pad.

2. LITERATURE REVIEW

Over the past ten years, researchers have tried a number of investigations and new ways to innovate new brake pad material. Adegbola et al. [13] used 65% cow bone particles with 35% phenolic resin as a binder to develop composite material for brake pad application using a compressive moulding process. There was a significant increase in interfacial bonding as the size of the cow bone particle decreased from 850 μm to 250 μm. The mechanical properties of the sample with 250 μm particle size were improved. From the experimental result it was evident that as the cow bone increased the wear rate increased, while the density and hardness of the brake pad decreased. The friction co-efficient result was within normal automobile brake pads standard. Therefore, cow bones particles are a suitable substitute for asbestos brake pads. Achebe et al. [14] examined the properties of an asbestos-free automobile brake pad developed with palm kernel fiber (PKF) as filler material combined with epoxy resin as a binder. They produced three sets of composition with procedures, equipment and standard materials to decide their possible performance. From the result the hardness, and specific gravity of the brake pad sample were increased as the filler content increased, showing that

PKF can be used as a filler material and also as a substitute material for manufacture of the asbestos brake pad. Aigbodion et al. [15] produced non-asbestos brake pads using bagasse and phenolic resin was used as binder to substitute asbestos brake pads which are carcinogenic. From the results it showed that bagasse can be used as an asbestos substitute in the manufacture of brake pads by using 100 µm sieve of bagasse grade with 70 % and 30 % composition of resin. They investigated its mechanical, physical and tribological properties. Microstructural results showed that resin was uniform in the bagasse distribution. Their results showed that, as the sieve grade of bagasse increased, the hardness, density and compressive strength of the developed samples decreased whereas the wear rate increased as bagasse sieve grade size increased. The finer sieve particle size of the brake pad material resulted in better properties. The results showed that by using bagasse of 100 µm sieve grade with 70 % and 30 % composition of resin, bagasse can be employed as a substitute for the production of asbestos-free brake pads.

Kim et al. [16] investigated the friction composite material performance with cashew nut-shell liquid (CNSL) and potassium titanate with phenolic resin as a binder. They evaluated friction properties using an organic formulation. They suggested that brake pad composites that can be compressed with a low hardness and high porosity which tends to lower the noise propensity. The result indicated that the resin increased the COF during sliding but showed high noise propensity. The phenolic resin improved the wear rate of the friction material whereas both CNSL and potassium titanate failed to improve wear resistance. Acharya and Samantrai [17] investigated the wear rate and friction coefficient properties of rice husk and epoxy resin matrix as a binder using pin on-disc apparatus to study the wear rate of rice husk composites reinforced with 5 wets %, 10 wets %, 15 wet %, 20 wet %. The morphological properties of the composites were analysed using a scanning electron microscope (SEM). During the testing conditions, the result showed that wear rates decreased as the rice husk fiber increased. The positive effect of rice husk reinforcement reflected the improvement of the tribological properties of the epoxy composite. Bashar et al. [18] used coconut shells as a filler to produced asbestos-free brake pads with other constituents and used epoxy resin as binder matrix. They conducted several tests to investigate the composition and optimal performance compared to the Honda (Enuco) model brake pad made in Nigeria. The results showed that a high percentage of ground CS powder provided hardness, low breaking strength, impact strength and compressive strength, indicating that CS powder increased the brittleness of the pads. Ahmed et al. [19] developed an asbestos free break-pad using watermelon peels together with a pure water sachet as a binder. The preparation of the brake pad was accomplished by varying the resin (pure water sachet) from 5 wt% to 30 wt%. The properties of the sample developed were tested. The result of their work showed that, the hardness, specific gravity and compressive strength of developed samples increased as the wt% of the resin increased. Good bonding was showed with addition of 25 wt% resin in asbestos-free brake pads production. This work showed that watermelon peels particles can be utilised as a suitable substitute for asbestos material in the production brake pads.

Olabisi et al. [20] used pulverized cocoa beans shells (CBS) as filler material with epoxy resin as a binder to produced asbestos-free brake pads. They investigated the properties of the sample produced. After an investigation, the outcomes of the work showed that cocoa beans shells (CBS) can be used as a substitute for asbestos filler material in friction lining of automotive brake pads production. The result showed that the wear rate, tensile strength, and compressive strength increased as the CBS filler content of the brake pad decreased, while the COF of brake pad sample increased as the weight percentage filler content increased. This showed that CBS as a filler can be employed as alternative for asbestos friction lining material and for production of automotive brake pads. Cho et al. [21] investigated the effects of 16 ingredients such as cashew nuts, phenolic resin as a binder and another 14 constituents such

as rock wool aramid fiber, magnesium, potassium titanate, Ca (OH) 2, graphite, rubber, Fe3O4, ZrSiO4, MoS2, CU chip, Boso4, sb2s3 and stone on the properties of friction materials. The results indicated that the COP of the sample increased with an increase in phenolic resin. The friction material physical properties affected the characteristics of the friction. In spite of this, the morphology of the constituents also affected the friction performance strongly. Ademoh and Olabisi [22] produced brake pads using maize husks as a filler with epoxy resin as a binder. They studied the properties of the sample, namely, mechanical, physical and tribological. It was noted that when the wt% of MH filler content in the sample decreased, the wear rate, hardness, compressive strength, and tensile strength, increased while density and friction coefficient of the sample increased as the wt% of MH filler content increased. The results showed that the brake pad produced was eco-friendly and suitable for asbestos-free brake pad friction material. Swamidoss and Prasanth [23] used pineapple leaf fiber (PALF) to develop an asbestos-free brake pad. Epoxy resin was used as a binder because it has good mechanical properties. The samples were varied with different percentage of PALF and gave good properties. The hardness, compressive strength, and wear rate of samples produced decreased as the wt% of PALF increased. This research results showed that pineapple leaf fiber can be used effectively as a substitute material for asbestos in brake pads production. Wisdom and Abraham [24] produced non-asbestos brake pads using corn husk fiber (CHF) as an alternative filler. The CHF was milled and sieved into sieve grades of 100 µm and 200 µm. The different proportions of CHF and silicon carbide were mixed together with other ingredients such as graphite, steel dust in a fixed ratio, while phenolic resin (phenol formaldehyde) was used as a binder to produce a brake pad from compressional molding. They investigated the properties of the sample produced. The result showed that the hardness, density compressive strength, and porosity of the developed samples decreased as the sieve size of CHF increased, while the wear rate increased as the sieve size of the CHF increased. From the results obtained, the brake pad samples developed were in close agreement when compared with commercial brake pads. This showed that CHF can be utilised as a possible replacement filler material for asbestos material. Darlington et al. [25] combined coconut shell powder and palm kernel shell to developed asbestos-free brake pad using other additives. Polyester resin was used as a binder. Three different samples were produced by varying both coconut shell and palm kernel shell constituents. The results revealed that the properties of the samples developed met the properties of commercial brake pads due to their high density and high wear rate and could be used as an alternative for commercial products because they were eco-friendly. Ruzaidi et al. [26] used palm ash to produce non-asbestos brake pads by varying the composition of polychlorinated biphenyls waste (PCB) and palm ash. Thermoset resin was employed as a binder. The wear properties and morphology analysis of the developed brake pad used five different ratios. The results showed that as the palm ash content increased in the composition, the compressive strength also increased. The results showed that a high content of PA composition gave better wear rate and mechanical properties. This showed that PA and PCB can be employed as a suitable replacement for asbestos brake pads production at less cost. Yawas et al. [27] and Yakubu et al. [28] developed asbestos-free brake pads from Periwinkle shells (PSP) and phenolic resin as a binder. They varied different sieve size of PSP in the range 710 µm to 125 µm and 35 % of resin. They investigated the tribological properties, mechanical as well as physical properties of the periwinkle shells-based brake pad as well as the morphology of the constituents. The results of their research showed that the hardness, density and compressive strength of the developed samples increased as the PSP size decreased from 710 µm to 125 µm and showed good interfacial bonding. The wear rate of the sample developed increased as the PSP increased. The research demonstrated that PSP could be used as an alternative filler material for the production of asbestos-free brake pads. Shahril Anuar Bahari et al. [29]

investigated the properties such impact resistance and hardness of asbestos-free brake pads produced from rice husk dust (RHD) using phenol formaldehyde as a binder. The RHD used different sizes (80 mesh and 100 mesh) with other materials at 10 and 30 % composition. Concerning the brake pad produced with fine mesh size, the results showed that when the percentage of RHD decreased, the COF also increased, while the wear rates decreased as the percentage of RHD decreased in the mixture. For that reason, RHD improved the frictional performance of the brake pad developed. Therefore, the smaller RHD particles performed better as a filler material in the composition. This study showed that a high percentage of RHD positively affected the result of hardness and impact resistance properties. Adeyemi et al. [30] developed asbestos-free brake pads from a mixture of palm kernel shells (PKS), cocoa beans shells (CBS) and maize husks (MH). The binder used was an epoxy resin. The properties of the sample produced were investigated. The properties of brake pad samples developed with the three mixtures were compared with single filler materials, for instance CBS and MH based sample pads. The results showed that as the wt% of epoxy resin matrix in the preparation increased, the friction coefficient of the sample decreased, while the tensile strength and compressive strength of the sample produced increased. However, the density and hardness were inconsistent. The results showed that mixture of agro-waste based material such as CBS, MH and PKS can be used as an asbestos alternative filler material for brake pad friction materials.

Ishola et al. [31] employed palm kernel shell (PKS) with other components to developed non-asbestos brake pads and phenolic resin as a binder using compressive moulding by varying the PKS particle sizes. The PKS was sieved into grades of 100 µm, 200 µm, and 350 µm respectively. The properties of the developed samples were investigated. The study results indicated that the PKS grain size influenced the properties such as hardness, compressive strength, and wear rate of the developed brake pad. The 100 µm PKS powder grain size produced the best brake pad. This showed that PKS powder can be used as a substitute material in the production of asbestos-free brake pads. Lawal et al. [32] developed an asbestos-free brake pad with sawdust and other additives. Epoxy resin used as a binder, using compressive molding with varied sieve sawdust particles of 100 µm, 355 µm and 710 µm and a ratio of 55 % (sawdust), 15 % (steel dust), 10 % (silicon carbide), 5 % (graphite) and 15 % (epoxy resin). They investigated density, compressive strength, hardness and microstructure of the sample produced. From the study, the finer the sieve size of the sawdust the better their properties. The density, compressive strength, and hardness of the samples decreased as the particles size of the sawdust increased. The samples produced were closely correlated when compared with asbestos brake pads. For that reason, sawdust can be employed for asbestos-free brake pads.

Unaldi and Kus [33] developed ecological brake pads using miscanthus as reinforcement material with other material such as alumina, cashew and calcite materials in powder form with phenolic resin as binder. A trial and error approach was used to find the optimum ratio. The compositions of the brake pad materials between 5 wt. % and 20 wt. % were determined by using Taguchi method to know the effect on the brake pads properties. The result showed that as the phenolic resin ratio in the samples increased, hardness values as well as the density of the samples increased, while the porosity values of the developed brake pad decreased. The phenolic resin had no effect on wear rate. The miscanthus component affected the wear rate performance of the brake pad sample.

Ma et al. [34] examined the mechanical properties of bamboo fiber reinforced friction materials with binder (Phenolic resin) for brake pads using a constant speed friction tester. The studies showed that the wear rate of the 3 wt% fiber of bamboo fiber reinforced friction material was lower than other materials and carbonized bamboo fiber reduced the wear rate of

the sample, the noise of the brake pad and also provided a constant COF. The presence of bamboo fiber in novel materials improved the friction performance. Solomon et al. [35] developed and evaluated asbestos-free brake pads produced from groundnut shell (GS) particles. This was done to take advantage of the properties of GS, which are mainly deposited as waste. Two samples were produced by varied GS as filler materials with 45 % and 50 % of phenolic resin separately as a binder. The results showed that as the filler material size decreased the compressive strength and density increased. This showed that GS particles can be used as good substitute for asbestos in the production of automotive brake pads when compared with asbestos and industrial waste. Ikpambese et al. [36] studied the properties of asbestos-free brake pad materials using palm kernel fiber with epoxy resin binder. They varied the percentages of 100 µm PKFs with Al_2O_3, C_aCO_3 and epoxy polymer with other constituents to produce brake pads. They investigated properties and microstructure analysis. The values obtained from PKFs parameters were within the normal requirement for commercial brake pad performance.

2.1. The Raw Materials Preparation

Existing agricultural waste cannot be used directly in the formulation of the final brake pad. Therefore, some treatments such as mechanical and chemical treatments are required earlier in the brake pads composition. The following are some of the natural fiber treatment methods proposed according to the literature.

2.1.1 Palm Kernel Fiber

Several studies such as Achebe et al. [14] and Ikpambese et al. [36] used palm kernel fiber as a filler in brake pad applications. The palm kernel fiber (PKF) was prepared by being suspended in caustic soda solution for 24 hours after the extraction to remove the leftover red oil. Then, the fiber was washed thoroughly with water and dried in the sun for a week. Dried palm kernel fibers were ground into a powder by hammer mill and then sieved using < 100 µm opening grade size sieve [36].

2.1.2. Banana Peel

The banana peels used by Idris et al. [37] were dried and milled at 250 rpm in the ball mill to banana powder form non-carbonized (BUNCP). The powder was pour into a crucible furnace and fired up at a temperature of 1200 °C in an electric resistance furnace to became banana peel ash carbonized (BCp).

2.1.3. Coconut fiber

Maleque et al. [38], collected coconut fiber which they thoroughly washed with ethanol in order to remove the impurities. A crusher machine was used to sieve the ground fiber into fine powder ranging from 100 µm to 200 µm size. Four different mixtures were prepared (BP1, BP2, BP3 and BP4) using powder metallurgy technique by varying the coconut fiber contents at 0, 5, 10 and 15 percentage volume fractions as well as binders, abrasive materials friction modifiers, and solid lubricants to produced natural fiber brake pad materials reinforced with aluminium. In this composition, coconut fiber was employed as a filler material. A mixing process method was used for obtaining metallurgy powder uniformity. All materials were in powder form. The produced samples were heated and compressed at 170 °C in a hot compacting mould using a holding time of 20 kg load for 60 seconds. A hydraulic press machine was used for compaction at a fixed temperature and pressure, after which the material was sintered at 200 °C for 5 hours in an oven [38].

2.1.4. Groundnut Shell

Groundnut shell was collected and washed with water to remove sand and put in a sodium hydroxide solution having a composition ratio of 1:15 with water to remove impurities such as lignin and pectin. After this, the GS was washed in distilled water to reduce the sodium hydroxide in the shell and sun dried till all the moisture content in the shell dried up. The dried shell was ground in a grinding machine to reduce its size, after which the shell was sieved into a 150 and 350 um sieve size. The shell particles were then mixed in a two-roll mixing mill together with other constituents [35].

2.1.5. Maize Husk

Maize husk (MH) collected by Ademoh and Olabisi [22] was cleaned to remove impurities and dried in the sun on a screed surface. Subsequently, it was pulverized in a hammer mill into powder and were sieved with 300 μm aperture sieve size to produce fine powder. Chemicals experimental were categorized and placed in clear-labelled glass bottles for simple identification.

3. BRAKE PAD COMPOSIT PREPARATION

The sample preparation of palm kernel fiber (PKF) was performed by Achebe et al. [14] using a cylindrical mold. The binder (epoxy resin) was varied from 10 to 30 wt% with a space of 10 wt% and PKF from 20 to 40 wt% with a gap of 10 wt%. The weighed solid substances were mixed together in a bowl with a stir bar until uniformity was achieved prior to the addition of the resin. At room temperature, a cylindrical mold was used to hold each individual formulation and a hydraulic press exerted a pressure of 8.8 kPa, used 100 KN force for 2 minutes. After released the load, the samples produced were cured at 250^{o}C for 1.5 hours. The samples developed was polished with a polishing machine using various sizes grades of grinding paper to get the final product.

Ademoh and Olabisi [22] and Bashar et al. [18] used powder metallurgy techniques to produce test brake pad specimens using maize husk filler to secure pre-cast mixtures to the surface of backing steel metal plates. Initially a controlled test was conducted in which 250 g of epoxy was cast inside the moulds to verify the correct quantity of mixture that filled the cavity. The wt% of maize husk filler and epoxy resin was varied while silica and iron oxide, pulverized graphite, and calcium carbonate (C_aCO_3) was constant. The wt% of the friction modifier abrasive, reinforcement and fillers were measured and mixed together for 15 minutes to get homogeneity in the mixing vessel. The amount of epoxy resin and hardener was added together to form a matrix, and mixed together for 10 minutes to obtain a homogeneous mixture. The formed adhesive was poured into a cavity mould in which powdered talc was used to facilitate removal of the components after casting and cured for 80 min to 120 min. The curing time varied in relation to the epoxy resin ratio to hardener in the mixture changes, and the flow resistance of the adhesive decreased as the weight of matrix binder increased. The epoxy resin ratio to hardener was 1:2 for constituents and 1:3 for compositions 2 and 3 [22].

4. RESULTS AND DISCUSSION

4.1. Effect of binder (Resin phenolic) on the brake pad performance using banana peels

The results of this review showed the effect of phenolic resin on banana peel brake pads performance. when the wt% of binder increased, the wear rate of banana peel particles decreased. This may have occurred due to the high microstructure packaging which affected the banana peel and the resin causing stronger bonding. Also, as a result of the additional

resin in the banana peel particles higher compressive strength and hardness value were obtained from the sample [37]. When the wt% of the resin in the preparation increases, the friction coefficient of the sample also increased.

4.2 Effect of epoxy resin binder and palm kernel fiber on brake pad performance

The presence of PKF and low binder content (epoxy resin) in the mixture increased the wear rates of samples A and B at the same time the wear rate of sample C decreased. This meant sample A and B had a low wear rate and sample C had high wear rate. When the wt% of PKF increased in the composition, the compressive strength of the sample also increased. The reason for the increase may be attributed to the percentage and ratio of the composite in the three developed samples. The samples' hardness values increased when the wt% of PKF samples increased in the composition [14].

4.3. Effect of epoxy resin binder on the brake pad performance with maize husk filler

A study by Ademoh and Olabisi [23] showed that by maize husk filler content can improve the wear rate, hardness, compressive strength, thermal conductivity and tensile strength of a brake pad composite. Friction coefficient, density, water and oil absorption increased as the content of MH filler increased. From the experimental results, properties of the MH filler brake pads produced had good effects on brake pad performance.

Table 1 Summary of the recent study on effect of fiber, fillers and binders on brake pad performance

Material	Binder Matrix	Input Parameter (Varied wt%)	Effect on Mechanical, Physical and Tribological Properties	Outcome	Ref.
Cow bone	Phenolic resin	Particle size of cow bone	↑wt% CB sieve grade from (250 µm to 850 µm) = ↑water & oil absorption, wear rate ↑wt% CB sieve grade = ↓COF, density ↑wt% CB sieve grade = ↑% charred properties	CB particle size decreased from 850 µm to 250 µm, and an increase in the amount of interfacial bonding. 250 µm CB particle size improved the performance of the brake pad more than the higher particle sizes.	[13]
Palm kernel fiber	Epoxy resin	Particle size of palm kernel fiber	↑wt% PKF content = ↑hardness, wear rate, specific gravity ↑wt% PKF content = ↓water and oil absorption	PKF is a potential replacement for asbestos brake pad material in the brake Pads production.	[14]
Bagasse	Phenolic resin	Bagasse	↑wt% sieve grade of bagasse = ↓compressive strength, hardness and density ↑wt% sieve grade of bagasse = ↑wear rate and percentage charred ↑wt% sieve grade of bagasse = ↑oil soak, water soak,	100 µm sieve grade of bagasse with a composition of 70% and phenolic resin of 30% can be applied as a substitute material in the production of asbestos brake pad	[15]
Cashew Nut-Shell liquid (CNSL) and Potassium	Phenolic resin	Cashew nut-shell liquid	↑wt% PS or CNSL = ↑COF at moderate temperature 100 ˚C ↑wt% Potassium titanate = ↓COF ↑wt% PR = ↑Wear resistance	The friction material wear resistance improved with the additional of phenolic resin	[16]

titanate				while CNSL failed to improve wear resistance.	
Rice Husk Fiber	Epoxy resin	Rice husk	↑RHF = ↓Abrasive wear rate	The positive effect of both untreated and treated RH reinforcement showed the progress on tribological properties of epoxy composites. Addition of the RH to epoxy resin has improved abrasive wear rate. ER is very efficient in improving the wear rate	[17]
Coconut Shell Powder	Epoxy resin	Coconut content and Epoxy resin	↑wt% CSP = ↓breaking strength, hardness, compressive strength and impact strength	CSP was well spread in the resin and it employed as a filler material in the brake pad friction materials. A higher percentage of ground CSP gave low strength, hardness, compressive strength, and impact strength; this showed that an increase in coconut shell powder increased the brittleness of the brake pad	[18]
Watermelon peels	Pure-water sachet	Pure-water sachet resin	↑wt% PWS =↑compressive strength, hardness and specific gravity ↑wt% PWS =↓wear rate ↑wt% PWS =↓oil soak, water soak	The result achieved proper bonding at additional 25 wt% pure-water sachet with watermelon peel particles	[19]
Cocoa Beans Shells	Epoxy resin	Cocoa Beans Shells	↓wt%. CBS = ↑wear rate, tensile strength, compressive strength ↑wt%. CBS = ↑COF wt% ER = ↑compressive strength	CBS properties showed that it can be employed as a substitute filler material in the brake pad instead of asbestos in brake pad friction material	[20]
Aramid Pulp, Rockwool, Potassium titanate and others	Phenolic resin	Phenolic resin	↑wt% PR = ↑hardness ↑wt% PR = ↓porosity & compressibility ↑wt% PR & MGO = ↑COF ↑wt% PR Rockwool, Zircon & Ca $(OH)_2$ = improved wear rate resistance ↑wt% APF = ↑hardness, porosity & compressibility ↑wt% PT & CN = ↓hardness, ↑wt % PT & CN = ↑porosity and compressibility	The friction performance was affected by the thermal stability and morphology of the constituents	[21]
Maize Husk Fiber	Epoxy resin	Hardener resin & Maize husk powder	↓wt% MHF content = ↑ wear rate, hardness, tensile strength, thermal conductivity, and compressive strength ↑wt% MHF = ↑density, COF, water	MHFs are suitable alternatives for asbestos-free friction materials in automotive brake	[22]

			and oil absorption	pads	
Pineapple leaf	Epoxy resin	Pineapple leaf	↑wt% pineapple leaf = ↓compressive strength, hardness & wear ↑wt% pineapple leaf = ↑water absorption	ER was used as a binder because it has good mechanical properties	[23]
Corn Husk	Phenolic resin	Corn Husks	↑wt% SC and CH = ↓compressive strength, hardness, densities and porosity ↑wt% SC and CH = ↑wear rate and percentage charred.	The higher the percentage volume of the CH particles from A–E, the higher wear rate, porosity, density and percentage charred	[24]
Coconut Shell Powder and Palm kernel shell.	Polyester resin	Coconut shell Powder and Palm Kernel Shell	↑wt% filler = ↑water absorption	Polyester resin type of binder used affects the wear rate. CSP and PKS cannot meet the properties of commercial brake pads due to their high density and high wear rate	[25]
Palm ash and Polychlorinated biphenyls	Phenolic resin	Particle size of Palm Ash	↑wt% PA content = ↑compressive strength ↑wt% PA content = ↓water absorption ↑wt% PA content = better wear properties	Asbestos-free brake pad components showed wear rate properties compare to asbestos brake pads.	[26]
Periwinkle shell	Phenolic resin	Periwinkle shell particle size	↓wt % PSP = ↑compressive strength, hardness and density ↓wt% PSP = ↓wear rate	Samples containing 125 µm of PS as a filler material showed good properties in all the test samples	[27]
Periwinkle shell	Thermoset resin	Periwinkle Shell particle size	↑wt% PSP = ↑wear rate increased	PS had good co-efficient of friction for automobile brake pads	[28]
Rice Husk Dust	Phenol Formaldehyde	Rice Husk Dust	↓wt% RHD = ↓wear rate ↓wt% RHD = ↑COF	Smaller particle size of RHD performed better as a filler material within a higher percentage of the composition. Higher percentage of RHD has a good result on hardness and impact resistance properties.	[29]
Cocoa Beans Shells, Palm Kernel Shells and Maize Husks	Epoxy resin		↑wt% ER = ↑tensile strength and compressive strength ↑wt% ER matrix formulation = ↓COF, abrasion resistance, and water soak	(CBS), maize husks (MH) and (PKS) can employed as replacement for filler materials in the production of brake pad as they showed improvement on their properties. The density, hardness, thermal conductivity, and oil soak varied	[30]

				inconsistently	
Palm Kernel Shell	Phenolic resin	Palm Kernel Shell	↑wt% PKS from 100 µm to 350 µm = ↑wear rate, porosity and ↑wt% PKS = ↑wt.% ash content ↑wt% PKS = ↓hardness values, compressive strength	The effect of wt.% increase in PKS on wear and porosity is rather unstable or unclear. The wt.% of PKS had direct effect on the ash content, while the hardness and compressive strength decrease.	[31]
Saw-Dust	Epoxy resin	Sawdust Particles	↑wt% SDP = ↓ density, compressive strength, hardness, ash-content & water absorption of the developed samples.	The finer the size sieve of the particle, the better the properties. SD of 100µm particles size had properties that can employed as a substitute material for asbestos brake pad	[32]
Miscanthus	Phenolic resin		↑wt% miscanthus = ↓density and hardness values ↑wt% miscanthus = ↑porosity and wear rate values ↑wt% cashew = ↓density and hardness values ↑wt% cashew = ↑porosity values, ↓wear rate ↑wt% phenolic resin = ↑density and hardness values ↑wt% phenolic resin = ↓porosity values	The properties of the developed brake pad such as hardness, density, porosity and wear rate were affected more by the Miscanthus and phenolic resin in the combination. PR constituent has no effect on wear rate.	[33]
Bamboo Fiber	Phenolic resin	Bamboo Fiber	↑wt% BF (-3 wt.%.) = ↓wear rate ↑wt% BF (+3 wt.%.) = ↑ wear rate	BF in the preparation of fiction materials improved the brake pad performance. COF of BF filled material was higher than material without BF	[34]
Groundnut Shell	Phenolic resin	Particle size of groundnut shell	↑wt% PR = ↑compressive strength ↑wt% GS = ↑water & oil absorption rate ↓wt% GS = ↑density & compressive strength ↑interfacial bonding = ↓water & oil absorption rate, porosity	The water and oil absorption rate for GS-based brake pad was closed to the conventional brake pad with a % deviation of 0.001 and 0.022. GS-based brake pads are environmental friendly and cost effective	[35]
Palm kernel fiber	Epoxy resin	Resins varied	↑ Speed = ↑wear rate, COF, noise level, stopping time & temperature ↑ Speed = π specific gravity, moisture content, hardness, surface roughness, porosity, oil and water absorption	PKF increased the softness of the friction materials. Better performance of non-asbestos brake pad can be achieved by using PKF as a substitute material for asbestos by	[36]

				using epoxy resin as binder.	
Banana Peels	Phenolic resin	Phenolic resin	↑wt% PR = ↑compressive strength, hardness & specific gravity ↑wt% PR = ↓wear rate and charred percentage ↑ wt% PR = ↓water absorption, oil absorption	The banana peels prototype shows that the formulation without adding any binder in preparation can be used in brake pad production. The properties of BP particles showed that it can be used as a substitute material to produce asbestos brake pads material.	[37]
Coconut Fiber	Phenolic resin	Coconut Fiber	wt% coconut fibres (BP2 and BP3) = ↑higher density & ↓porosity wt% coconut fibres (BP3) = ↑compressive strength	Microstructure studied showed a equal distribution of resin as the coconut fiber acted as filler in the preparation of the friction material.	[38]
Sea Shell	Epoxy resin	Process Parameters	Δ in process parameters affect the compressive strength hardness, tensile strength, impact, COF, flexural strength and wear rate	All factors have a large effect on the tribological and mechanical properties because their p-values are less than 1%. The brake pads sample provided a better COF, as the optimum value (0.48) which is within G-class (0.45-0.55) type brake pads recommended by the (SAE) for automobiles.	[39]
Pulverized Cow hooves	Epoxy resin	Pulverized Cow Hooves and Epoxy resin	↑wt% ER = ↑compressive strength, hardness, relative density and coefficient of friction ↓wt% PCH = ↑compressive strength, hardness, relative density & COF ↑wt% ER = ↓water absorption, oil absorption and wear rate ↓wt% PCH = ↓ water absorption, oil absorption and wear rate	When the wt% ER increased, the wt% of the PCH decreased, a suitable bonding was obtained	[40]
Periwinkle Shell	Phenolic resin	periwinkle shell particles	↑wt%PSP = ↑wear rate, sliding speed & temperatures load	The friction coefficient obtained from the work was within the automobile brake pad standard. Therefore, PSP can be utilised as alternative for asbestos in the production of brake pad.	[41]
Fly Ash & Other materials	Phenolic resin	Filler materials	↑wt% filler materials = ↓tensile strength ↑wt% PR = ↑hardness ↑wt% FA = ↓COF	The availability of fibers content in the binder matrix increases hardness	[42]

			↑wt%RP, Vermiculite & CDP = ↓hardness & ↑porosity	and tensile strength, which is expected because the hard fibers reinforced in the soft matrix.	
Snail Shell & Rubber Seed Husk	Epoxy resin	Snail Shell	↑wt% SS sieve grade = ↓compressive strength, hardness & densities. ↑wt% SS sieve grade = ↑oil soak, water soak & wear rate properties	By using a 125 µm SS sieve-grade with 65% SS -10% RSH & -25% resin of composition, SS & RSH can use effectively as an alternative for asbestos brake pad production	[43]
Palm slag, Calcium carbonate ($CaCO_3$), and Dolomite	Phenolic resin	Filler materials	↑wt% DF = ↑compressive strength ↑wt% PSL = ↑hardness value	PSL had substantial potential as an alternative filler material to present fillers in composite formulations for the production of brake pads. When compared with conventional asbestos brake pads, PSL and CaCO3 brake pads offered better wear rate properties than dolomite	[44]

Table notes:	CBS = Cocoa Beans Shells
↑wt% = Percentage weight increase	PKS = Kalm Kernel Shells
↓wt% = Percentage weight decrease	ES = Epoxy Resin
↑ = increased	PSF = Periwinkle Shell Fiber
↓ = decreased	PCH = Pulverized Cow Hooves
% = Percentage	PA = Palm Ash
CB = Cow Bone	PSP = Periwinkle Shell Particle
PKF = Palm Kernel Fiber	RHD = Rice Husk Dust
PSL = Palm Slag	CH = Corn Husk
DF = Dolomite Filler	PS = Phenolic Resin
CaCO3 = Calcium Carbonate	RP = Rubber Powder
RHF = Rice Husk Fibers	SDP = Saw-Dust Particles
GA = Gum Arabic	FA = Flash Ash
BP = Banana Peels	SS = Snail Shell
PWS = Pure-Water Sachet	RSH = Rubber Seed Husk
CSP = Coconut Shell Powder	SC = Silicon Carbide
CN = Cashew Nuts	CDP = Cashew dust powder
APR = Aramid Pulp Fiber	BF = Bamboo Fiber
PT = Potassium Titanate	COF = Coefficient of friction
CNSL = Cashew Nut-Shell Liquid	GS = Groundnut Shell
MHF = Maize husk filler	II = Constant
	SAE= Society of Automobile Engineers

5. CONCLUSION

Although asbestos brake pads have good tribological and mechanical properties, they are carcinogenic in nature. From the studies, better physical properties were obtained with coconut fiber brake pads as the percentage of composition was optimized. In brake pads produced by using banana peel, there was an improvement in the tribological properties of the sample when the percentage of phenolic resin increased, although increasing the percentage of resin can lead to development of toxic substances and low shelf life. In the case of palm kernel fiber, both filler materials and binder affected the mechanical, tribological, and physical properties of the brake pad sample developed. These studies also indicate that chemical and physical treatments also used to subdue poor wettability and enable higher moisture absorption.

The wear rate improved with the addition of filler material in the brake pad sample preparation. Wear rate of the developed composite also affected by the speed significantly. The smaller quantity of the filler, binder and fiber material had effect on the composite wear rate and gave better.

The performance of the composite material such as mechanical and physical properties have been reported to be affected by the filler materials in the composition. In addition, various studies so far have found that as the composite filler material content decreases the properties for examples hardness, compressive strength, thermal conductivity and tensile strength, of the composite produced increase, while the density, oil and water absorption of the developed brake pad sample increases when the filler content of the composite increases.

REFERENCES

[1] Carus, M., Eder, A., Dammer, L., Korte, H., Scholz, L., Essel, R. et al., Wood-Plastic Composites (WPC) and Natural Fibre Composites (NFC). Nova-Institute: Hürth, Germany: Nova-Institute, 2015.

[2] Nagesh, S., Siddaraju, C., Prakash, S. and Ramesh, M. Characterization of Brake Pads by Variation in Composition of Friction Materials. *Procedia Materials Science*, 5, 2014, pp. 295-302.

[3] Navin, C., Hashmi, S., Lomash, S., and Naik, A. Development of Asbestos Free Brake Pad. *Journal of the Institution of Engineers*, 85, 2004, pp. 13-16.

[4] Lee P. W. and Filip, P. Friction and Wear of Cu-Free and Sb-Free Environmental Friendly Automotive Brake Materials. *Wear*, 302, 2013, pp. 1404-1413.

[5] Saffar A., and A. Shojaei. Effect of Rubber Component on the Performance of Brake Friction Materials. *Wear*, 274, 2012, pp. 286-297.

[6] Kumar M. and Bijwe, J. Composite Friction Materials Based on Metallic Fillers: Sensitivity of μ to Operating Variables. *Tribology International*, 44, 2011, pp. 106-113.

[7] Kumar M. and Bijwe, J. Role of Different Metallic Fillers in Non-Asbestos Organic (NAO) Friction Composites for Controlling Sensitivity of coefficient of Friction to Load and Speed. *Tribology International*, 43, 2010, pp. 965-974.

[8] Han, Y., Tian, X. and Yin, Y. Effects of Ceramic Fiber on the Friction Performance of Automotive Brake Lining Materials. *Tribology Transactions*, 51, 2008, pp. 779-783.

[9] Bijwe, J. Composites as Friction Materials: Recent Developments in Non-Asbestos Fiber Reinforced Friction Materials—a Review. *Polymer Composites*, 18, 1997, pp. 378-396.

[10] P. J. Blau, "Compositions, functions, and testing of friction brake materials and their additives," Oak Ridge National Lab., TN (US)2001.

[11] Rohatgi, P. K., Menezes, P. L. and Lovell, M. R. Tribological Properties of Fly Ash-Based Green Friction Products. In: Nosonovsky M., Bhushan B. (eds) *Green Tribology. Green Energy and Technology*. Berin: Springer, 2012, pp. 429-443.

[12] Chan D. and Stachowiak, G. Review of Automotive Brake Friction Materials. *Journal of Automobile Engineering, Proceedings of the Institution of Mechanical Engineers, Part D*, 218, 2004, pp. 953-966.

[13] Adegbola, J., Adedayo, S. and Ohijeagbon, I. Development of Cow Bone Resin Composites as a Friction Material for Automobile Braking Systems. *Journal of Production Engineering,* 20, 2017, 69-74.

[14] Achebe, C., Chukwuneke, J., Anene, F. and Ewulonu, C. A Retrofit for Asbestos-Based Brake Pad Employing Palm Kernel Fiber as the Base Filler Material. Proceedings of the Institution of Mechanical Engineers. *Journal of Materials: Design and Applications: Part L*, 2018, p. 1464420718796050.

[15] Aigbodion, V., Akadike, U., Hassan, S., Asuke, F. and Agunsoye, J. Fevelopment of Asbestos-Free Brake Pad using Bagasse. *Tribology in Industry*, 32, pp. 12-17, 2010.

[16] Kim, Y. C., Cho, M. H., Kim, S. J. and Jang, H. The Effect of Phenolic Resin, Potassium Titanate, and CNSL on the Tribological Properties of Brake Friction Materials. *Wear*, 264, 2008, pp. 204-210.

[17] Acharya S. and Samantrai, S. The Friction and Wear Behavior of Modified Rice Husk Filled Epoxy Composite. NIT Rourkela-Institutional Repository, 2012. Available: http://dspace.nitrkl.ac.in/dspace/handle/2080/1786

[18] Bashar, D.-A., Madakson, P. B., and Manji, J. Material Selection and Production of a Cold-Worked Composite Brake Pad. *World Journal of Engineering and Pure & Applied Sciences*. 2, 2012, p. 92.

[19] Ahmed, A. O., Umar, A., Aliyu, B. U., Omilabu, E. B. and Khalifa, S. Y. Development of Asbestos Free-Brake Pad Using Solid Waste. *ATBU Journal of Science, Technology and Education*, 6,2018, pp. 121-126.

[20] Olabisi, A. I., Adam, A. N. and Okechukwu, O. M. Development and Assessment of Composite Brake Pad Using Pulverized Cocoa Beans Shells Filler. *International Journal of Materials Science and Applications*, 5, 2016, pp. 66-78.

[21] Cho, M. H., Kim, S. J., Kim, D. and Jang, H. Effects of Ingredients on Tribological Characteristics of a Brake Lining: an Experimental Case Study. *Wear*, 258, 2005, pp. 1682-1687.

[22] Ademoh N. A. and Olabisi, A. I. Development and Evaluation of Maize Husks (Asbestos-Free) Based Brake Pad. *Development*, 5, 2015.

[23] Swamidoss V. F. and Prasanth, Fabrication and Characterization of Brake Pad Using Pineapple Leaf Fiber (Palf), *International Journal of Research in Computer Applications and Robotics*, 3, pp. 107-111, March 2015.

[24] Asotah W. and Adeleke, A. Development of Asbestos Free Brake Pads using Corn Husks. *Leonardo Electronic Journal of Practices and Technologies,* 31, 2017, pp. 129-144.

[25] Egeonu D. and Okolo, C. O. P. Production of Eco-Friendly Brake Pad Using Raw Materials Sourced Locally In Nsukka. *Journal of Energy Policies and Policy,* 5(11), 2015.

[26] Ruzaidi, C., Kamarudin, H., Shamsul, J., Al Bakri, A. M. and Alida, A. Morphology and Wear Properties of Palm Ash and PCB Waste Brake Pad. Proc. of International Conference on Asia Agriculture and Animal (ICAAA 2011), 2011, pp. 145-149.

[27] Yawas, D., Aku, S. and Amaren, S. Morphology and Properties of Periwinkle Shell Asbestos-Free Brake Pad. *Journal of King Saud University-Engineering Sciences*, 28, 2016, pp. 103-109.

[28] Yakubu, A. S., Amaren, S. and Saleh, Y. D. Evaluation of the Wear and Thermal Properties of Asbestos Free Brake Pad Using Periwinkles Shell Particles. *Usak University Journal of Material Sciences*, 2, 2013, pp. 99-108.

[29] Bahari, S. A., Isa, K. H., Kassim, M. A., Mohamed, Z. and Othman, E. A. Investigation on Hardness and Impact Resistance of Automotive Brake Pad Composed with Rice Husk Dust. *AIP Conference Proceedings 2nd*, 2012, pp. 155-161.

[30] Adeyemi, I. O. Development of Asbestos-Free Automotive Brake Pad Using Ternary Agro-Waste Fillers. *Development*, 3(7), 2016.

[31] Ishola, M. T., Oladimeji, O. O. and Paul, K. O. Development of Ecofriendly Automobile Brake Pad Using Different Grade Sizes of Palm Kernel Shell Powder. *Current Journal of Applied Science and Technology,* 23, 2017, pp. 1-14.

[32] Lawal, S. S., Katsina Christopher, B. and Alegbede, A. T. Development and Production of Brake Pad from Sawdust Composite. *Leonardo Journal of Sciences*, 16, 2017, pp. 47-56.

[33] Unaldi M. and Kus, R. The effect of the brake pad components to some physical properties of the ecological brake pad samples. *IOP Conference Series: Materials Science and Engineering*, 2017, p. 012032.

[34] Ma, Y., Shen, S., Tong, J., Ye, W., Yang, Y. and Zhou, J. Effects of Bamboo Fibers on Friction Performance of Friction Materials. *Journal of Thermoplastic Composite Materials*, 26, 2013, pp. 845-859.

[35] Solomon, W., Lilly, M. and Sodiki, J. Production of Asbestos-free Brake Pad Using Groundnut Shell as Filler Material. *International Journal of Science and Engineering Invention*, 4, 2018, pp. 21-27.

[36] Ikpambese, K., Gundu, D. and Tuleun, L. Evaluation of Palm Kernel Fibers (PKFs) for Production of Asbestos-Free Automotive Brake Pads. *Journal of King Saud University-Engineering Sciences*, 28, 2016, pp. 110-118.

[37] Idris, U., Aigbodion, V., Abubakar, I. and Nwoye, C. Eco-Friendly Asbestos Free Brake-Pad: Using Banana Peels. *Journal of King Saud University-Engineering Sciences*, 27, 2015, pp. 185-192.

[38] Maleque, M., Atiqah, A., Talib, R. and Zahurin, H. New Natural Fibre Reinforced Aluminium Composite for Automotive Brake Pad. *International Journal of Mechanical and Materials Engineering*, 7, 2012, pp. 166-170.

[39] Abutu, J., Lawal, S., Ndaliman, M., Lafia-Araga, R., Adedipe, O. and Choudhury, I. Effects of Process Parameters on the Properties of Brake Pad Developed from Seashell as Reinforcement Material Using Grey Relational Analysis. *Engineering Science and Technology*, 21, 2018, pp. 787-797.

[40] Bala, K. C., Okoli, M. and Abolarin, M. S. Development of Automobile Brake Lining Using Pulverized Cow Hooves. *Leonardo Journal of Science*, 15, 2016, pp. 95-108.

[41] Amaren, S., Yawas, D. and Aku, S. Effect of Periwinkles Shell Particle Size on the Wear Behavior of Asbestos Free Brake Pad. *Results in Physics*, 3, 2013, pp. 109-114.

[42] Natarajan, M., Rajmohan, B., and Devarajulu, S. Effect of Ingredients on Mechanical and Tribological Characteristics of Different Brake Liner Materials. *International Journal of Mechanical Engineering and Robotics Research*, 1, 2012, pp. 145-157.

[43] Abhulimen E. and Orumwense, F. Characterization and Development of Asbestos Free Brake Pad, using Snail Shell and Rubber Seed Husk. *African Journal of Engineering Research*, 5, 2017, pp. 24-34.

[44] Ghazali, C. M. R., Kamarudin, H., Jamaludin, S. B., and Abdullah, M. Comparative Study on Thermal, Compressive, and Wear Properties of palm Slag Brake Pad Composite with Other Fillers. *Advanced Materials Research*, 328, 2011, pp. 1636-1641.

CHAPTER 4: SYNTHESIS OF CARBON NANOSPHERES FROM PALM KERNNEL FIBER

To cite this article: O. E Ige, F. L. Inambao, G. A. Adewumi, and N. Revaprasadu, "Synthesis of Natural Carbon Nano-spheres from Palm Kernel Fiber," *International Journal of Mechanical Engineering and Technology,* vol. 10, no. 12, pp. 625-641, 2019.

International Journal of Mechanical Engineering and Technology (IJMET)
Volume 10, Issue 12, December 2019, pp. 625-641, Article ID: IJMET_10_12_056
Available online at http://www.iaeme.com/ijmet/issues.asp?JType=IJMET&VType=10&IType=12
ISSN Print: 0976-6340 and ISSN Online: 0976-6359

SYNTHESIS OF NATURAL CARBON NANO-SPHERES FROM PALM KERNEL FIBER

Oluwafemi E. Ige*, Freddie L. Inambao, Gloria A. Adewumi
Department of Mechanical Engineering, School of Engineering,
University of KwaZulu-Natal, Howard College, Durban, 4041, South Africa,

Neerish Revaprasadu
University of Zululand, X1001, Kwadlangezwa 3886, South Africa
https://orcid.org/0000-0001-9922-5434
*Corresponding Author Email: inambaof@ukzn.ac.za

ABSTRACT

*In the field of energy and environmental applications, carbon nanomaterials have enormous potential. It is necessary to develop a broad variety of green and eco-friendly synthesis methods using natural, renewable, and cheaper waste products. In this work, carbon nano-spheres were synthesized using palm kernel fiber as a renewable raw material. The process involved carbonization, physical activation and finally ethanol vapor treatment. The synthesized carbon nanomaterials were characterized using high-resolution transmission electron microscopy (HRTEM), X-ray diffraction (XRD), field emission gun scanning electron microscope (*FEG-SEM*), energy dispersive x-ray spectroscopy (EDX), Fourier transform infrared microscopy (FTIR) and thermo-gravimetric analysis (TGA) for their morphological and structural characterization. Scanning electron microscope (SEM) studies confirm carbon nano-spheres production with diameters between 10 nm and 60 nm. The synthesized carbon nano-spheres can be used as reinforcement materials in brake pad production and in medicine for drug delivery.*

Keywords: Carbon nano-spheres, Palm kernel fiber, Characterization, Synthesis.

Cite this Article: Oluwafemi E. Ige, Freddie L. Inambao, Gloria A. Adewumi and Neerish Revaprasadu, Synthesis of Natural Carbon Nano-Spheres from Palm Kernel Fiber. *International Journal of Mechanical Engineering and Technology* 10(12), 2019, pp. 625-641.
http://www.iaeme.com/IJMET/issues.asp?JType=IJMET&VType=10&IType=12

1. INTRODUCTION

The present trend in science is to use biomass materials, especially agricultural and industrial waste, as basic raw materials for composite formation. Many studies have focused on the use of lignocellulosic materials such as coconut shell [1, 2], rice husk, palm kernel fiber [3], pineapple leaf, kenaf [4] and palm kernel shells [5, 6] amongst others, as composite materials. Their advantages include hardness and high strength, high carbon content, high lignin content

and low ash material content. The use of natural fibers in the preparation of a composite has various advantages when compared to synthetic fibers due to their low cost, renewability, low density, and biodegradability [7, 8]. Synthetic fibers, for example carbon and glass fibers, generate serious environmental and health hazard issues for employees in the production of these composites compared to natural fiber composites [9]. Presently, studies are increasingly concerned about the use of abundant biomass waste as a raw material for activated carbon (AC) [10]. Due to biomass accessibility and low toxicity, different biomass sources are used for nanomaterial production obtained from carbon [11, 12].

Much attention is being paid to the preparation of AC from agri-products. Due to their low-cost, AC derived from biomass has the potential to be used for brake-pad applications [13]. Palm kernel fibers (PKF) are good raw materials for AC production because of its well-developed porosity and surface area. A further advantage is the high carbon content and the low price. PKF containes 49.6 % of carbon content [14]. PKF is largely produced in South-east Asia (Malaysia, Indonesia, and Thailand), Africa (Nigeria and Cameroon) and southern China. It is very cheap because it is a waste product [10]. As a result, it is recommended to use this low-cost and abundant waste by converting into AC. Carbon is a multifunctional element because it has distinctive properties resulting varying shaped structures [15]. The wide range of carbon-related materials with ability to bond structures, textures or surface chemistry has drawn the attention of many researchers regarding the production of AC [16], characterization [17], and its surface modification [18].

1.1. Synthesis of Carbon Nano-spheres

Because of their high surface area, chemical inertness, good mechanical stability, and unique electrical properties, carbon nano-spheres (CNSs) have many potential uses in nanocomposites such as lithium ion batteries [19, 20], super-capacitors [21, 22], catalysts [23, 24], brake pad preparation [25, 26], drug delivery [27-30] and cement composite [31]. Carbon nanotubes (CNTs) and nanostructures have received considerable attention in recent years [32]. Since CNTs or CNSs have been discovered to be an appropriate material for a multitude of applications, each application needs certain features or characteristics such as pore diameter, high aspect ratio, alignment, chirality, dispersion, shape etc. The CNSs represent the spherical form of carbon that can be divided into semi-crystalline or crystalline.

CNSs can also be classified as hollow, solid or core-shell spheres. There are three different types of CNSs depending on their diameter: wall graphitized spheres (2 nm to 20 nm), less graphitized spheres (50 nm to 1000 nm), and carbon beads (> 1000 nm) [32]. Besides such characteristics, it is also required in a reproducible technique to be able to generate the product in large capacities. CNSs have several advantages compared to other types of carbon (for example, carbon nanotubes, activated carbon powder and graphene), namely: uniform particle size, surface morphology, high specific surface area, low toxicity, good dispersion, and outstanding biocompatibility. CNSs have the desired properties that can be achieved through the reaction parameters adjusted from a carbon source, catalyst, substrate, and synthesis method. The synthesis approaches for CNT production are chemical vapor deposition (CVD) [33-37], laser ablation [38-40] and arc discharge [41, 42]. The arc discharge and laser ablation methods are costly because of the high-power equipment and they are mostly used for production of single-walled carbon nanotubes (SWCNTs). Both methods produced a small amount of CNTs with a large amount of impurities.

CVD is the most common method for CNT synthesis because it provides better control, directness, mass production, simplicity, and cost-effectiveness [33-37]. CNTs can be produced at relatively low temperatures and their size can be controlled by varying the catalyst particle size. The production of CNTs happens at reasonably low temperatures. CVD

is utilized for large volume production of CNTs. Due to its acceptance, various studies on CNT synthesis have been published in the literature, periodically emphasizing the achievement of the synthesis in recent developments [43-45]. In standard synthesis, the carbon precursor is gasified and flows into the reaction chamber with a substrate to be coated using a carrier gas. The carbonization of the carbon-rich materials at high temperatures in an inert atmosphere is the most common method used for AC preparation which is then followed by the activation process before being converted to carbon nanomaterials. The process of activation is divided into chemical and physical methods. The physical activation method involves the treatment of char achieved from carbonization by using oxidizing gas, steam or CO_2 (carbon dioxide) at temperatures (400 ℃ to 1000 ℃) [46]. The chemical activation process involves the mixing of initial material together with an activation reagent and the mixture is heated at a low temperature in an inert atmosphere [47]. The characteristics of the chemical activation agent (dehydration and oxidation) demand extremely low activation temperatures compared to the physical activation method [48]. A comparative study involving chemical and physical activation has been reported using biomass fiber as AC [49]. Hidayu and Muda [47] produced AC from agri-waste (palm kernel shell and coconut shell) by physical activation and chemical activation with the activation temperature of 800 ℃ for physical activation and 550 ℃ for chemical activation. Guo *et al.* [50] prepared AC from palm kernel fiber and palm kernel shell using a physical activation method; the process was improved by changing the holding time and the conditions of CO_2 i.e. activation temperature and the flow rate.

Chen *et al.* [34] synthesized carbon nanofibers from AC produced from palm kernel shell, coconut shell, and wheat straw agri-waste using the chemical vapor deposition method (CVD). The presence of iron in the AC ash was used as a natural catalyst for the development of the nanofiber. Tan *et al.* [51] used coconut husk fibers to produce AC by using both chemical and physical activation methods, later treated with potassium hydroxide (KOH) and with CO_2 gasification. The reaction product of hydrogen and carbon monoxide was reduced by the reaction rate between carbon and CO_2. Kumar *et al.* [52] conducted a study on natural sources with the aim of synthesizing carbon nanomaterials. The study demonstrated the use of fossil hydrocarbons, botanical hydrocarbons, and natural waste materials as sources of hydrocarbon for the synthesis of CNT and graphene. CNT synthesis based on fossil hydrocarbons is very expensive and not available. Furthermore, many of the liquid and gaseous fossil hydrocarbons are explosive or toxic and they are not good for human health and the environment. In addition, carbon nanomaterials grown from natural materials based on carbon have the advantage of producing scalable quantities, being environmentally friendly, low-cost, and allowing rapid production techniques.

In this present work, palm kernel fiber was selected as a precursor to producing carbon nanomaterials since it is available as an agri-waste material in Nigeria and has low market value. This study presents results from synthesis and characterization of CNSs from PKF, the materials were synthesized with the non-appearance of catalysts or acids for 240 hours. The production of the CNSs occurred in three stages consisting of carbonization, physical activation, and ethanol vapor treatment. The characterization of the sample was conducted by using TEM, SEM, TGA, FTIR, XRD, and EDX (elemental analysis) techniques. The developed nanomaterial can be used to improve thermal bake pad applications, lithium-ion batteries, reinforcement materials, and medical drugs.

2. EXPERIMENTAL

Palm kernel fiber for this research study was obtained after extraction from local farmers in Ado-Ekiti, Nigeria. PKF was washed with hot water and dried to reduce the fiber moisture content, then was cut close to 1 mm size with scissors as shown in Figure 1.

Figure 1 Palm kernel fiber

A heat-resistant quartz tube positioned in a horizontal tube furnace with a maximum temperature of 1200 ℃ was used for fiber carbonization in an inert atmosphere (Carbolite furnace type MTF 12/25/250). Approximately 16.0 g of the dried PKF samples were placed in a quartz tube, then put at the centre of the horizontal furnace tube (Figure 2).

Figure 2 Experimental setup

Pure nitrogen gas which operated at 80 $scfm^{-1}$ flow rates was employed as purge gas at one side when pyrolysis was in progress. On the other side of the tube, was a beaker that contained water for the exhaust. The furnace's temperature was raised from 25 °C to 600 ℃ and the carbonization process lasted 120 min to produce carbonized PKF as shown in Figure 3a. The developed char was physically activated under CO_2 gas at 850 ℃ for 60 min. The produced AC was placed in a tube positioned in a tube furnace, flushed with nitrogen gas and heated at a temperature of 1000 ℃ for 60 min^{-1}. The system was cooled down under the flow of nitrogen gas for 5 ℃ min^{-1} after 60 minutes to produce CCNs as shown in Figure 3b.

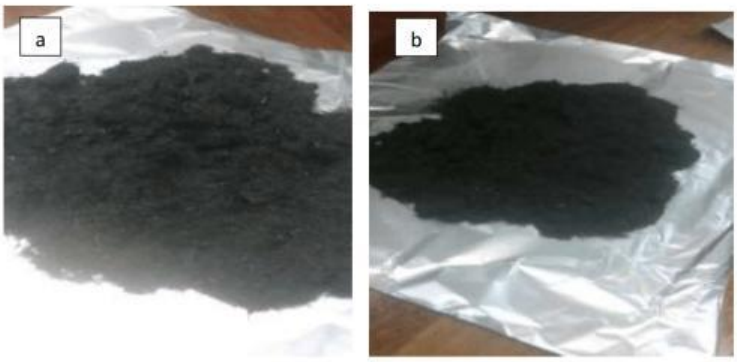

Figure 3 (a). Carbonized PKF Materials **(b)** Synthesized nanomaterial

2.1. Characterization

Transmission electron microscopy (TEM) analysis was used to study the microstructure and the samples' phase identification using a JEOL HRTEM 2100 running at an accelerating voltage of 20 kV. The sample of PKF CNS required for HRTEM measurements was approximately 0.0002 g mixed with ethanol and vibrated for 20 minutes by using an 80 Hz Watt transistorized sonic cleaner. TEM sample analysis preparation was performed by placing a drop of nanomaterial solution in a formvar-coated Cu grid (150 meshes).

The morphology and elemental composition of the synthesized nanomaterial were studied using a field emission gum scanning electron microscope (FEGSEM) Zeiss, Germany (Ultra Plus, FEGSEM). The FEGSEM together with the energy dispersive x-ray spectrometer (EDX) was used for elemental composition analysis. Thermo-gravimetric analysis (TGA) was conducted using a Perkin Elmer simultaneous thermal analyzer (STA) 6000. The synthesized material weighed between 17 mg to 28 mg. The nanomaterial thermal degradation was studied in the temperature from 30℃ to 600℃ under nitrogen flow of 10 ml/min with heating rate of 10 ℃/min and held for 10.0 min at 600 ℃. Fourier transform infrared spectra (FTIR) of CNS were acquired by using a Perkin Elmer Spectrum 400 series FTIR in ATR (attenuated total reflectance) mode. Four consecutive scans with 4.0 cm^{-1} resolution were made for each spectrum. The scan range was 650 cm^{-1} to 4000 cm^{-1}.

The crystallinity and graphitization of the PKF synthesized CNS sample was investigated using the black loading preparation method for x-ray diffraction (XRD) sample analysis. The Co-Kα radiation and PANalytical Empyrean Diffractometer with an X'Celerator detector (Netherlands made) were used to analyze the sample. The configuration of the generator was 40 kV and 40 mA. The thermal gravimetric analysis (TGA) was conducted by means of a simultaneous thermal analyzer (STA) 6000 PerkinElmer.

3. RESULT AND ANALYSIS

3.1. Morphology and Particle Size Distribution

Figure 4a displays SEM images of carbonized PKF at 600 ℃ for 120 min. The pyrolyzed PKF was activated physically under CO_2 at 1000 ℃ for 30 min to increase porosity. Figure 4b presents the KPF charcoal SEM image after being physically activated, showing some porosity.

The wide FE-SEM image in Figure 4c at 100 nm and 100 000 magnification shows that the synthesized CNSs sample had a smaller number of uniform CNSs ranging from 10 nm to

65 nm in diameter with agglomerations of particles and a smooth morphology surface. Figure 5 shows the histogram of the particle size distribution of the synthesized carbon nano-spheres, which reveals a wide-ranging distribution of sizes.

3.2. Analysis of Elemental Composition

The EDX analysis in Figures 4d to 4f analysed the composition of the elements of carbonized PKF fiber at 600 ℃ for 120 minutes, AC at 850 ℃ with CO_2 and synthesized carbon nanosphere at 1000 ℃ with ethanol vapor treatment for 30 min. The carbonized PKF had the following elements: carbon (89.33 %) oxygen (7.92 %), magnesium 0.91 %, potassium 1.15 % and calcium 0.69 % as shown in Table 1.

Table 1 Elemental composition of carbonized PKF, zctivated PKF, and synthesis palm kernel fiber

Material Sample	Carbonized PKF Wt.%	Activated Carbon Wt.%	Carbon nano-sphere Wt.%
C	89.33	87.59	89.40
O	7.92	7.80	6.52
Na		0.09	
Mg	0.91	0.79	1.27
Al		0.09	
Si		0.16	
P		0.81	
S		0.23	
Cl		0.05	
K	1.15	1.09	1.12
Ca	0.69	1.02	1.17
Fe		0.09	0.52
Cu		0.18	
Total	100.00	100.00	100.00

Elemental analysis of AC showed carbon 87.59 %, oxygen 7.80 % and other constituents. From the EDX spectra in Figure 4f the elemental analysis of the carbon nano-spheres (CNS) showed carbon content of 89.40 % after ethanol vapor treatment at 1000 ℃.

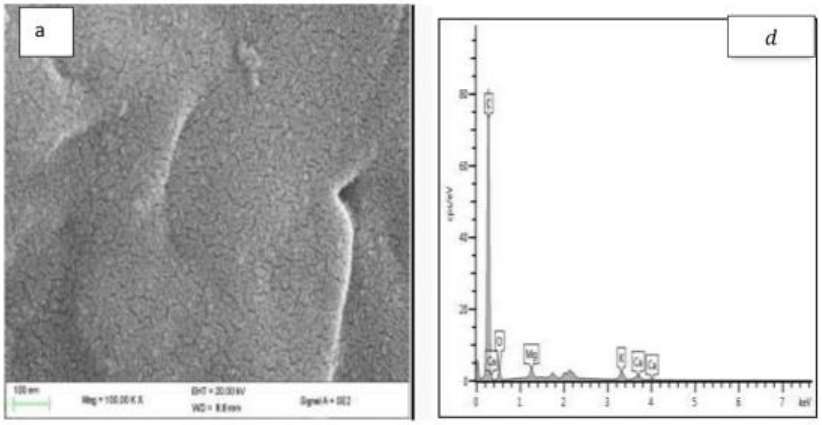

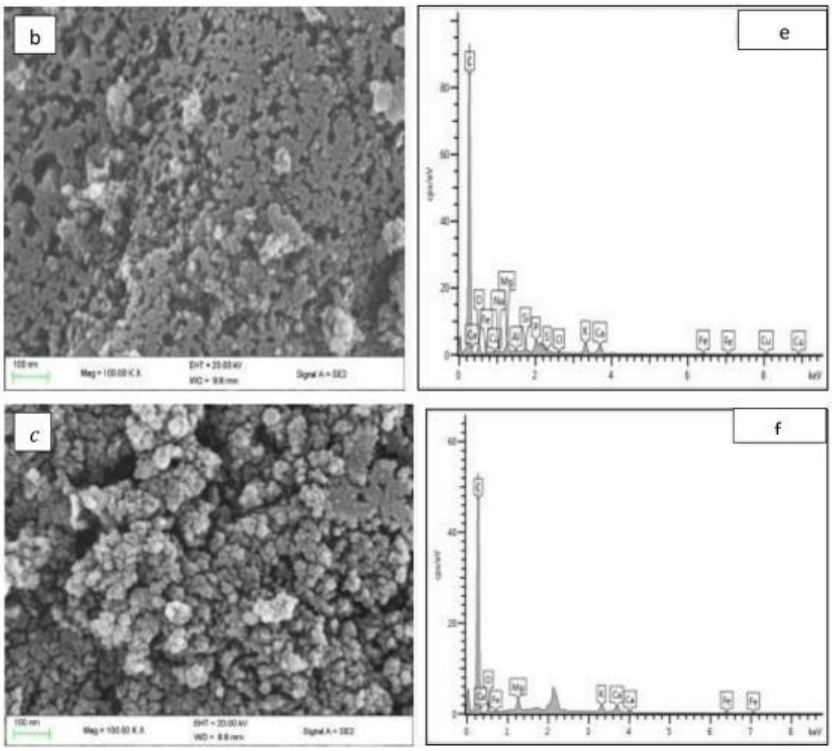

Figure 4 (a) SEM images of carbonized palm kernel fiber at 600 ℃ for 120 min **(b)** SEM image of activated carbon physically activated under CO_2 at 1000 ℃ (4c) SEM image of CNS at 1000 ℃ with ethanol vapor treatment **(d)** EDX of carbonized PKF at 600 ℃ **(e)** EDX of PKF activated carbon at 850 ℃ **(f)** EDX of CNS at 1000 ℃

The high carbon content showed that the CNS treatment with ethanol vapor at 1000 ℃ formed CNSs. Table 1 shows the elemental composition of carbonized PKF, AC and CNSs. As a result of the increase in temperature from 600 ℃ for carbonization to 850 ℃ for activation and 1000 ℃ to produce carbon nanosphere, the oxygen was reduced.

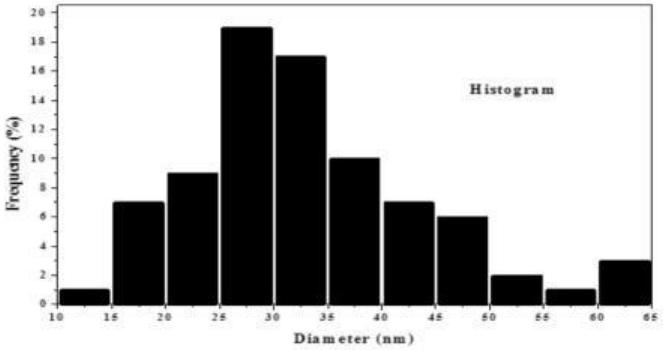

Figure 5 Carbon Nano-sphere particle size distribution

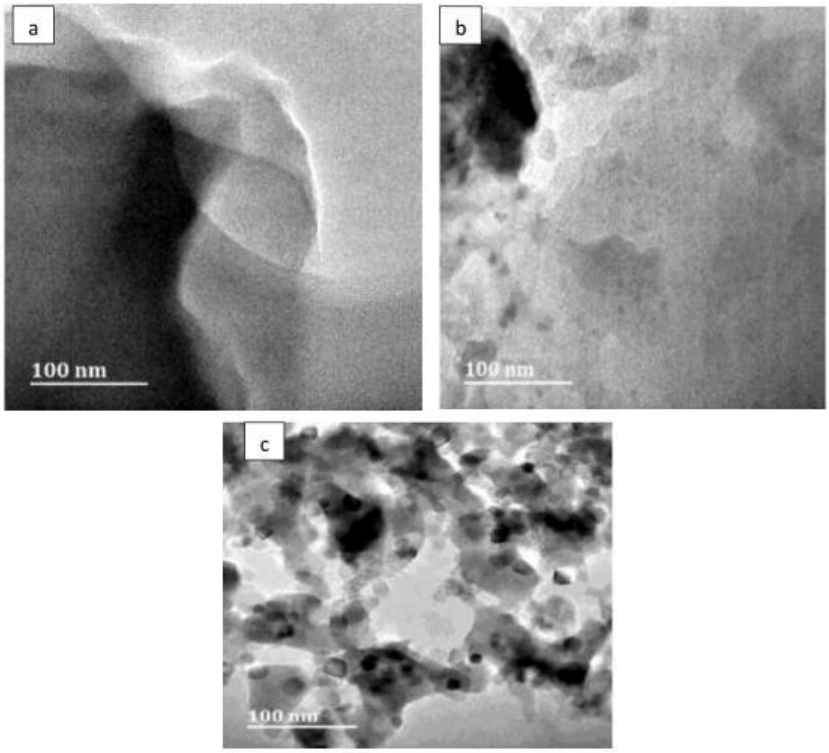

Figure 6 (a) HRTEM image of carbonized palm kernel fiber **(b)** HRTEM image of activated carbon **(c)** HRTEM image of synthesized carbon nano-spheres

3.3. Structural Analysis

The XRD pattern of PKF, carbonized PKF, AC and synthesized carbon nano-spheres obtained is shown in Figure 7 a-d.

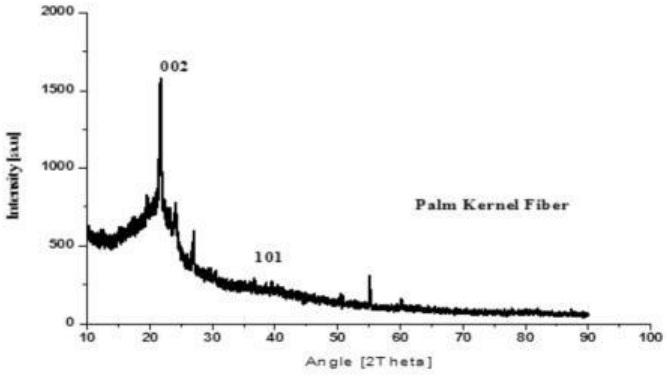

Figure 7a XRD pattern of Palm kernel fiber (PKF)

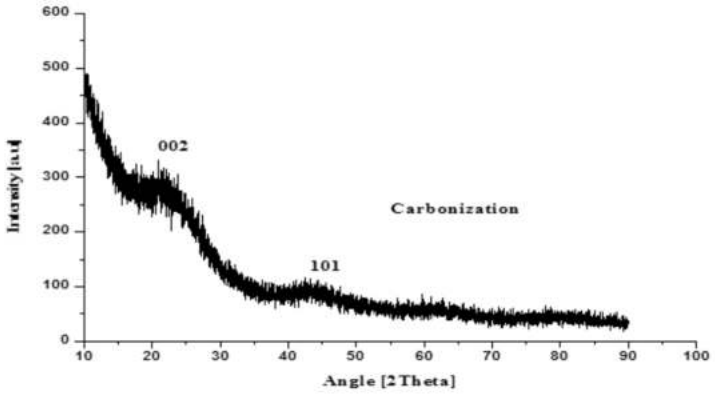

Figure 7b XRD pattern of carbonized material

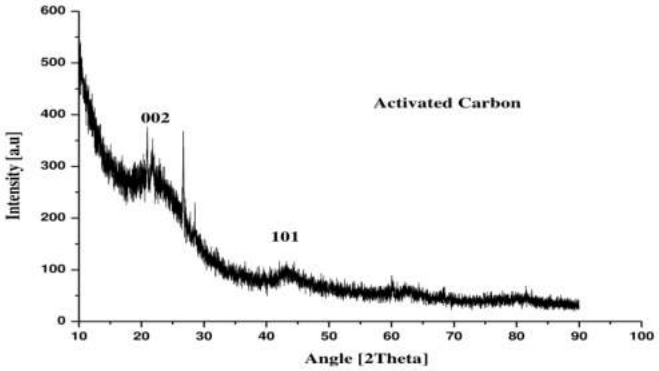

Figure 7c XRD pattern of activated carbon

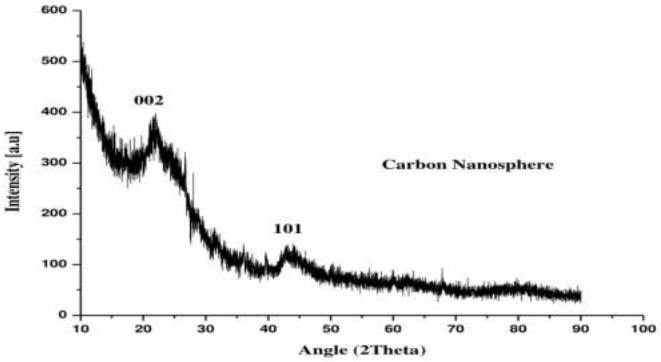

Figure 7d XRD pattern of the carbon nano-spheres synthesized

The XRD results showed two diffraction peaks. The diffraction peaks at about 2θ = 22.11481° (d = 4,0163Å) and 42.95507° (d = 2,1039Å) are attributed to the (002) and (101) planes of graphite structure respectively. This confirmed the CNS structure. The peaks (002) in PKF confirmed the hemicellulose and high lignin contents in the material. These two peaks 2θ = (~22°) and (~43°) showed low crystallinity of the CNS samples and a large amount of amorphous carbon structures. The FTIR spectrum of PKF, carbonized PKF, AC and synthesized carbon nano-spheres produced from PKF is shown in Figure 8a-d. The synthesized CNS functional groups were studied using FTIR analysis. The peak at 3400 cm^{-1} in the FTIR spectrum was related to the O-H stretching vibration of active alcoholic, phenolic, and carboxylic groups and also contributed by the hydroxyl group in PKF as shown in Figure 8a. Another peak between 2800 cm^{-1} and 2900 cm^{-1} was attributed to C-H stretching vibration functional groups of CH_2 and-CH_3 as shown in Figure 8a. The ketones, aldehydes or carboxyl peak C = O was observed at 1720 cm^{-1} which represents stretching vibration of the carbonyl groups of the hemicellulose element as shown in Figure 8a-d.

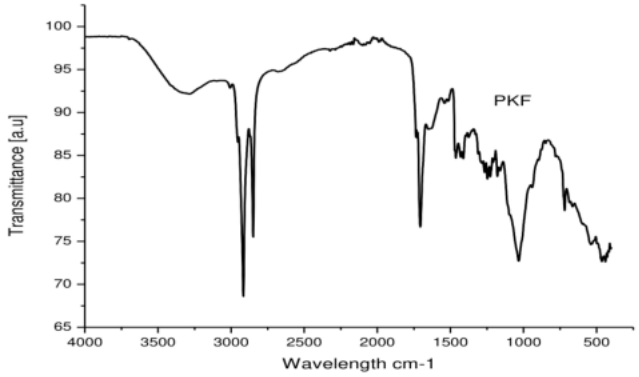

Figure 8a FTIR spectra of Palm kernel fiber (PKF)

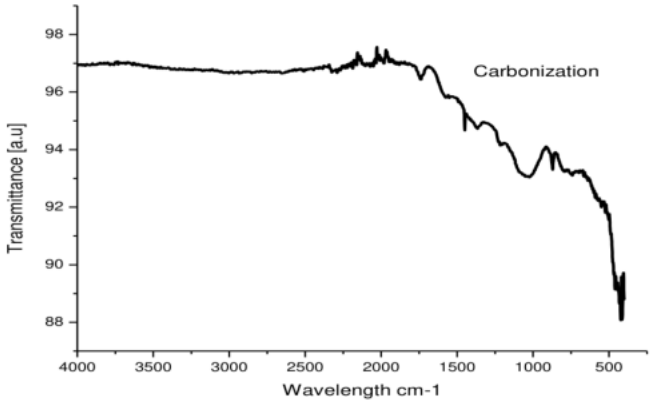

Figure 8b FTIR spectra of carbonized PKF

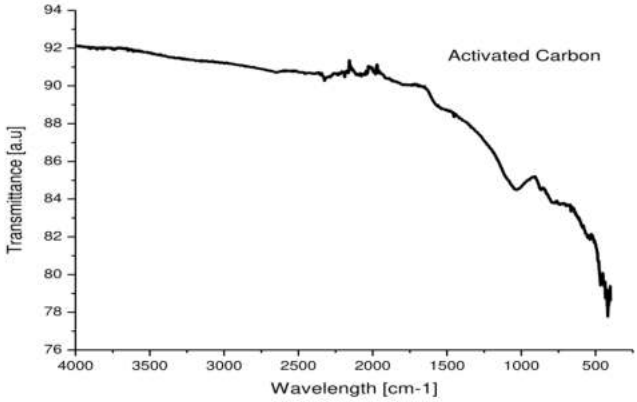

Figure 8c FTIR spectra of activated carbon

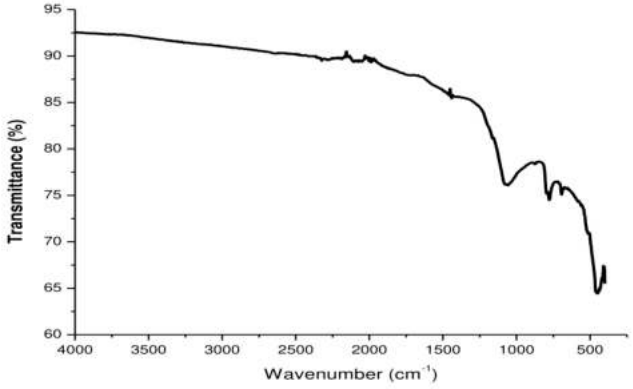

Figure 8d FTIR spectra of synthesized carbon Nano-spheres

The stretching vibrations of aromatics C = C at peak between 1440 cm^{-1} and 1610 cm^{-1} were related to lignin as shown in Figure 8a-d. The peak vibration at 1220 cm^{-1} showed a different quality of lignin components (C = O stretching) [53, 54]. The aromatic peaks C-H out-of-plane bending observed at 693 cm^{-1} and 776 cm^{-1} [55] represent the deformation of the carbons within the aromatic ring, whereas the stretching vibration at band 1071 belongs to C-O (hydroxyl, ester, or ether) [56] as shown in Figure 8a-d. In the CNS spectrum there are no other carbon peaks, indicating that a high purity product has been discovered.

3.4 Thermal Stability

The thermal stability of synthesized CNS material was investigated through TGA analysis (Figure 9).

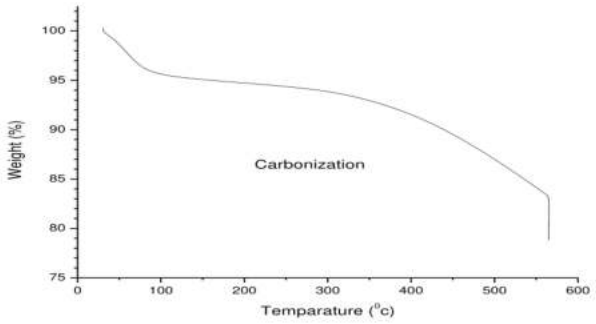

Figure 9a TGA curve of carbonized PKF

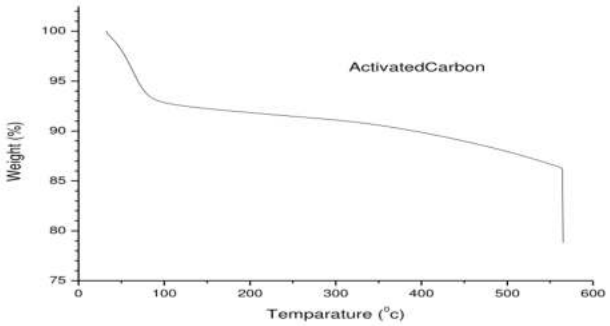

Figure 9b TGA curve of activated carbon

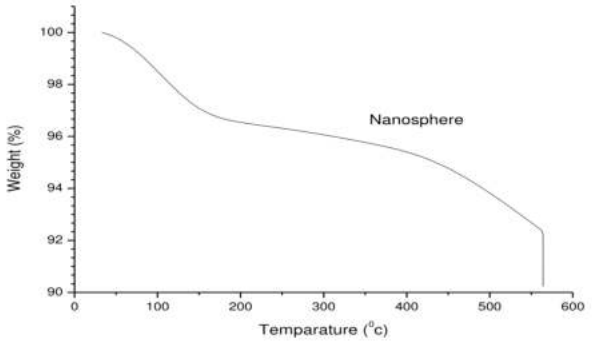

Figure 9c TGA curve of synthesized carbon Nano-spheres

The sample weight was 19.170 mg and was heated from 30 ℃ to 600 ℃ at a rate of 10 ℃/min under a nitrogen flow of 20 ml/min. From Figure 9a-c the first weight loss of 0.2 % for the carbonized material, AC, and synthesized nanosphere samples occurred at approximately between 70 ℃ and 120 ℃ due to the moisture and can be attached to the synthesized sample as a functional group such as an hydroxyl. Another weight loss of 5% occurs at a temperature between 120 °C and 400 °C.

The CNSs weight loss started from the range 400 °C to 560 °C in line with the decomposition of all the carbonaceous material functional groups. These results indicated that in this temperature region, the oxygen functional groups began to discharge, contributing to the activation of aromatization.

4. CONCLUSION

A simple method to synthesize CNS from PKF was reported in this paper. For the preparation of CNSs from palm kernel fiber (a bio-based raw material), an overall time-efficient and cost-effective approach was followed. The process of synthesized CNSs involved carbonization, followed by physical activation under CO_2 gas, and, finally, treating the AC by nitrogen gas through ethanol vapor. The formation of carbon nano-spheres was studied by EDX, XRD, FTIR SEM, TEM, and TGA analysis. SEM analysis recorded CNNSs with diameters between 10 nm and 60 nm. The findings also showed that the CNS were spheres with smooth surfaces. Carbon dioxide (CO_2) and carbon monoxide (CO) were decomposed from oxygen-containing functional groups through the thermal decomposition of CNSs. This method makes CNS preparation easier, sustainable, non-toxic and more cost-effective. The synthesized CNS has potential for use as reinforcement material in brake pad applications due to its simple manufacturing process, non-toxicity and cost-effectiveness.

REFERENCES

[1] Maleque M. and Atiqah, A. Development and Characterization of Coir Fibre Reinforced Composite Brake Friction Materials. *Arabian Journal for Science and Engineering,* 38, 2013, pp. 3191-3199. https://doi.org/10.1007/s13369-012-0454-4

[2] Nam, T. H., Ogihara, S., Tung, N. H. and Kobayashi, S. Mechanical and Thermal Properties of Short Coir Fibre Reinforced Poly (Butylene Succinate) Biodegradable Composites. *Journal of Solid Mechanics and Materials Engineering,* 5, 2011, pp. 251-262. https://doi.org/10.1299/jmmp.5.251

[3] Ikpambese, K., Gundu, D. and Tuleun, L. Evaluation of Palm Kernel Fibers (Pkfs) for Production of Asbestos-Free Automotive Brake Pads. *Journal of King Saud University-Engineering Sciences,* 28, 2016, pp. 110-118. https://doi.org/10.1016/j.jksues.2014.02.001

[4] Lee, J., Ishak, Z. M., Taib, R. M., Law, T. and Thirmizir, M.A. "Mechanical, Thermal and Water Absorption Properties of Kenaf-Fiber-Based Polypropylene and Poly (Butylene Succinate) Composites," *Journal of Polymers and the Environment,* 21, 2013, pp. 293-302. https://doi.org/10.1007/s10924-012-0516-4

[5] Afolabi, M., Abubakre, O., Lawal, S. and Raji, A. Experimental Investigation of Palm Kernel Shell and Cow Bone Reinforced Polymer Composites for Brake Pad Production. *International Journal of Chemistry and Materials Research,* 3, 2015, pp. 27-40. https://doi.org/10.18488/journal.64/2015.3.2/64.2.27.40

[6] Ibhadode A. O. A., and Dagwa, I. M. Development of Asbestos-Free Friction Lining Material from Palm Kernel Shell. *Journal of the Brazilian Society of Mechanical Sciences and Engineering,* 1, 2008, pp. 1-2. http://dx.doi.org/10.1590/S1678-58782008000200010

[7] Jahan, A., Rahman, J. M., Kabir, M. H., Kabir, M. A., Ahmed, F., Hossain, M. A. *et al.* Comparative Study of Physical and Elastic Properties of Jute and Glass Fiber Reinforced LDPE Composites. *International Journal of Scientific & Technology Research,* 1, 2012, pp. 68-72.

[8] Tserki, V., Matzinos, P. and Panayiotou, C. Novel Biodegradable Composites Based on Treated Lignocellulosic Waste Flour as Filler. Part II. Development of Biodegradable Composites using Treated and Compatibilized Waste Flour. *Composites Part A: Applied Science and Manufacturing,* 37, 2006, pp. 1231-1238. https://doi.org/10.1016/j.compositesa.2005.09.004

[9] Jawaid M. and Khalil, H. A. Cellulosic/Synthetic Fibre Reinforced Hybrid Composites: A Review. *Carbohydrate Polymers,* 86, 2011, pp. 1-18. https://doi.org/10.1016/j.carbpol.2011.04.043

[10] Herawan, S. G., Hadi, M., Ayob, M. R. and Putra, A. Characterization of Activated Carbons from Oil-Palm Shell by CO2 Activation with no Holding Carbonization Temperature. *The Scientific World Journal,* 2013. http://dx.doi.org/10.1155/2013/624865

[11] Khalil, H., Jawaid, M., Firoozian, P., Rashid, U., Islam, A.and Akil, H. M. Activated Carbon from Various Agricultural Wastes by Chemical Activation with KOH: Preparation and Characterization. *Journal of Biobased Materials and Bioenergy,* 7, 2013, pp. 708-714. https://doi.org/10.1166/jbmb.2013.1379

[12] Saba, N., Paridah, T. M., Abdan, K. and Ibrahim, N. A. "Preparation and Characterization of Fire Retardant Nano-Filler from Oil Palm Empty Fruit Bunch Fibers," *BioResources,* vol. 10, pp. 4530-4543, 2015. https://doi.org/10.15376/biores.10.3.4530-4543

[13] Castro, J. B., Bonelli, P. R., Cerrella, E. G. and Cukierman, A. L. Phosphoric Acid Activation of Agricultural Residues and Bagasse from Sugar Cane: Influence of the Experimental Conditions on Adsorption Characteristics of Activated Carbons. *Industrial & Engineering Chemistry Research,* 39, 2000, pp. 4166-4172. https://doi.org/10.1021/ie0002677

[14] Rincon S. and Gomez, A. Comparative Behaviour of Agricultural Biomass Residues during Thermochemical Processing. *Global NEST Journal,* 14, 2012, pp. 111-117. https://doi.org/10.30955/gnj.000866

[15] Pierson, H. O. Handbook of Carbon, Graphite, Diamond and Fullerenes. Park Ridge, NJ: Noyes Publications, 1993.

[16] Lozano-Castello, D., Lillo-Rodenas, M., Cazorla-Amorós, D. and Linares-Solano, A. Preparation of activated Carbons from Spanish Anthracite: I. Activation by KOH. *Carbon,* 39, 2001, pp. 741-749. https://doi.org/10.1016/S0008-6223(00)00185-8

[17] Cuesta, A., Dhamelincourt, P., Laureyns, J., Martinez-Alonso, A. and Tascón, J. D. Raman Microprobe Studies on Carbon Materials. *Carbon,* 32, 1994, pp. 1523-1532. https://doi.org/10.1016/0008-6223(94)90148-1

[18] Figueiredo, J. L., Pereira, M., Freitas, M. and Orfao, J. Modification of the Surface Chemistry of Activated Carbons. *Carbon,* 37, 1999, pp. 1379-1389. https://doi.org/10.1016/S0008-6223(98)00333-9

[19] Cui, G., Hu, Y. S., Zhi, L., Wu, D., Lieberwirth, I., Maier, J. *et al.* A One-Step Approach Towards Carbon-Encapsulated Hollow Tin Nanoparticles and their Application in Lithium Batteries. *Small,* 3, 2007, pp. 2066-2069, 2007. https://doi.org/10.1002/smll.200700350

[20] Zhu, T. Chen, S. J. and Lou, X. W. Glucose-Assisted One-Pot Synthesis of Feooh Nanorods and their Transformation to Fe3O4@ Carbon Nanorods for Application in Lithium Ion Batteries. *The Journal of Physical Chemistry C,* 115, 2011, pp. 9814-9820. https://doi.org/10.1021/jp2013754

[21] Zhu J. and He, J. Facile Synthesis of Graphene-Wrapped Honeycomb Mno2 Nanospheres and their Application in Supercapacitors. *ACS Applied Materials & Interfaces,* 4, 2012, pp. 1770-1776. https://doi.org/10.1021/am3000165

[22] Frackowiak, E. Carbon Materials for Supercapacitor Application. *Physical Chemistry Chemical Physics,* 9, 2007, pp. 1774-1785. https://doi.org/10.1039/b618139m

[23] Zhao, X., Zhu, H. and Yang, X. Amorphous Carbon Supported MoS_2 Nanosheets as Effective Catalysts for Electrocatalytic Hydrogen Evolution. *Nanoscale,* 6, 2014, pp. 10680-10685. https://doi.org/10.1039/C4NR01885K

[24] Chang, B., Tian, Y., Shi, W., Liu, J., Xi, F. and Dong, X. Magnetically Separable Porous Carbon Nanospheres as Solid Acid Catalysts. *RSC Advances,* 3, 2013, pp. 20999-21006. https://doi.org/10.1039/C3RA43208D

[25] Raja P. and Ramkumar, P. Tribological Effects of Multiwall Carbon Nanotube (MWCNT) on Cu Based Hybrid Composite Brake Friction Material for Medium Duty Automotive Applications. SAE Technical Paper 0148-7191, 2018. https://doi.org/10.4271/2018-28-0048

[26] Hwang, H., Jung, S., Cho, K., Kim, Y. and Jang, H. Tribological Performance of Brake Friction Materials Containing Carbon Nanotubes. *Wear,* 268, 2010, pp. 519-525. https://doi.org/10.1016/j.wear.2009.09.003

[27] Oh, W.-K., Yoon, H. and Jang, J. Size Control of Magnetic Carbon Nanoparticles for Drug Delivery. *Biomaterials,* 31, 2010, pp. 1342-1348. https://doi.org/10.1016/j.biomaterials.2009.10.018

[28] Ganeshkumar, M., Ponrasu, T., Sathishkumar, M. and Suguna, L. Preparation of Amphiphilic Hollow Carbon Nanosphere Loaded Insulin for Oral Delivery. *Colloids and Surfaces B: Biointerfaces,* 103, 2013, pp. 238-243. https://doi.org/10.1016/j.colsurfb.2012.10.043

[29] Liu, J., Yang, T., Wang, D.-W., Lu, G. Q. M., Zhao, D. and Qiao, S. Z. A Facile Soft-Template Synthesis of Mesoporous Polymeric and Carbonaceous Nanospheres. *Nature Communications,* 4, 2013, p. 2798. https://doi.org/10.1038/ncomms3798

[30] Gbadeyan, O. J. Low Friction Hybrid Nanocomposite Material for Brake Pad Application. Master's dissertation, Durban University of Technology, Durban, 2017.

[31] Han, T., Wang, H., Jin, X., Yang, J., Lei, Y., Yang, F. *et al.* Multiscale Carbon Nanosphere–Carbon Fiber Reinforcement for Cement-Based Composites with Enhanced High-Temperature Resistance. *Journal of Materials Science,* 50, 2015, pp. 2038-2048. https://doi.org/10.1007/s10853-014-8655-8

[32] Serp, P., Feurer, R., Kalck, P., Kihn, Y., Faria, J. andFigueiredo, J. A Chemical Vapour Deposition Process for the Production of Carbon Nanospheres. *Carbon,* 4, 2001, pp. 621-626. https://doi.org/10.1016/S0008-6223(00)00324-9

[33] Awasthi, S., Awasthi, K., Kumar, R. and Srivastava, O. Functionalization Effects on the Electrical Properties of Multi-Walled Carbon Nanotube-Polyacrylamide Composites. *Journal of Nanoscience and Nanotechnology,* 9, 2009, pp. 5455-5460. https://doi.org/10.1166/jnn.2009.1160

[34] Chen, X.-W., Timpe, O., Hamid, S. B., Schlögl, R. and Su, D. S. Direct Synthesis of Carbon Nanofibers on Modified Biomass-Derived Activated Carbon. *Carbon,* 47, 2009, pp. 340-343. https://doi.org/10.1016/j.carbon.2008.11.001

[35] Terrado, E., Redrado, M., Muñoz, E., Maser, W., Benito, A. and Martínez, M. Aligned Carbon Nanotubes Grown on Alumina and Quartz Substrates by a Simple Thermal CVD Process. *Diamond and Related Materials,* 15, 2006, pp. 1059-1063. https://doi.org/10.1016/j.diamond.2005.10.071

[36] Tempel, H., Joshi, R. and Schneider, J. J. Ink Jet Printing of Ferritin as Method for Selective Catalyst Patterning and Growth of Multiwalled Carbon Nanotubes. *Materials Chemistry and Physics,* 121, 2010, pp. 178-183. https://doi.org/10.1016/j.matchemphys.2010.01.029

[37] Sengupta J. and Jacob, C. Growth Temperature Dependence of Partially Fe Filled MWCNT using Chemical Vapor Deposition. *Journal of Crystal Growth,* 311, 2009, pp. 4692-4697. https://doi.org/10.1016/j.jcrysgro.2009.09.029

[38] Thess, A., Lee, R., Nikolaev, P., Dai, H., Petit, P., Robert, J. *et al.* Crystalline Ropes of Metallic Carbon Nanotubes. *Science,* 273, 1996, pp. 483-487. https://doi.org/10.1126/science.273.5274.483

[39] Tamir S. and Drezner, Y. New Aspects on Pulsed Laser Deposition of Aligned Carbon Nanotubes. *Applied surface science,* 252, 2006, pp. 4819-4823. https://doi.org/10.1016/j.apsusc.2005.06.053

[40] Le Normand, F., Cojocaru, C. S., Ersen, O., Legagneux, P., Gangloff, L., Fleaca, C. *et al.* Aligned Carbon Nanotubes Catalytically Grown on Iron-Based Nanoparticles Obtained by Laser-Induced CVD. *Applied Surface Science,* 254, 2007, pp. 1058-1066. https://doi.org/10.1016/j.apsusc.2007.08.054

[41] Ebbesen, T. and Ajayan, P. Large-Scale Synthesis of Carbon Nanotubes. *Nature,* 358, 1992, p. 220. https://doi.org/10.1038/358220a0

[42] Zhao, T., Liu, Y. and Zhu, J. Temperature and Catalyst Effects on the Production of Amorphous Carbon Nanotubes by a Modified Arc Discharge. *Carbon,* 43, 2005, pp. 2907-2912. https://doi.org/10.1016/j.carbon.2005.06.005

[43] Jourdain V. and Bichara, C. Current Understanding of the Growth of Carbon Nanotubes in Catalytic Chemical Vapour Deposition. *Carbon,* 58, 2013, pp. 2-39. https://doi.org/10.1016/j.carbon.2013.02.046

[44] Mubarak, N., Abdullah, E., Jayakumar, N. and Sahu, J. An Overview on Methods for the Production of Carbon Nanotubes. *Journal of Industrial and Engineering Chemistry,* 20, 2014, pp. 1186-1197. https://doi.org/10.1016/j.jiec.2013.09.001

[45] Annu, A., Bhattacharya, B., Singh, P. K., Shukla, P. and Rhee, H.-W. Carbon Nanotubes using Spray Pyrolysis: Recent Scenario. *Journal of Alloys and Compounds,* 691, 2017, pp. 970-982. https://doi.org/10.1016/j.jallcom.2016.08.246

[46] Matali, S., Khairuddin, S., Sharifah, A. and Hidayu, A. Removal of Selected Gaseous Effluent using Activated Carbon Derived from Oil Palm Waste: An Overview. in 2013 IEEE Symposium on Business, Engineering and Industrial Applications, Kuching, Sarawak, 2013.

[47] Hidayu A. and Muda, N. Preparation and Characterization of Impregnated Activated Carbon from Palm Kernel Shell and Coconut Shell for CO2 Capture. *Procedia Engineering,* 148, 2016, pp. 106-113. https://doi.org/10.1016/j.proeng.2016.06.463

[48] Zhu, Z., Liu, Z., Liu, S., Niu, H., Hu, T., Liu, T. *et al.* NO Reduction with NH3 over an Activated Carbon-Supported Copper Oxide Catalysts at Low Temperatures. *Applied Catalysis B: Environmental,* 26, 2000, pp. 25-35. https://doi.org/10.1016/S0926-3373(99)00144-7

[49] Shamsuddin, M., Yusoff, N. and Sulaiman, M. Synthesis and Characterization of Activated Carbon Produced from Kenaf Core Fiber using H3PO4 Activation. *Procedia Chemistry,* 19, 2016, pp. 558-565. https://doi.org/10.1016/j.proche.2016.03.053

[50] Guo, J., Gui, B., Xiang, S.-X., Bao, X.-T., Zhang, H.-j. and Lua, A. C. Preparation of Activated Carbons by Utilizing Solid Wastes from Palm Oil Processing Mills. *Journal of Porous Materials,* 15, 2008, pp. 535-540. https://doi.org/10.1007/s10934-007-9129-z

[51] Tan, I., Ahmad, A. and Hameed, B. Preparation of Activated Carbon from Coconut Husk: Optimization Study on Removal Of 2, 4, 6-Trichlorophenol using Response Surface Methodology. *Journal of Hazardous Materials,* 153, 2008, pp. 709-717. https://doi.org/10.1016/j.jhazmat.2007.09.014

[52] Kumar, R., Singh, R. K. and Singh, D. P. Natural and Waste Hydrocarbon Precursors for the Synthesis of Carbon-Based Nanomaterials: Graphene and CNTs. *Renewable and Sustainable Energy Reviews,* 58, 2016, pp. 976-1006. https://doi.org/10.1016/j.rser.2015.12.120

[53] Fierro, V., Torné-Fernández, V., Celzard, A. and Montané, D. Influence of the Demineralisation on the Chemical Activation of Kraft Lignin with Orthophosphoric Acid. *Journal of Hazardous Materials,* 149, 2007, pp. 126-133. https://doi.org/10.1016/j.jhazmat.2007.03.056

[54] Parshetti, G. K., Kent Hoekman, S. and Balasubramanian, R. Chemical, Structural and Combustion Characteristics of Carbonaceous Products Obtained by Hydrothermal Carbonization of Palm Empty Fruit Bunches. *Bioresource Technology,* 135, 2013, pp. 683-689. https://doi.org/10.1016/j.biortech.2012.09.042

[55] Lua A. C. and Yang, T. Effect of Activation Temperature on the Textural and Chemical Properties of Potassium Hydroxide Activated Carbon Prepared from Pistachio-Nut Shell. *Journal of Colloid and Interface Science,* 274, 2004, pp. 594-601. https://doi.org/10.1016/j.jcis.2003.10.001

[56] Li, M., Li, W. and Liu, S. Control of the Morphology and Chemical Properties Of Carbon Spheres Prepared From Glucose By A Hydrothermal Method. *Journal of Materials Research,* 27, 2012, pp. 1117-1123. https://doi.org/10.1557/jmr.2011.447

CHAPTER 5: THE EFFECT OF SYNTHESIS TEMPERATURE ON CARBON NANOSPHERES FROM PALM KERNEL FIBER

To cite this article: O. E. Ige, F. L. Inambao, G. A. Adewumi, "The Effect of Synthesis Temperature on Carbon Nanospheres from Palm Kernel Fiber," *International Journal of Engineering Research and Technology*, vol. 13, no. 11, pp. 3099-3108, 2020.

International Journal of Engineering Research and Technology. ISSN 0974-3154, Volume 13, Number 11 (2020), pp. 3099-3108

The Effect of Synthesis Temperature on Carbon Nanospheres from Palm Kernel Fiber

Oluwafemi E. Ige*, Freddie L. Inambao[1], Gloria A. Adewumi

Department of Mechanical Engineering, University of Kwazulu-Natal, Durban, South Africa.

[1]0000-0001-9922-5434 (Freddie Inambao)

Abstract

Carbon nanospheres (CNS) were synthesized successfully from palm kernel fiber activated carbon. Palm kernel fiber (PKF) which is an agro-waste was carbonized followed by physical activation with CO_2, then go along with treated utilizing ethanol vapor at temperature of 700 °C, 850 °C and 1000 °C. The temperature effect on developed synthesized nanomaterials was investigated using scanning Fourier transform infrared microscopy (FTIR), electron microscopy (SEM), energy dispersive x-ray spectroscopy (EDX), transmission electron microscopy (TEM), x-ray diffraction (XRD), and thermo-gravimetric analysis (TGA). The temperatures were varied from 700 °C to 1000 °C with intervals of 150 °C. The SEM results showed highest purity and the largest number of carbon-nanospheres being formed at a synthesis temperature of 1000 °C. The results indicate that CNS diameter, growth rate, crystallinity and density can be affected by increase in temperature. The CNS diameters were found to increase when the synthesis temperature increased. The results of the TEM showed that, within the temperature range of 700 °C to 1000 °C, the CNSs diameter increased continuously from 3 nm to 65 nm. XRD analysis showed that the synthesized carbon nanomaterials were amorphous. In general, the results showed that the synthesis temperature affects the diameter, density and crystallinity of carbon nanomaterials. The synthesis temperature of 1000 °C appears to be the ideal temperature for high quality and high yield CNSs production. The presence of iron (Fe) in the EDX results showed that such synthesized CNSs can be used as reinforcement materials in the manufacture of automobile brake pads.

Keywords: Carbon nanosphere, characterization, bio-based precursors, temperature

I. INTRODUCTION

The increasing need for more environmentally friendly and biodegradable material requires the development of nanomaterials.

Since Iijima's innovation of multi-walled carbon nanotubes in 1991, global enthusiasm in academic and industrial circles for carbon nanotubes (CNTs) and their distinctive characteristics has been high because of their nanoscale structures [1] Carbon-based nanostructures with various morphologies have created great interest in scientific research due to their outstanding and distinctive characteristics. The attention of scientists around the world has been drawn to research on new material technology, development and improvement of materials properties and the discovery of alternative precursors that impart the desired properties to the materials.

Chemical vapor deposition (CVD) [2, 3], laser ablation [4], and arc discharge [5] are the commonly used synthesis methods to produce CNTs. Among the variety of synthetic methods, CVD is the most effective technique for large-scale CNTs [6, 7]. The capability to grow nanotubes exactly on the nanomaterials by using the CVD method allows sufficient control for production of high purity nanotubes. The quantity of carbon that enables better CNT nucleation is reduced as particle size decreases [8-10].

Since the innovation of carbon nanotubes, carbon nanoparticles carbon nanofibers, and carbon nanostructures are becoming commercially significant and their importance has grown rapidly over the past decade. CNTs have been widely examined due to their unique mechanical, magnetic and electronic properties [11-13]. The CNTs are regarded as possible filler materials to enhance the mechanical properties as well as physical properties of polymer composites [14]. CNT applications are eco-friendly and offer good opportunities as well as new technology for various sectors which include biotechnology, aerospace, automotive and electronics industries.

By using ethanol as the carbon resource in the CVD method has positive impacts for instance, low temperature reaction, high product purity and the potential for reduced cost for large-scale production [15, 16]. Generally, the temperature of synthesis is a factor affecting crystallinity [17], density [18], diameter, growth rate [17-20], yield, morphology [21, 22] and purity [23] of nanomaterials. Investigations of temperature effect on CNT growth parameters have shown that the temperature range from 800 °C to 1000 °C is the optimal temperature which results in the highest yield of CNTs [23, 24]. When the temperature increases from 750 °C to 950 °C the

diameter, crystallinity, growth rate and density of CNTs can be measured and high levels of crystalline perfection can be achieved at temperature of 950 °C [18]. The interchange of temperature from 700 °C to 830 °C has been shown to result in structural defects in CNTs and graphite sheets grown [25].

Muataz et al. [20] varied the temperatures reaction of CNT from 500 °C to 850 °C and the result indicated that CNT growth was seen from 600 °C and high purity was obtained at a temperature of 850 °C. The study by Lee et al. [19] showed that the thicker layers of the compartment appear at 1100 °C more frequently. When the temperature gradually increased from 850 °C to 1100 °C, the comparative amount of crystalline graphitic sheets also increased. Toussi et al. [26] showed that a small amount of CNTs were formed at temperatures below 700 °C, while more shapeless carbons were formed in the CNTs at temperatures above 900 °C. Their study found that the optimum temperature for CNT growth was between 800 °C and 900 °C and the ideal temperature growth was at 850 °C. Pham et al. [27] reported that below the synthesis temperature of 800 °C, tube length growth and diameter was minimal, while the highest tube crystallinity was achieved at a temperature range between 800 °C and 840 °C. Madani et al. [17] presented the temperature effect variation on the growth of CNTs utilizing CVD and the results revealed that the CNTs diameters increased when the temperature of synthesis increased, but the CNTs growth crystallinity decreased.

Zhao et al. [28] revealed that the CNTs multiplied quicker as the temperature increased, while the catalyst showed a significant increase for a little while, followed by a decrease. As temperature increased from 805 °C to 830 °C, the crystallinity improved a little while the height and the yield of CNT forests tripled in the course of increasing from 800 °C to 1100 °C. Shamsudin et al. [24] achieved 99.99 % optimum growth at a temperature of 900 °C. According to Jiang and Lan [29], at a low temperature of 450 °C, CNTs can be synthesized from carbonaceous solids, as opposed to high temperature synthesis. This paper presents the result of the temperature effect on synthesis of carbon nanomaterials at 700 °C, 850 °C and 1000 °C for 30 min treated with ethanol vapor. In the manufacturing of CNTs, nanospheres and nanosheets, the synthesis temperature performs a significant role. Generally, the temperature of synthesis is a factor that affects the final purity, morphology and yield of a nanomaterial.

II. EXPERIMENTAL PROCEDURE

The material used in this study was palm kernel fiber (PKF) of the *Elaeis guineensis* species and was obtained from a local palm oil mill in Ado Ekiti, Nigeria, after extraction of the oil. PKF was washed with hot water to remove leftover red oil and sun dried for 60 days. The PKF were placed in a quartz tube (heat-resistant) in a horizontal (MTF 12/38/400: Model) tube furnace to produce carbon nanospheres (CNSs). PKF carbonization was done at 600 °C for 120 mins in an inert atmosphere. In the experimental procedure 15 g of PKF was stored in a quartz tube and heated to the desired reaction temperature in a horizontal furnace at 5 °C min^{-1} heating rate until carbonized. This was followed by physical activation with CO_2, for 60 min, then treated at 700 °C, 850 °C and 1000 °C for 30 min using ethanol vapor. Ethanol was used to generate an aerosol using an ultrasonic (GMH-200: Type) air humidifier which operated at 50 Hz. Nitrogen gas was gone through the aerosol in order to generate a inert air for reaction and deliver the of drops aerosol to the reactor space. At the desired temperature the aerosol line was shut, allowing the nitrogen gas to cool the system.

III. MATERIAL CHARACTERIZATION

The morphology of the synthesized CNS was investigated utilizing FEGSEM (Zeiss, Germany Model: Ultra Plus) with an EDX in-built which was used for elemental composition analysis. The sample phase identification and microstructure were examined using JEOL 1400 TEM and a JEOL HRTEM 2100 model at a speed voltage of 20 kV. The sample of CNS needed for HRTEM measurements was approximately 0.0002 g mixed with ethanol using an 80 Hz Watt transistorized sonic cleaner for 20 min. The TEM preparation of the carbon nanosphere mixed with ethanol was achieved by putting a droplet of the solution on formvar with painted 150 meshes of copper grids. The TEM sample was dry at lower temperature and watched at 100 kV speed voltage.

For TEM, the iTEM software and Gatan camera were used to store and process the images taken digitally from the camera (Megaview III). The backloading preparation method was used for the preparation of XRD samples of the PKF nanomaterial. The Netherlands made PANalytical Empyrean Diffractometer with a Co-Kα radiation and X'Celerator detector was used to analyze the sample. The generator configuration was 40 kV and 40 mA. A PerkinElmer Product was used to study the FTIR of the sample. A PerkinElmer synchronized thermal analyzer (STA) 6000 was used to establish the thermal stability of the synthesized nanosphere material.

IV. RESULTS AND DISCUSSION

A. SEM

Increasing the temperature of the furnace can increase the frequency of impact of the elements found in carbon activated PKF resulting in various structures being formed as shown in Fig. 1.

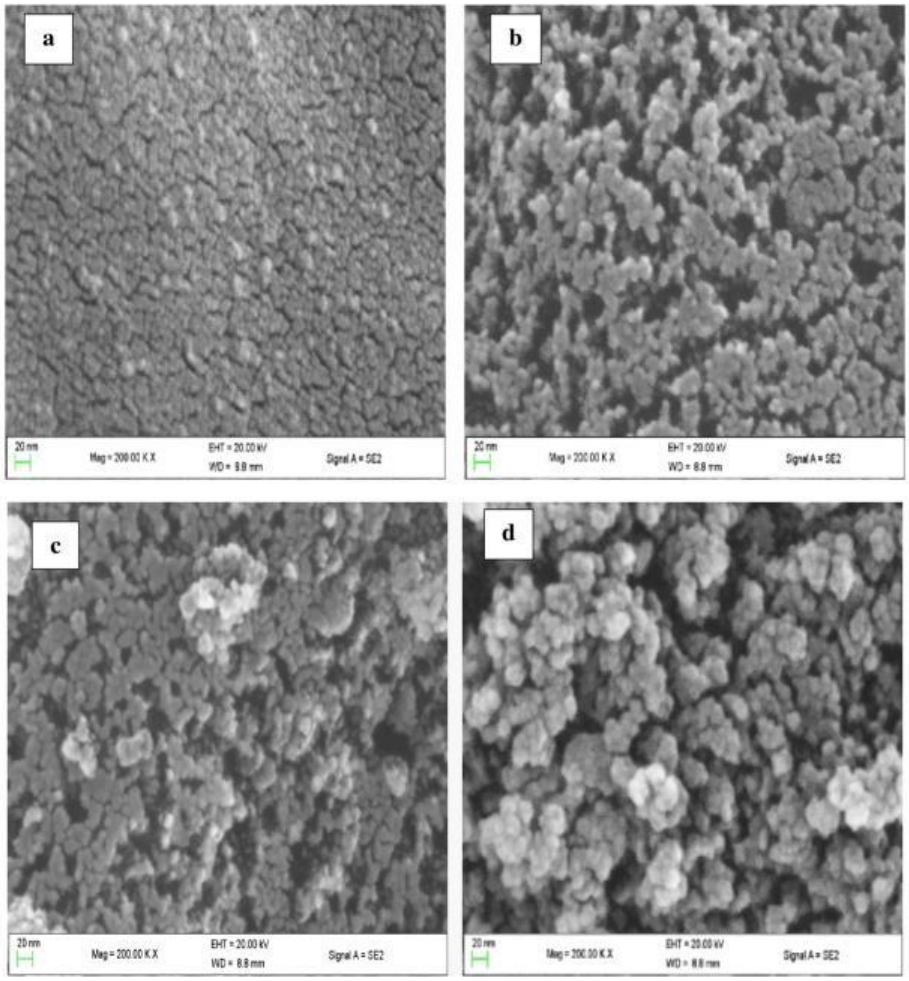

Fig. 1 SEM images of (a) PKF carbon activated, synthesized nanomaterials at (b) 700 °C (c) 850 °C and (d) 1000 °C

Fig. 1 (b-d) shows the SEM images of CNS produced from PKF at different buildup temperatures 700 °C, 850 °C and 1000 °C. FEGSEM and HRTEM were used to characterize the temperature effect on the synthesized nanomaterials developed. Fig. 1a shows the SEM image of physically activated PKF produced at 850 ° C for 60 min under CO_2. The micrographs SEM image from Fig. 1b to d present carbon sheets, carbon-nanoparticles (CNPs) and carbon-nanospheres (CNSs). The SEM image at 700 °C from Fig. 1b indicates the presence of tiny sphere particles or sheet-like structure grown with irregular morphology. Low density nanospheres with small diameter ranging from 3 nm to 20 nm were formed. This indicates that the synthesis temperature of 700 °C was not enough to produced carbon nanospheres/nanotubes. At the temperature of 850°C, a small sphere-like morphology was noticed as shown in Fig. 1c. At this temperature several carbon nanospheres with small quantities of amorphous carbon were developed.

The results showed a huge increase in hydrocarbon pyrolysis with particle distribution size ranging 10 nm to 65 nm when the synthesis temperature increased from 850 °C to 1000 °C, as shown in Figure 1d. Increasing the temperature to 1000 °C produced clean nanospheres with aligned and uniform diameter distribution size. The SEM micrographs of all developed

samples display a strong difference in the structure of the synthesized materials at the different temperatures. Thus, the morphological analysis under atmospheric pressure showed that the temperature build-up played an important role in the synthesis of uniform CNSs.

B. Elemental Composition Analysis

A FEGSEM built-in with EDX was employed to analyze the activated carbon elemental composition and synthesized nanomaterials at different temperatures. Table I shows the PKF activated carbon EDX analysis and synthesized nanomaterials at temperatures of 700 °C, 850 °C and 1000 °C. From the table there is a high carbon content in all samples with the highest yield for all synthesis temperatures from nanomaterials synthesized at 850 °C. After the carbonized PKF was physically activated at 850 °C under CO_2, it was followed by treatment for 30 min with ethanol vapor to produce carbon nanospheres. This temperature has the highest carbon nanomaterials yield because the synthesis temperature is high enough to produce carbon nanospheres while also decreasing amorphous carbon. In addition, EDX showed a high carbon content of 88.10 %, 90.06 % and 89.40 % respectively in all synthesized carbon nanosphere samples; this confirmed the treatment of the nanomaterials with ethanol vapor. From Table I it is evident that as the synthesis temperature increased the oxygen content reduced which agrees with previous results obtained [30].

Table I. EDX analysis of PKF carbon activated, and nanomaterials at the different temperature

Element	**Activated Carbon Wt.%**	**Nanomaterial Synthesized at 700°C Wt.%**	**Nanomaterial Synthesized at 850°C Wt.%**	**Nanomaterial Synthesized at 1000°C Wt.%**
C	87.59	88.10	90.06	89.40
O	7.80	6.85	6.76	6.52
Mg	0.79	0.76	0.54	1.27
Al	0.32	0.97	0.52	1.17
Si	0.97	1.29	0.57	-
K	1.09	1.53	1.20	1.12
Fe	0.23	0.50	0.34	0.52
Cu	1.20	-	-	-
Total	100.00	100.00	100.00	100.00

The elemental composition in PKF carbon activated for CF included oxygen (O), carbon (C), and potassium (K), which are normally originated from plants. The existence of oxygen in all samples developed can be credited to the carbonized PKF physically activated under CO_2 and ethanol aerosol. The existence of silicon (Si) was noticed in the synthesized nanomaterials which can be attributed to the reaction of the material in the quartz tube. The results from both FESEM and EDX established that the samples produced form PKF activated carbon are carbon nanospheres. The presence of iron (Fe) in all the samples as seen in Table I showed that the nanomaterial can be used as additive materials in the production of brake pads.

C. High-Resolution TEM (HRTEM)

The TEM analysis was conducted using a JEOL HRTEM 2100 model to study the morphological changes and the material deflections and the actual transition that appears in the carbon nanomaterial structure. Fig. 2(c) shows small quantities of CNSs at 850 °C with particle size distribution as seen in the TEM image varying from 10 nm to 40 nm diameter; however, the sphere structure was not clearly identified. At this temperature, increased numbers of CNSs with a smaller amount of deformation and a higher CNS yield was observed with fewer impurities.

As seen in Fig. 2(c), the TEM images show uniform nanosphere sizes, while some nanospheres have some deformation and are very weak. The TEM at 1000 °C as seen in Figure 2 (d) shows that high purity and high yield CNSs were formed with high agglomeration. The distribution size diameter of nanospheres range from 10 nm to 65 nm, while nanospheres with 25 nm to 35 nm diameter occur at a higher frequency than those of 40 nm to 65 nm diameter.

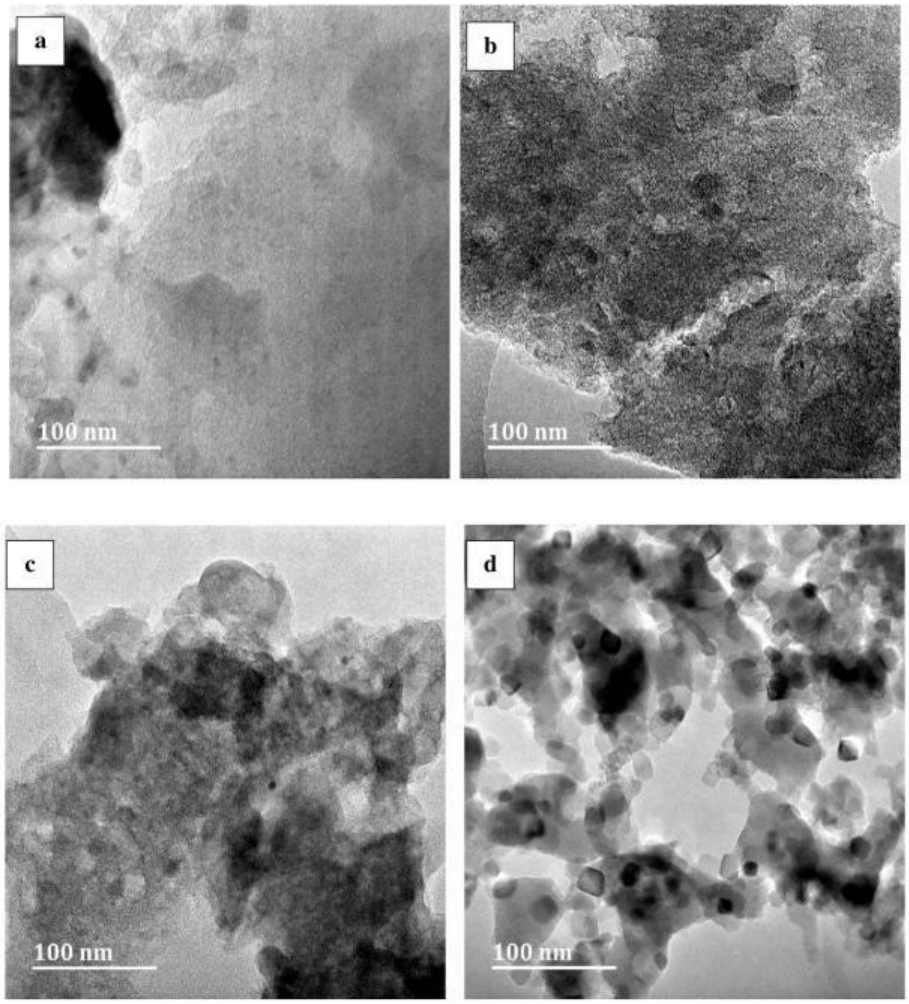

Fig. 2: TEM images of (a) PKF carbon activated, synthesized nano materials at (b) 700 °C (c) 850 °C and (d) 1000 °C

At 700 °C, the absence of carbon nanomaterial growth indicates that the temperature at that level was not adequate high to transform the PKF carbon activated into tubes or spheres. As ethanol vapor was added and the temperature increased, the state of PKF activated carbon content in the tube was modified, thereby activating the carbon nanospheres growth on carbon activated. It was noticed that temperature of 1000 °C is appropriate to develop nanospheres.

D. XRD Analysis

The structural characterization of carbon nanomaterial samples at different synthesis temperatures was achieved using XRD technique using the Netherlands made PANalytical Empyrean Diffractometer including Co-Kα radiation and X'Celerator detector. Fig. 3 is the XRD pattern obtained from activated carbon at 850 °C for 60 min and synthesized nanomaterials at temperature for 30 min. All the synthesized nanomaterials result at 700 °C, 850 °C to 1000 °C displayed two major broad diffraction peaks in Fig. 3 (b-d). The 2Θ value (002) diffraction peak was found at 22.11°, whereas the (101) diffraction peak was discovered at 42.96°, indicating hexagonal graphite structural planes.

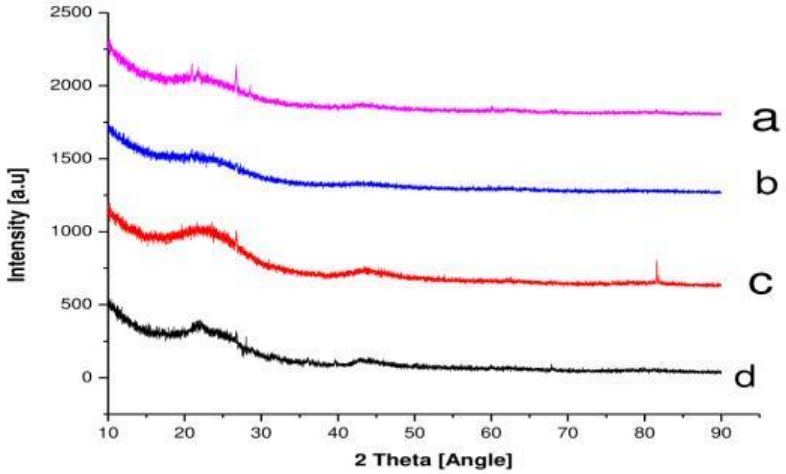

Fig. 3 XRD of (a) PKF carbon activated, synthesized nanomaterials at (b) 700 °C (c) 850 °C and (d) 1000 °C

The peak located at (002) confirmed the presence of lignin and hemicellulose contents found in PKF and all the samples were amorphous in nature. These two peak values exhibit low crystallinity and high amorphous carbon structure of the nanomaterials sample and are in accordance with results from other studies [23, 29].

E. SAED

The HRTEM was utilized to establish the effect of temperature on crystallinity of nanomaterials. Fig. 4 shows the image of the SAED and HRTEM rings of the nanospheres produced in the research. From Fig. 4(a) and (c) it is evident that the CNSs have a strongly regular crystalline structure. The HRTEM reveals a small portion of nanosphere grown at temperature of 850 °C and a graphite structure near the edge of the sphere as shown in Fig. 4(a). Increasing in temperature from 850 °C to 1000 °C, the HRTEM image of CNS showed that most CNSs were formed at unique depths with sphere curves as shown in Fig. 4(c). The SAED pattern has wide diffraction rings that show the presence of nanosphere crystallinity and graphitic nature which agrees with the planes (002) and (101) and displays agreement with the results from XRD.

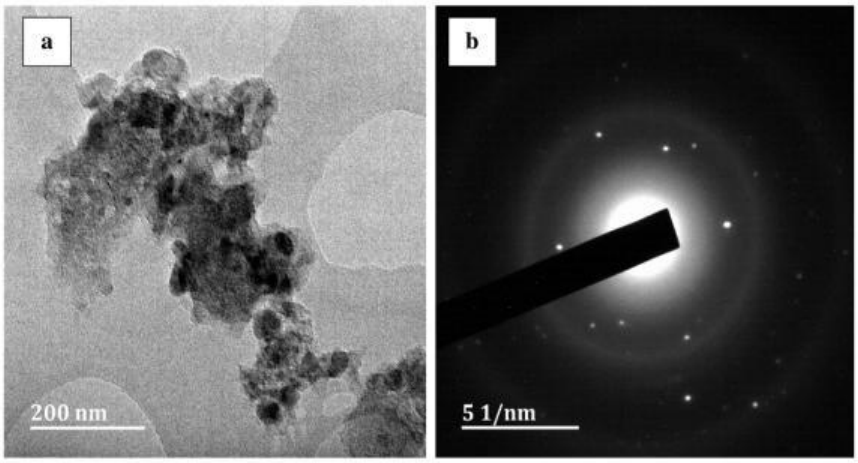

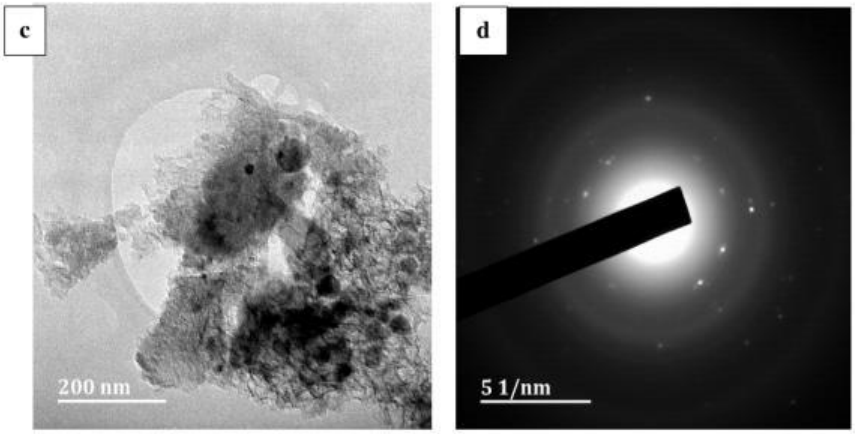

Fig. 4 (a) HRTEM of CNS synthesized at 850°C (b) SAED at 850°C, (c) HRTEM of CNS synthesized at 1000 °C and (d) SAED at 1000°C

The rings brighter areas in Fig. 4b and d agree with the hexagonal graphite reflection 002, whereas the next constant ring observed the diffraction pattern agrees to the hexagonal graphite reflection 101. The SAED pattern from CNS samples at 850 °C as shown in Fig. 4b show some sets of diffuse diffraction and unclear spots, showing that the material has a little crystalline or amorphous carbon, while the diffraction rings from Fig. 4d showed that the CNS samples at 1000 °C present amorphous carbon structures and crystalline together.

F. TGA

TGA was used to examine the thermal stability of the synthesized nanomaterial at different temperatures as shown in Fig. 5. The analysis was carried out under nitrogen gas (20 ml/min flow rate) and heating rate (10 °C/min) from 30 °C to 600 °C. The synthesized nanomaterials at 700 °C, 850 °C and 1000 °C began to vaporize at the temperature of approximately 200 °C, 350 °C and 430 °C respectively. The early weight loss for all the nanomaterials happened at temperatures within 100 °C to 150 °C as a result of the moisture content, as well as loss of the synthesized sample functional group and other non-carbon material present in the sample. The synthesized nanospheres at 700 °C began to decay at a temperature of about 200 °C (thermal decomposition), which was caused by the presence of amorphous carbon at a lower synthesis temperature.

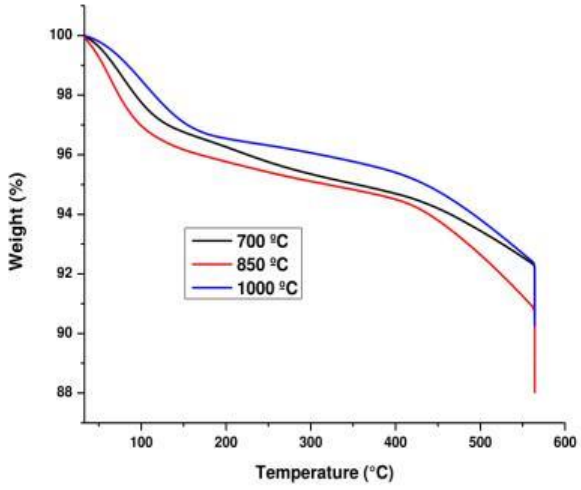

Fig. 5 TGA results for Synthesized nanomaterials at (b)700 °C (c)850 °C and (d) 1000 °C

The initial degradation temperature for synthesized nanospheres prepared at 850 °C started at 350 °C due to less amorphous carbon produced by longer reaction times, which led to production of better nanospheres. At 1000 °C, the synthesis temperature was high enough that almost no amorphous carbon was burned. The nanomaterial synthesized at 1000 °C started degrading at 430 °C which agrees with the decomposition of carbonaceous materials functional groups, while the whole weight loss for synthesized nanomaterials took place at 560°C. This indicates that small diameter nanospheres were formed at low temperature and nanosphere diameter increased when the temperature of the synthesis increased.

In conclusion, the synthesized nanospheres thermal stability improved at 1000 °C. The TGA results agreed with the EDX and SEM results and showed that within this temperature range, functional oxygen groups started to release, causing aromatization activation. The results also provide clear evidence that the crystalline perfection degree of CNSs increases with increasing temperature.

G. FTIR

The FTIR was measured between 400 cm^{-1} to 4 000 cm^{-1} to characterize the synthesized nanomaterial functional groups using Perkin Elmer Product

Fig. 6 shows the FTIR spectrum of activated carbon PKF and synthesized nanomaterials from PKF at 700 °C, 850 °C and 1000 °C for 30 min. From the FTIR result, all the PKF synthesized nanomaterials showed strong peaks at 1071 cm^{-1} to 1220 cm^{-1} which indicates different characteristics of lignin composition (O-H bending vibrations and C-O stretching) groups, which reduced as the temperature increased.

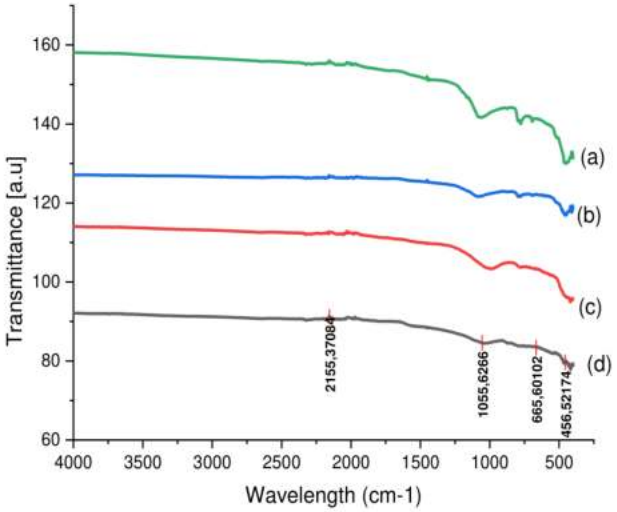

Fig. 6 FTIR of (a) PKF carbon activated, synthesized nanomaterials at (b) 700°C (c) 850°C and (d) 1000°C

The FTIR spectra of all synthesized nanomaterial samples show similar vibrational modes as well as different strengths and energy changes. As shown in Fig. 6 (b) and (c), the FTIR at 700 °C and 850 °C reveals plane peaks of bending C-H compounds between 693 cm^{-1} and 776 cm^{-1}, signifying the carbon bend inside the aromatic ring. When the synthesis temperature increased 850 °C to 1000 °C, the FTIR spectrum shows that there are no other peaks which indicates that the nanomaterial product has high purity.

V. CONCLUSION

Synthesized carbon nanospheres were successfully produced using ethanol vapor through activated carbon made from palm kernel fiber at temperatures of 700 °C to 1000 °C synthesis with 150 °C increase. The SEM analysis results showed highest purity and number of carbon-nanospheres formed at 1000 °C. The results indicate that CNS diameter, growth rate, crystallinity and density can be affected by increase in temperature. Also, the temperature played a major role in the production of high quality and high yield CNSs. We noticed that at 1000 °C, the carbon nanospheres (CNSs) were formed from synthesized nanomaterials of different sizes and shapes. The SEM images showed that the temperature growth affected the CNSs growth rate as well as their diameter and density. As the temperature increased, the increase in growth rate of synthesized CNSs was most likely due to the increased carbon diffusion and reaction rate. It was also discovered that the temperature was an influential factor in regulating the structure of the CNSs.

In conclusion, synthesis temperature greatly affects the diameter, density and crystallinity of carbon nanomaterials synthesized from PKF. The synthesis temperature of 1000 °C can be considered as the ideal temperature for production of high quality and high yield CNSs. The EDX result showed the presence of iron (Fe) in the sample which makes PKF nanomaterials good candidates as additive material in the production of brake pads.

NOMENCLATURE

CNS	Carbon Nanospheres
PKF	Palm Kernel Fiber
CF	Carbon Fiber
O	Oxygen
C	Carbon
K	Potassium
CO_2	Carbon dioxide
SI	Silicon
Fe	Iron
SEM	Scanning Electron Microscope
XRD	X-Ray Diffraction
EDX	Energy Dispersive X-Ray
CVD	Chemical vapor deposition
TGA	Thermo-gravimetric analysis
SAED	Selected Area Electron Diffraction
CNTs	Carbon nanotubes
CNPs	Carbon-Nanoparticles
FEGSEM	Field Emission Gun Scanning Electron Microscope
FTIR	Spectroscopy Fourier Transform Infrared Microscopy
TEM	Transmission Electron Microscopy
HRTEM	High-Resolution Transmission Electron Microscopy

REFERENCES

[1] S. Iijima, "Helical microtubules of graphitic carbon," Nature, vol. 354, p. 56, 1991.

[2] S. Awasthi, K. Awasthi, R. Kumar, and O. Srivastava, "Functionalization effects on the electrical properties of multi-walled carbon nanotube-polyacrylamide composites," J. Nanosci. Nanotechnol., vol. 9, pp. 5455-5460, 2009.

[3] X.-W. Chen, O. Timpe, S. B. Hamid, R. Schlögl, and D. S. Su, "Direct synthesis of carbon nanofibers on modified biomass-derived activated carbon," Carbon, vol. 47, pp. 340-343, 2009.

[4] A. Thess, R. Lee, P. Nikolaev, H. Dai, P. Petit, J. Robert, et al., "Crystalline ropes of metallic carbon nanotubes," Science, vol. 273, pp. 483-487, 1996.

[5] T. Ebbesen and P. Ajayan, "Large-scale synthesis of carbon nanotubes," Nature, vol. 358, p. 220, 1992.

[6] K. Awasthi, R. Kumar, H. Raghubanshi, S. Awasthi, R. Pandey, D. Singh, et al., "Synthesis of nano-carbon (nanotubes, nanofibres, graphene) materials," Bull. Mater. Sci., vol. 34, p. 607, 2011.

[7] C. He, N. Zhao, C. Shi, and S. Song, "Fabrication of carbon nanomaterials by chemical vapor deposition," J. Alloys Compd., vol. 484, pp. 6-11, 2009.

[8] C. L. Cheung, A. Kurtz, H. Park, and C. M. Lieber, "Diameter-controlled synthesis of carbon nanotubes," J. Phys. Chem. B, vol. 106, pp. 2429-2433, 2002.

[9] D. Kondo, S. Sato, and Y. Awano, "Low-temperature synthesis of single-walled carbon nanotubes with a narrow diameter distribution using size-classified catalyst nanoparticles," Chem. Phys. Lett., vol. 422, pp. 481-487, 2006.

[10] W.-H. Chiang and R. M. Sankaran, "In-flight dimensional tuning of metal nanoparticles by microplasma synthesis for selective production of diameter-controlled carbon nanotubes," J. Phys. Chem. C, vol. 112, pp. 17920-17925, 2008.

[11] E. W. Wong, P. E. Sheehan, and C. M. Lieber, "Nanobeam mechanics: elasticity, strength, and toughness of nanorods and nanotubes," Science, vol. 277, pp. 1971-1975, 1997.

[12] M. S. Dresselhaus, G. Dresselhaus, and P. C. Eklund, Science of Fullerenes and Carbon Nanotubes: Their Properties and Applications. Amsterdam: Elsevier, 1996.

[13] M. J. Treacy, T. Ebbesen, and J. Gibson, "Exceptionally high Young's modulus observed for individual carbon nanotubes," Nature, vol. 381, p. 678, 1996.

[14] J. Njuguna, K. Pielichowski, and S. Desai, "Nanofiller- reinforced polymer nanocomposites," Polym. Adv. Technol., vol. 19, pp. 947-959, 2008.

[15] Q. Liu and Y. Fang, "New technique of synthesizing single-walled carbon nanotubes from ethanol using fluidized-bed over Fe–Mo/MgO catalyst," Spectrochimica Acta A, vol. 64, pp. 296-300, 2006.

[16] S. Maruyama, R. Kojima, Y. Miyauchi, S. Chiashi, and M. Kohno, "Low-temperature synthesis of high-purity single-walled carbon nanotubes from alcohol," Chem. Phys. Lett, vol. 360, pp. 229-234, 2002.

[17] S. S. Madani, K. Zare, and M. Ghoranneviss, "Role of growth temperature in CVD synthesis of Carbon

nanotubes from Ni-Co bimetallic catalysts," Int. J. Nano Dimension, vol. 7, pp. 240-246, 2016.

[18] C. J. Lee, J. Park, Y. Huh, and J. Y. Lee, "Temperature effect on the growth of carbon nanotubes using thermal chemical vapor deposition," Chem. Phys. Lett, vol. 343, pp. 33-38, 2001.

[19] Y. T. Lee, J. Park, Y. S. Choi, H. Ryu, and H. J. Lee, "Temperature-dependent growth of vertically aligned carbon nanotubes in the range 800− 1100° C," J. Phys. Chem. B, vol. 106, pp. 7614-7618, 2002.

[20] A. Muataz, F. Ahmadun, C. Guan, E. Mahdi, and A. Rinaldi, "Effect of reaction temperature on the production of carbon nanotubes," Nano, vol. 1, pp. 251-257, 2006.

[21] J. O. Alves, J. A. S. Tenório, C. Zhuo, and Y. A. Levendis, "Characterization of nanomaterials produced from sugarcane bagasse," J. Mater. Res. Technol., vol. 1, pp. 31-34, 2012.

[22] I. Abdullahi, N. Sakulchaicharoen, and J. E. Herrera, "Selective synthesis of single-walled carbon nanotubes on Fe–MgO catalyst by chemical vapor deposition of methane," Diamond Relat. Mater., vol. 41, pp. 84-93, 2014.

[23] N. Jeong, Y. Seo, and J. Lee, "Vertically aligned carbon nanotubes synthesized by the thermal pyrolysis with an ultrasonic evaporator," Diamond Relat. Mater., vol. 16, pp. 600-608, 2007.

[24] M. Shamsudin, N. Asli, S. Abdullah, S. Yahya, and M. Rusop, "Effect of synthesis temperature on the growth iron-filled carbon nanotubes as evidenced by structural, micro-raman, and thermogravimetric analyses," Adv. Condens. Matter Phys., vol. 2012, 2012.

[25] L. Sun, S. Xie, J. Mao, Z. Pan, B. Chang, W. Zhou, et al., "Effects of temperature oscillations on the growth of carbon nanotubes by chemical vapor deposition," Appl. Phys. Lett., vol. 76, pp. 828-830, 2000.

[26] M. Sani, M. Rahman, M. Noor, K. Kadirgama, and M. Izham, "IOP Conference Series: Materials Science and Engineering," ed: IOP Publishing, 2011.

[27] Q. N. Pham, L. S. Larkin, C. C. Lisboa, C. B. Saltonstall, L. Qiu, J. D. Schuler, et al., "Effect of growth temperature on the synthesis of carbon nanotube arrays and amorphous carbon for thermal applications," Physica Status Solidi (a), vol. 214, p. 1600852, 2017.

[28] B. Zhao, Y. Liang, C. Jiang, J. Li, and J. Yang, "Effects of growth temperature on carbon nanotube forests synthesized by water-assisted chemical vapor deposition," Nanosci. Nanotechnol. Lett., vol. 6, pp. 488-492, 2014.

[29] Y. Jiang and C. Lan, "Low temperature synthesis of multiwall carbon nanotubes from carbonaceous solid prepared by sol–gel autocombustion," Mater. Lett., vol. 157, pp. 269-272, 2015.

[30] S. Alam, S. Bangash, and F. Bangash, "Elemental analysis of activated carbon by EDS spectrophotometry and X-rays diffraction," J. Chem. Soc. Pak, vol. 31, pp. 46-58, 2009G.

CHAPTER 6: DEVELOPMENT OF BIO-BASED HYBRID NANOCOMPOSITES FOR BRAKE PAD APPLICATION

To cite this article: O. E. Ige, F. L. Inambao, and O. J. Gbadeyan, "Development and Study of Tribological Performance of Bio-Based Hybrid Nanocomposites for Brake Pad Application," *International Journal of Mechanical and Production Engineering Research and Development* (IJMPERD). ISSN (P): 2249-6890; ISSN (E): 2249-8001. Vol. 11, Issue 2, Apr 2021, 89-106

International Journal of Mechanical and Production Engineering Research and Development (IJMPERD)
ISSN (P): 2249–6890; ISSN (E): 2249–8001
Vol. 11, Issue 2, Apr 2021, 89–106

DEVELOPMENT AND STUDY OF TRIBOLOGICAL PERFORMANCE OF BIO-BASED HYBRID NANOCOMPOSITES FOR BRAKE PAD APPLICATION

OLUWAFEMI E. IGE, PROFESSOR FREDDIE L. INAMBAO & OLUWATOYIN J. GBADEYAN

Department of Mechanical Engineering, University of KwaZulu-Natal, Durban, South Africa

ABSTRACT

In this study, a novel bio-based hybrid nanocomposite brake pad (BHN) has been developed and investigated to serve as a functional replacement for metallic, ceramic, and hazardous asbestos-based brake pad materials. Carbon nanospheres (CNSs) synthesized from agro-waste were incorporated with other carbon-based constituents and additives to produce brake pads. The tribological, mechanical, and solvent absorption properties of BHN brake pads were examined with caution and compared with conventional (CON) brake pads. In this work, the properties of friction materials varied with CNSs loading made with different parameters; the experimental results showed that the brake pad performance changed with each pad formulation. The BHN brake pad material showed better performance than the CON brake pad in most tests. The friction coefficient (COF) of the BHNs brake pad samples (0.3 to 0.5) was within the standard of SAE J661 CODE. The BHN brake pad (0.18 % to 1.97 %) absorbed lower water content than the CON brake pads (2.02 %), and most BHN brake pads similarly absorbed a smaller amount of oil (0.11 % to 0.42 %) compared to the CON brake pad. Scanning electron microscopy (SEM) image of CON brake pad worn surface was inconsistent with stress yielding surface texture, while homogenous dispersion, wear debris, flakes, and plateaus were observed in the BHN brake pad. These improved properties were attributed to CNSs incorporation and the homogenous dispersion of additives forming a synergistic effect, producing a tougher structure, which eventually improved BHN brake pad performance.

KEYWORDS: Brake pad, wear, carbon nanospheres, friction composite, scanning electron microscope

Received: Dec 15, 2020; **Accepted**: Jan 05, 2021; **Published**: Mar 08, 2021; **Paper Id**.: IJMPERDAPR20219

Original Article

INTRODUCTION

Friction material for automotive braking system application must meet various safety-related guidelines. The expected properties of a brake pad to enable it to perform its function include but are not limited to better tribological properties relating to stopping distance and durability (under regular braking requirements) and fade resistance (at high temperature). Over the years materials that meet this requirement have been designed but challenges remain such as high wear rate, irritating noises, and vibration when these pads are working [1]. Consequently, several experimental designs have been used for commercial brake friction materials to enhance the wear resistance, reduce vibration and eliminate noise when applying brakes [2-7]. The commercial use of a single material never succeeded in meeting the multi-faceted requirements for brake pad application. As a result, multiphase composite materials with up to ten or more components have been used as brake pad friction materials. Materials such as metallic fibers [8-10], organic fibers [11], and ceramic fibers [12] have been used to improve wear resistance and friction stability at high temperature among all the numerous components used at present in commercial brake friction materials. Due to brake pads playing a critical role in vehicle safety, fabricating reliable and secure brake pads has become the focus of friction materials formulation. The polymer-based friction material in automotive braking systems consists of several parts, including friction modifiers, thermosetting binders, reinforcing fibers, and fillers [13]. These additives are incorporated to improve tribological and mechanical

properties and achieve a suitable brake pad for the braking system. Despite several combinations of material used for brake pad production, the use of carbon-based material continues to be preferred because it provides the required properties for brake pad application. In this regard, the introduction of carbon nanotubes (CNTs) as a filler for brake pad material development has been a huge breakthrough in brake pad production.

Studies have shown that the loading of CNTs increases the nominal contact area, enhances mechanical properties, decreases wear rate, and naturally reduces the friction coefficient [14-16] [17]. The effectiveness of CNTs on improving numerous nanocomposites properties makes it an additive of choice for brake pad manufacturing and also for use as alternative fillers in brake pad friction materials [4, 5, 18-20]. The increase in use of CNTs recently is due to its low-density, high rigidity, and high aspect ratios. Hwang et al. [1] investigated the effect of adding CNTs for brake friction materials production. The material compositions were prepared by replacing the barite with 1.7 % wt.%, 4.7 % wt.%, and 8.5 % wt.% of CNT. The results showed that adding CNTs could improve the thermal friction stability of the materials. Simultaneously, the specific wear rate reduced as the CNT content increased in the formation due to the composite reinforcement by CNT and the high temperature produced by CNTs. Besides, the COF was reduced as the CNT content increased, which could be the undispersed bundles of CNT on the contact surface. Lee et al. [21] examined the tribological properties of brake lining materials containing CNTs. The result also showed that additional CNT content enhanced the composite materials wear and thermal stability. In both situations, the COF decreased as the CNT content increased, which may be due to the lubricity of the CNT content. As stated by Han et al. [22], Jang et al. [23], Cho et al. [3], Deshmukh et al. [24], Kim et al. [25], and Gbadeyan and Kanny [6], braking performance (for example, stopping distance and other related tribological properties) fundamentally depend on a series of solid lubricants contained in the brake pads. Bearing this in mind, one those papers selected carbon-based constituents such as bio-based CNSs, binders, friction modifiers, and reinforcement materials based on the standard composition of the brake pad, inherent properties of the material, and compatibility. Multiwall carbon nanotubes (MWCNTs) and carbon nanotubes (CNTs) have demonstrated numerous advances in the properties of nanocomposites as alternate brake friction materials [4]. This output may be attributed to high toughness and high ratios with low density in CNTs. Although CNTs have many advantages, it is an expensive product and increases the production costs [5].

Similarly, limited studies have reported bio-based filler use for brake friction materials application [26]. In this study, carbon nano-spheres (CNSs) with the same properties as CNTs were synthesized from coil fiber and used as a friction modifier, and the reinforcement offered interlocking connections of other fillers to form carbon and carbon bonds. This structure generally enhances the tribological, thermal and mechanical properties of the composite materials [7, 27, 28]. This work investigates the mechanical and tribological properties of bio-based hybrid nanocomposite materials and evaluates existing brake pad material.

MATERIALS AND METHODS

Materials

The binder and hardener were purchased from ATM Composite in Durban, South Africa. CNSs were synthesized by UniZulu, South Africa, while friction modifier and reinforcement materials were purchased from Capital Lab Supplies in Durban, South Africa. The CNSs and friction modifiers were used as a friction additives and fillers. CNSs are a kind of black additive, generally used to enhance the properties of polymeric materials such as thermal conductivity, mechanical and tribological properties [29-32]. Thermal stability additives are often used to regulate brake pad wear and friction, while

friction modifiers are generally used as internal lubricants [33, 34]. In this work, reinforcement material was also used to enhance the thermal stability, creep, mechanical strength, and wear resistance of polymer materials [31, 35-37].

Table 1: Bio-Based Hybrid Nanocomposite Composition

	Samples					
	BHN 1	**BHN 2**	**BHN 3**	**BHN 4**	**BHN 5**	**BHN 6**
Materials	Composite in weight percentage (wt. %)					
Binder	98.1	98.6	98	98.6	97.9	98.7
Friction modifier	1	0.3	1	0.5	1	0.3
Carbon nanosphere	0.1	0.3	0.2	0.1	0.3	0.2
Reinforcement	0.8	0.8	0.8	0.8	0.8	0.8
Total	100	100	100	100	100	100

To produce bio-based hybrid nanocomposite material, binder was weighed into a beaker and heated up to 70 °C to reduce the viscosity of the resin and integrate carbon nanospheres and friction modifier. The binder, CNSs, and friction modifier were mixed with a mechanical stirrer at 500 rpm for 60 minutes to achieve uniform distribution. The weight percentage of additives (such as CNSs and friction modifier) was very low in the formulation, as carbon-based additives performance are always important in the polymer matrix. [12]. The biobased hybrid nanocomposite material was cooled down at room temperature and mixed with the catalyst in a ratio of 100 to30% by volume % to ease the process of curing. The reinforcements were added (0.8 wt. %) to the different compositions, as shown in Table 1. The mixture was poured into an open mold. Before pouring into the mold, the inner surface of the plastic mold was coated with wax to enable easy removal of the composite material after two days. The composite was de-molded and tested after it had cured for 14 days.

Hardness

Hardness is the amount of a solid matter resistance to several permanent changes when a compression force or indentation is applied. The hardness of the developed brake pad composite was tested using a Barcol impressor hardness tester produced by the Barber Colman company Illinois, USA. The Barcol impressor hardness tester is good for testing fabricated samples for production control. The hardness samples test was performed following ASTM D 2583 standard test specification [38]. The depth of the indenter point penetration was measured. The hardness test explains the hardness of a material dent point.

The Barcol impressor hardness tester (GYZJ-934-1 model) is widely used to calculate and determine the hardness of composite materials. The impresser has a toughened steel (intender) with an angle of 26º, and a flat point with a diameter of 0.157 mm and was mounted into a hollow spindle and pressed by a spring-loaded plunger. The indenter point of the Barcol impressor was positioned directly towards the face of the developed nanocomposite sample plate. A downward force was applied constantly by hand until the reading indicator reached a maximum, and the value was recorded. The average of the 15 values taken on developed biobased hybrid nanocomposite plate samples at random was reported.

The Absorption Test

The absorption rate of brake pads generally affects braking performance [39]. For that reason, the oil and water absorption of the brake pad samples should be investigated. The methods used in this work to determine the absorption of brake pads are outlined below.

Water Absorption

The water absorption of the brake pad sample was examined to determine the water absorption rate of the material and the effects of water or humidity exposure. Tests were in compliance with the standard test specification of ASTM D 570-98 [40]. The initial weight of each sample was weighed using a digital electronic balance (Kern Germany model D-72336) with an accuracy of 0.01 g and recorded as (W_0) to determine the water absorption rate. The samples were soaked for 24 hours in water at an ambient temperature. After this the samples were brought out from the water, dried with a dry thick towel, re-weighed, and the new weight was recorded as (W_1). Three samples cut from each brake pad were examined. The average of these three samples was used for graphical presentation and discussion. The water-absorption percentage was determined using equation (1).

$$P_{WA} = \frac{W_1 - W_0}{W_0} \times 100 \quad (1)$$

Where:

P_{WA} = Percentage of water absorption

W_0 = Initial weight of water sample

W_1 = Final weight of water sample

Oil Absorption

The oil absorption rate of the developed brake pad sample and its influence on oil was examined using a digital electronic balance (Kern Germany model D-72336) with accuracy of 0.01 g to weigh the initial weight of each sample and recorded as (W_1). The samples were soaked in engine oil for 24 hours at an ambient temperature. The rating of automotive engine oil used was SAE40. After this the sample was taken from the engine oil, dried with a thick dry towel, re-weighed, and the new weight was recorded as (W_2). Three samples taken from each brake pad developed were used and absorption percentages were recorded. The average of nine samples recorded was used for graphical representations and discussion. The oil absorption percentage was determined using equation (2).

$$P_{OA} = \frac{WO_1 - WO_0}{W_{O0}} \times 100 \quad (2)$$

Where:

P_{OA} = Percentage of oil absorption

WO_0 = Oil sample initial weight

WO_1 = Oil sample final weight

Therefore, as per Edokpia et al. [41], the change between the initial and the final weight of each sample was used to calculate the absorption rate.

Wear Rate

The wear (abrasion) rate refers to the gradual loss of material because of relative motion on the contact surface. An in-house built pin-on-disc tribometer was employed to examine the non-lubricated sliding wear behavior of the bio-based

hybrid nanocomposite samples by varying the Vol.% of carbon nanospheres (0.1 Vol.%, 0.3 Vol.%, 0.3 Vol.%, 0.3, 0.1 Vol.% and 0.2 Vol.%) in accordance with ASTM G-99. The tribometer was designed precisely for wear measurements and friction. The COF was calculated according to the data of frictional force. A digital electronic balance (Kern Germany model D-72336) with accuracy of 0.01 g was used to measure the BHN brake pad samples. The wear test was performed on a 230 mm diameter wear track at different sliding distance from 433.6 m/s to 2168.0 m/s with a fixed load of 30 N and 0.7 m/s sliding speed. The sample wear loss is calculated as the difference between the initial and final weight of the sample. The average of the six samples were recorded. The samples' worn surfaces were investigated using a scanning electron microscope (SEM) to check the wear tracks after the friction test. Based on the wear properties studied, the potential of the wear mechanisms was addressed.

Coefficient of friction

The friction coefficient of the sample friction material is related to the time and conditions of the test at 30 N friction force and a sliding speed of the disc of 0.7 m/s. The sample density data was used to convert the mass loss into volume loss. The specific wear rate and coefficient of friction of the sample were calculated using equation (3) and equation (4), respectively.

$$\kappa = \frac{\Delta V}{\mathrm{N}.\chi} \ \# \tag{3}$$

Where:

κ = Specific wear rate

V = The volume change (in m^3)

χ = Total sliding distance (in m)

$$\mu = \frac{\mathrm{M}}{r.N} \tag{4}$$

Where

μ = Friction coefficient

M = Torque induced in the specimen due to friction (in N-mm)

r = The disc radius (mm)

N = Normal load acting on the specimen (in N) [42].

Structure and Morphology

The worn surface of the bio-based hybrid nanocomposite brake pad was sputter-coated with an ultra-thin gold film before microstructure analysis and then examined with SEM. After wear investigation, the BHN brake pad worn microstructure surfaces were analyzed to determine the wear mechanisms under sliding, using a Carl Zeiss Environmental SEM (EVO HD 15 model) operating 1000 times zoom under controlled atmospheric conditions at 20 kV [43-45].

RESULTS AND DISCUSSION

Hardness

As shown in Table 2, the hardness values of the newly developed and CON brake pads were recorded. The hardness value of the CON was 27.3. In each formulation the variation in hardness values were distinct. This showed that the different formulations of brake pads provided different hardness values. In addition, CON and BHN 4 brake pads had the same hardness values, which shows the same surface rigidity.

Table 2: Hardness Properties of BHN and CON Brake Pads

Biobased Hybrid Nanocomposite Sample	Hardness	Remarks	
CON	27,3		
BHN 1	24,6	-10	
BHN 2	30,7	13	
BHN 3	26,3	-4	
BHN 4	27,3	0	
BHN 5	23,5	-14	
BHN 6	31,7	16	

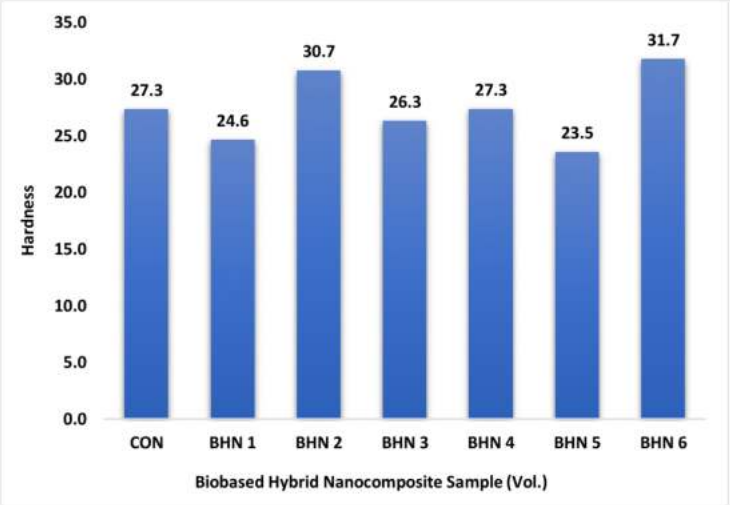

Figure 1: Hardness Properties of BHN and CON Brake Pads.

The high content of friction modifier in the BHN 2 and BHN 6 formulations caused a slight reduction in hardness properties of the developed brake pads. This result is in line with the studies by Gbadeyan [5] and Rukiye et al. [46] in which a higher graphite content reduced the hardness properties of the brake pad. As can be seen in Figure 1, the hardness value of the conventional pad is higher than almost all bio-based nanocomposite brake pad formulations except BHN 2 and BHN 6. The hardness properties of CON brake pads is due to the loading and homogeneous dispersion of the ceramic additive.

The higher hardness values for BHN 2 and BHN 6 can be attributed to the loading of CNSs in the composition. Therefore, the hardness values of BHN 2 and BHN 6 should be observed because they have better surface toughness than conventional brake pads. Thus, the results show that the hardness properties of the BHN and conventional brake pad were similar.

Compressive Modulus

As shown in Figure 2 the values of the compression modulus from the linear fraction of the engineering stress and strain bar was compared in graph form with different BHNs and the CON brake pad formulations. The results show that compared to CON, the BHN 2, BHN 3 and BHN 6 brake pads showed higher elastic modulus. This can be attributed to the homogenous distribution of CNSs and graphite nano-powders in the composition. A synergistic interlocking bond with the matrix was formed by this component, which works together to produce a more stable structure that results in better stiffness. Figure 2 shows that the compressive strains of BHN 1, BHN 4, and BHN 5 were lower when compared with the CON pad. When loaded with additives, the brittle behavior of the BHN brake pads group caused the material to break rapidly during testing.

Table 3: Compressive Modulus of BHN and CON Brake Pads.

Biobased Hybrid Nanocomposite Sample	Compressive Modulus (GPa)	Remarks (%)
CON	9,30	
BHN 1	4,50	-51,6
BHN 2	11,11	19,4
BHN 3	12,32	32,5
BHN 4	5,11	-45,0
BHN 5	6,74	-27,5
BHN 6	10,75	15,6

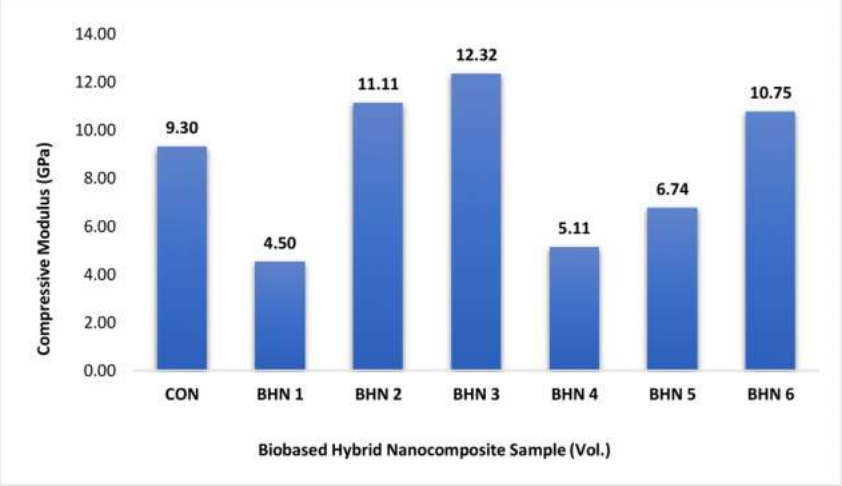

Figure 2: Compressive Modulus of BHN and CON Brake Pads.

The Absorption Test

The absorption rate of brake pads generally affects the braking performance [39]. For that reason, the oil and water absorption of the brake pad samples should be investigated. Therefore, the methods used to determine the absorption of brake pads were tested as laid out below.

Water Absorption

Table 4 shows the conventional and developed brake pad water absorption rate and is illustrated in Figure 3. The water absorption value of the two brake pads had low variation from 0.18 5 % to 2.02 % compared with the value 5.03 % recorded by Dagwa and Ibhadode [47] and 5 % to 9 % by Mayowa et al. [48]. The moisture absorption rate of BHN brake pad samples ranged from 0.18 % to 1.97 % which is low compared to the CON brake pads (2.02 %) as shown in Figure 3. Brake pads BHN 2 and BHN 3 showed water absorption values of 0.18 % and 0.22 %, respectively. The water absorption rate of the two samples were relatively low compared to that of the CON brake pads. This major reduction may be due to the interconnecting bond created by the additives.

Table 4: Water Absorption Rate of BHN and CON Brake Pads.

Biobased Hybrid Nanocomposite Sample	Water absorption (%)	Remarks
CON	2,02	
BHN 1	0,44	78
BHN 2	0,18	91
BHN 3	0,22	89
BHN 4	0,27	87
BHN 5	0,49	76
BHN 6	1,97	3

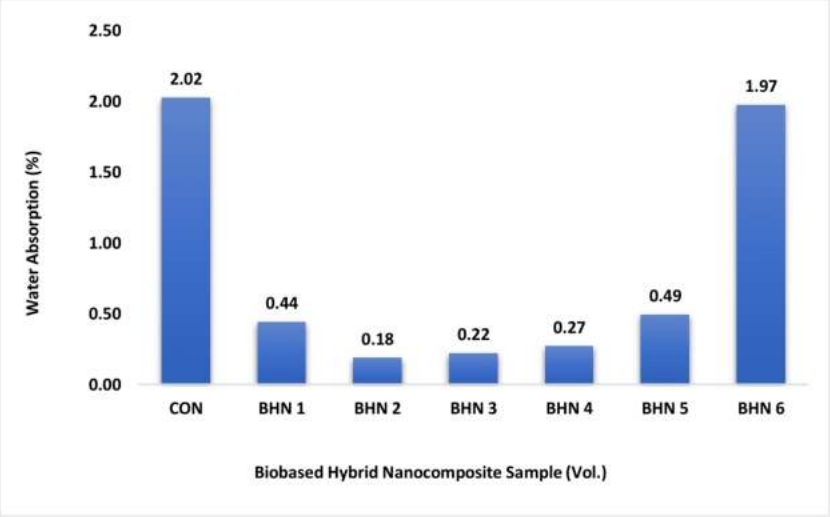

Figure 3: Water Absorption Rate of BHN and CON Brake Pads.

The water absorption of BHN brake pads and CON brake pads compared favorably with the standard conventional brake pad values of 0 % to 4 % [43]. Kim et al. [49] reported that the water absorption increases the weight and thickness of the brake pad, which eventually reduces the brake pad mechanical properties such as compressibility and hardness. These results indicate that the BHN brake pads' low moisture absorption rate prevented performance phenomena variability, for example COF, which agrees with the COF illustrated in Figure 6.

Oil Absorption

Table 5 shows the values of oil absorption rates of the BHN and CON brake pad samples. The results indicate that the oil absorption rate of BHN pads was lower than CON pads. The absorption of both pads was lower than the 2.34 % recorded by Mayowa et al. [48] and the 0.44 % reported by Dagwa et al. [47]. However, under the same conditions, most of the BHN brake pads absorbed a smaller amount of oil than the CON brake pads. The low absorption rate of the BHN samples could be due to the boundary bond being closer to the carbon-based material.

Table 5: Oil Absorption Rate of BHN and CON Brake Pad.

Biobased Hybrid Nanocomposite Sample	Oil absorption (%)	Remarks
CON	0,40	
BHN 1	0,32	20
BHN 2	0,28	31
BHN 3	0,19	52
BHN 4	0,16	60
BHN 5	0,11	71
BHN 6	0,42	-5

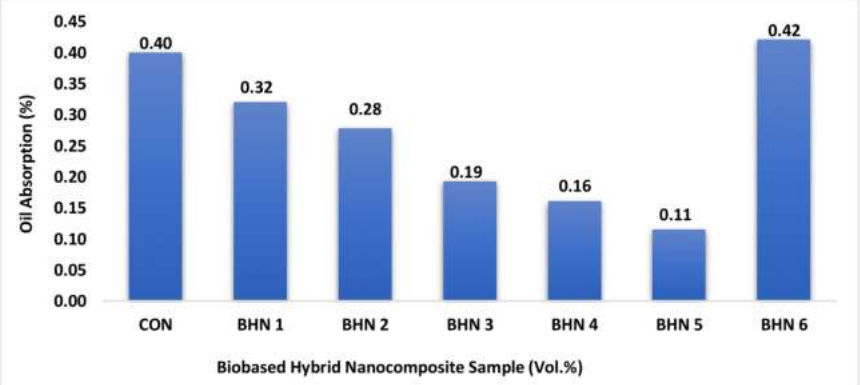

Figure 4: Oil absorption Rate of BHN and CON Brake Pad.

The BHN 6 pads absorbed more oil and had higher absorption capacity than all the rest of the BHN and CON pad samples. The increase in oil absorption could be due to the high loading of graphite nano powder and CNSs. The BHN 5

oil absorption rate was low (0.11 %) which was 71 % higher than the 0.40 % absorption rate achieved by CON pad samples.

Figure 4 shows the oil absorption graph of BHN and CON brakes pads for each sample after 24 hours. Increasing the concentration of CNSs reduces the matrix interface between the fibers. This creates holes that make the flow of fluid possible.

Wear Rate

The wear rate and friction coefficient of BHN brake pad with respect to three different speeds is shown in Table 6. The variation of BHN and CON brake pads wear rate at three different speeds is shown in Figure 5. As a function of speed, the correlation between the wear rates and formulation of brake pads was measured. The wear rate of all BHN and CON samples was reduced as the speed increased. This could be due to the improved heat resistance and toughness of the additives in the samples. Sample BHN 2 and BHN 6 brake pads showed a low wear rate compared to CON due to high surface hardness. This good wear resistance can be attributed to the uniform distribution of CNSs and binder quality in the matrix. In addition, the shared effect developed by carbon-based additives and the bonding properties of epoxy resin provide excellent component bonding that counteracts abrasion.

Table 6: Coefficient of Friction and Wear Rates of bio-Based Hybrid Brake Pads.

Bio-Based Hybrid Nanocomposite	Wear Rates (g/Nm) at Different Speeds (m/s)			Coefficient of Friction At Different Speeds (m/s)		
	433,6	1300,8	2168,0	433,6	1300,8	2168,0
CON	3,1E-08	1,82E-08	1,53E-08	0,564	0,557	0,581
BHN 1	8,3E-08	3,78E-08	2,44E-08	0,454	0,475	0,500
BHN 2	2,28E-08	1,77E-08	1,39E-08	0,525	0,531	0,555
BHN 3	2,00E-08	1,61E-08	1,43E-08	0,375	0,377	0,376
BHN 4	3,84E-08	1,67E-08	1,97E-08	0,320	0,352	0,364
BHN 5	3E-08	1,07E-08	9,53E-09	0,525	0,531	0,555
BHN 6	2,84E-08	9,31E-09	8,25E-09	0,388	0,394	0,423

The correlation of wear rate and speed on BHN 1, BHN 4, and BHN 5 was obvious as the speed increased. As the speed increased the brake pad samples showed a random wear rate. This performance may be due to gradual thermal stress build-up produced as sliding distance increases. Furthermore, it is evident that BHN 2, BHN 3, BHN 6 with 0.3 wt. % of was lower than other samples, including CON brake pads. This can be attributed to the uniform distribution of the CNSs potential resulting in effective wear resistance.

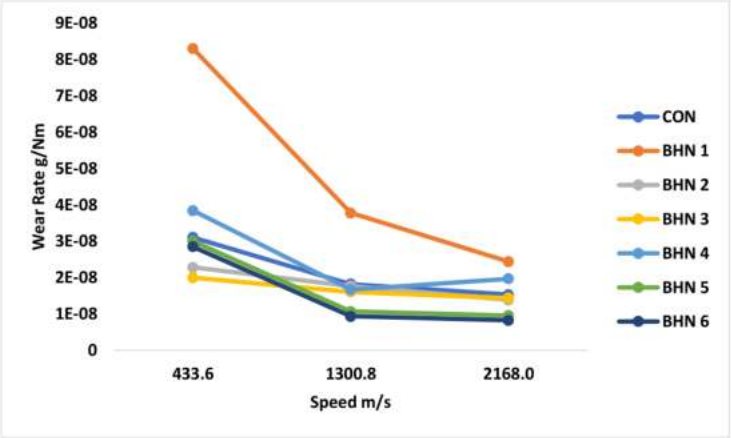

Figure 5: The Variation of Wear Rate With Speed.

This trend of variation of wear rate with speed is consistent with the report by Friedrich et al. [50] where a combination of fiber showed good wear resistance. As reported in the literature, adding CNTs generally improves the thermal and mechanical properties of composite materials. In this respect, the BHN brake pads' lower wear rate could be due to the synergistic functions of graphite nanoparticle (GN) and CNSs which work together to produce a coil resulting in higher strength, better heat absorption, stiffness, and toughness due to more stable structure [4, 50, 51]. The wear test shows that as the CNS content increases, the wear rate reduces. The results also show that by reinforcing the resin and other components, the CNSs improve the wear resistance of friction materials.

According to Ibhadode and Dagwa [52] and Ikpambese et al. [43], increasing the speed increases the contact between the rotor and the brake pads. Therefore, the increase in the wear rate of BHN 1, BHN 4, and BHN 5 are due to the increase in contact between the brake pad and the rotor as the speed increases. This speed increases thermal inductive stress and frictional heat, leading to the breakdown of additives, which finally leads to an increase in wear rates.

Friction Coefficient (COF)

For good brake pad performance, the friction coefficient value of a pad should range between 0.35 and 0.65 according to the SAE J661 CODE standard value recommended for vehicle brake pad application [53]. The friction coefficient obtained for BHN and CON brake pads was found to be between 0.320 to 0.581, which is within the standard of the SAE J661 CODE. Table 6 shows the relationship between the speed and the friction coefficient of BHN brake pads. As shown in Figure 6, the COF varies with different formulations of brake pads. As reported by Lee et al. [21] and Lawrence and Paul [39], this fictional performance in the brake pad material formulations can be due to the abrasive filler and friction modifier loading. Figure 6 shows that the BHN brake pads and CON brake pads keep a constant friction coefficient as the speed changes from 433.6 m/s to 2168 m/s. This development is consistent with research by Jang et al. [37] who reported a stable COF in different brake pad formulations.

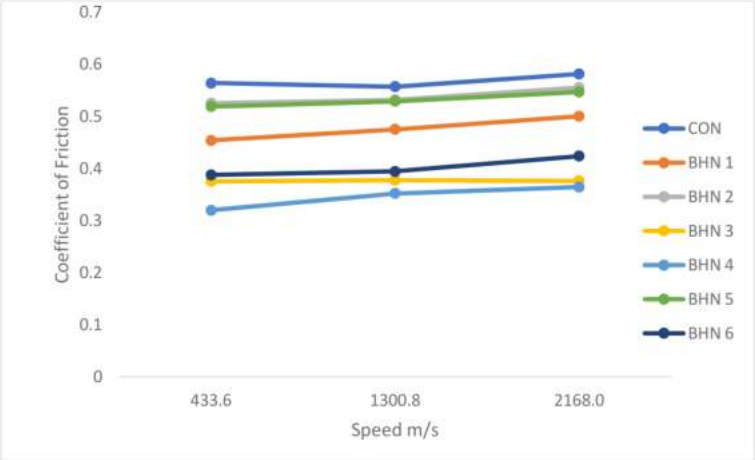

Figure 6: The Coefficient of Friction Variation with Speed.

The BHN brake pads BHN 2 and BHN 5 had a similar friction coefficient value of 0.555 μ which was higher than the COF values of other BHN brake pads. This behavior can be attributed to the amount of CNSs added to the composition. The result is in agreement with Ibhadode and Dagwa [52] who found that high fiber in the composition of brake pads increases COF. Likewise, the stable graphite formation in the composition may be the reason for BHNs' friction coefficient stability. The reduction in BHN 1, BHN 3, BHN 4, and BHN 6 COF may be due to graphite nanoparticles and CNSs interactive lubricating effect and the carbon bonding used as a friction modifier in the formulation of brake pad materials [21, 29].

Scanning Electron Microscopy

The morphology of the worn surface of CON and BHN brake pads filled with CNSs was investigated to determine the tribological performance of the brake pad samples under a SEM. Figure 7 shows the SEM micrographs of CON and BHN brake pad worn surfaces at 500X magnification.

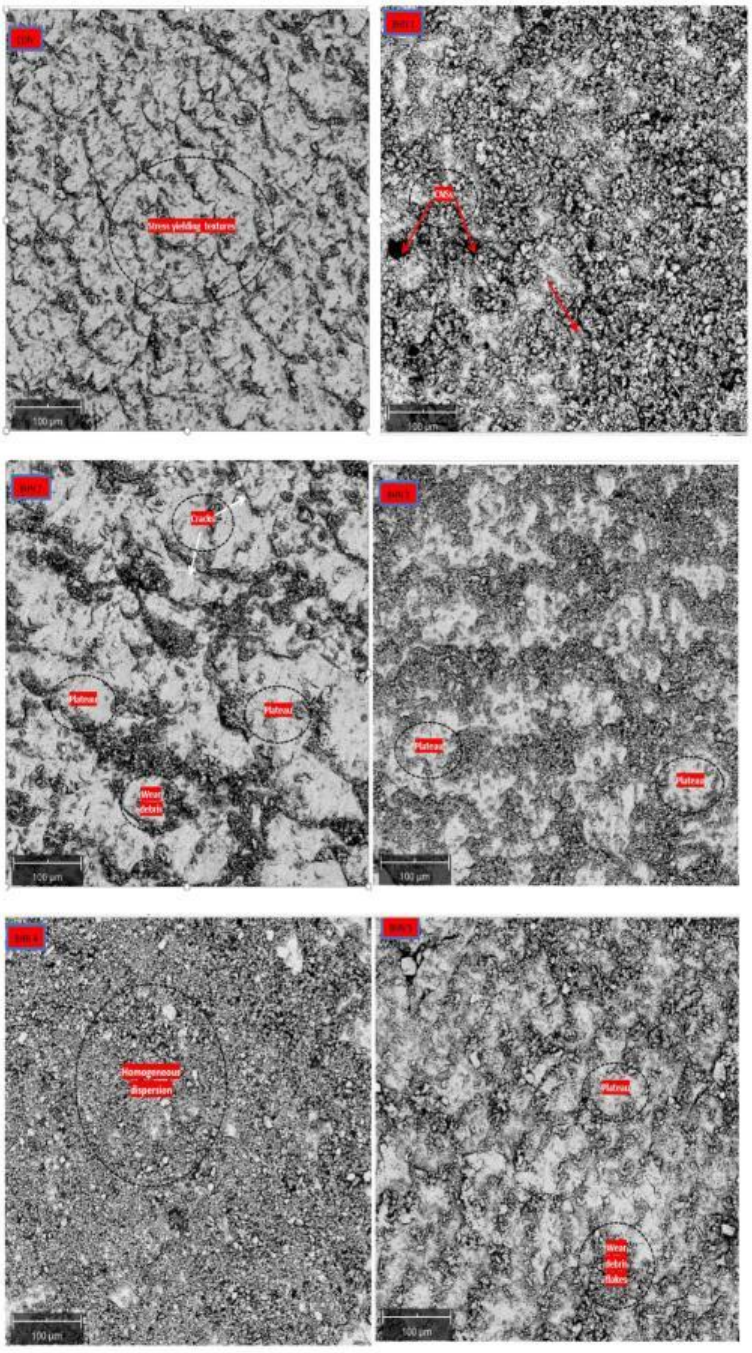
Stress yielding features
CNS
Crack
Plateau
Plateau
Wear debris
Plateau
Plateau
Homogeneous dispersion
Plateau
Wear debris flakes

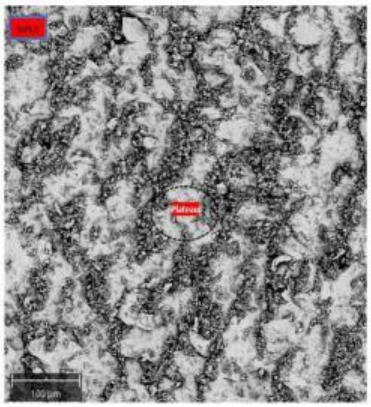

Figure 7: SEM Micrograph of BHN and CON Brake Pads Worn Surfaces.

The order of wear is CON, BHN 1, BHN 2, BHN 3, BHN 4, BHN 5, and BHN 6. In Figure 7 stress yielding textures are observed at the worn surface of the CON brake pad, which could be attributed to the crystallographic textures caused by the deformation of constituents. The stress surface textures may be due to the high amount of tough, abrasive material that controlled abrasion and increased the friction coefficient. Regarding the worn surfaces of the brake pads, homogenous dispersion of CNSs as well as cracks, wear debris, flakes, and plateaus are visible on BHN brake pad worn surfaces. The wear is reportedly structured by the formation of plateaus. The BHN brake pads worn surfaces revealed the structural formation of matrix-enclosed carbon fibers. The cracks were due to the material's toughness and brittleness. BHN1's worn surface clearly shows the presence of CNS bundles, which are tangled and closely embedded in nanocomposite material. Despite all the impact shock, the materials are still intact.

Samples BHN 2 and BHN 5 demonstrated suitable compaction of the wear debris. Therefore, the plateaus were formed at the interface with the metal fiber [54]. The width of plateaus of BHN 2, BHN 3, BHN 5, and BHN 6 nanocomposite samples was about 2 µm, which is in agreement with the 1 µm to 5 µm recorded by Eriksson and Jacobson [55]. The primary plateau was formed as the pads wear, which induces increased contact of the surface area between rotor and brake. As the contact area increases wear occurs and the surface becomes smooth. Therefore, the elastic contact component increases, and the actual contact area increases accordingly. The coefficient of friction increases with the defined applying force [54-57]. The smooth surface noticed on the BHN 4 brake pads worn surface may be due to homogenous dispersion of the carbon-based additive. This output may also be attributed to the constant friction coefficient, as shown in Figure 6, and can improve by keeping the brake pad and rotor contact.

CONCLUSIONS

This study aimed to develop a BHN brake pad application. A mixture of CNSs, graphite nanoparticles, steel nanoparticles, and epoxy resin were used to produce the BHN brake pad samples for solving the braking system problems. CNSs were used to enhance the mechanical and tribological properties of the pad. Graphite nanoparticles were employed as an internal lubricant to control the brake pad wear and friction. Loading of CNSs improved the tribological and mechanical properties of the BHN brake pad. The hardness of the CON brake pad is 27.3, which was slightly higher than the hardness found in

the BHN brake pads except for BHN2 and BHN6 that were 13 % and 16 % tougher. The uniform dispersion of silicon carbide (ceramic additives) in conventional brake pads results in improved hardness properties.

The water absorption value of BHN and CON recorded a lower rate ranging from 0.18 % to 2.02 %, which was better than the water absorption value recorded in the literature [47, 48]. However, the moisture absorption rate of BHN brake pads (0.18 % to 1.97 %) was lower compared to CON brake pads (2.02 %). The oil absorption rate of BHN and CON differs with several formations. Under the same conditions, most BHN brake pads absorbed less oil than CON brake pads. It was noted that BHN 5 had a 0.11 % lower oil absorption rate, which was 71 % better compared to CON brake pads. This performance was due to lower porosity and the interface bond with carbon-based materials. Therefore, the increase in the BHN pads' oil absorption rate can also be attributed to graphite nanoparticles' loading. According to Ibhadode and Dagwa [52], graphite has a porosity that varies from 0.7 % to 53 %. Enticingly, the BHN brake pads with better water/oil absorption properties than the CON pad and other existing pads may show better water/oil resistance when exposed during application.

Furthermore, the BHN brake pad has better tribological properties than the conventional brake pad. The COF of both brake pad samples ranged from 0.3 to 0.5, which was within SAE J661 CODE standard value (0.3-0.6) as recommended for vehicle brake pad application. The homogenous dispersion and increase in the CNSs increased the COF. The interactive effect of carbon additives and the binder quality led to a low wear rate of the BHN brake pads. The SEM image of the worn surface of CON brake pads reveal inconsistent and stress yielding surface textures, while homogenous dispersion, wear debris, flakes, and plateaus are observed in BHN brake pad surfaces. This structural formation provides better resistance to the effectiveness of the interaction of the asperities between the two rubbing surfaces, which eventually result in improved tribological properties. It may be concluded that the tribological properties of the BHN brake pads depend on CNS and graphite nanoparticle loading.

REFERENCES

1. *H. Hwang, S. Jung, K. Cho, Y. Kim, and H. Jang. Tribological performance of brake friction materials containing carbon nanotubes. Wear. 2010, https://doi.org/10.1016/j.wear.2009.09.003.*
2. *Y. C. Kim, M. H. Cho, S. J. Kim, and H. Jang. The effect of phenolic resin, potassium titanate, and CNSL on the tribological properties of brake friction materials. Wear. vol. 264, no. 3-4, pp. 204-210, 2008, https://doi.org/10.1016/j.wear.2007.03.004*
3. *P. Deshmukh, M. Lovell, W. G. Sawyer, and A. Mobley. On the friction and wear performance of boric acid lubricant combinations in extended duration operations. Wear. 2006, https://doi.org/10.1016/j.wear.2005.08.012.*
4. *O. J. Gbadeyan, K. Kanny, and T. Mohan. Influence of the multi-walled carbon nanotube and short carbon fibre composition on tribological properties of epoxy composites. Tribol. Mater. Surf. Interfaces. 2017, https://doi.org/10.1016/j.wear.2005.08.012*
5. *O. J. Gbadeyan. Low friction hybrid nanocomposite material for brake pad application. Master's dissertation, Durban University of Technology, Durban, South Africa, 2017.*
6. *O. J. Gbadeyan and K. Kanny. Tribological behaviors of polymer-based hybrid nanocomposite brake pad. J. Tribol. 2018, https://doi.org/10.1115/1.4038679*
7. *E. F. EL-kashif, S. A. Esmail, O. A. Elkady, B. Azzam, and A. A. Khattab. Influence of carbon nanotubes on the properties of friction composite materials. J. Compos. Mater. 2020; **54**, 2101-2111, 2020.*

8. H. Jang, K. Ko, S. Kim, R. Basch, and J. Fash. The effect of metal fibers on the friction performance of automotive brake friction materials. Wear 2004, https://doi.org/10.1016/S0043-1648(03)00445-9
9. J. Bijwe, M. Kumar, P. Gurunath, and Y. Desplanques. Optimization of brass contents for best combination of tribo-performance and thermal conductivity of non-asbestos organic (NAO) friction composites. Wear. 2008, https://doi.org/10.1016/j.wear.2007.12.016.
10. J. Bijwe and M. Kumar. Optimization of steel wool contents in non-asbestos organic (NAO) friction composites for best combination of thermal conductivity and tribo-performance. Wear. 2007, https://doi.org/10.1016/j.wear.2007.01.125.
11. B. Satapathy and J. Bijwe. Performance of friction materials based on variation in nature of organic fibres: Part I. Fade and recovery behaviour. Wear. 2004, https://doi.org/10.1016/j.wear.2004.03.003.
12. K. H. Cho, M. H. Cho, S. J. Kim, and H. Jang. Tribological properties of potassium titanate in the brake friction material; morphological effects. Tribol. Lett. 2008, https://doi.org/10.1007/s11249-008-9362-x.
13. K. N. Kumar and K. Suman. Review of brake friction materials for future development. J. Mech. Mech. Eng. vol. 3, pp. 1-29, 2017.
14. O. Jacobs, W. Xu, B. Schädel, and W. Wu. Wear behaviour of carbon nanotube reinforced epoxy resin composites. Tribol. Lett. 2006, https://doi.org/10.1007/s11249-006-9042-7.
15. A. B. Sulong, J. Park, N. Lee, and J. Goak. Wear behavior of functionalized multi-walled carbon nanotube reinforced epoxy matrix composites. J. Compos. Mater. 2006, https://doi.org/10.1177/0021998306061305.
16. X. H. Men, Z. Z. Zhang, H. J. Song, K. Wang, and W. Jiang. Functionalization of carbon nanotubes to improve the tribological properties of poly (furfuryl alcohol) composite coatings. Compos. Sci. Technol. 2008, https://doi.org/10.1016/j.compscitech.2007.07.008.
17. T. Sing, A. Patnaik, B. Satapathy, and B. Tomar. Development and optimization of hybrid friction materials consisting of nanoclay and carbon nanotubes by using analytical hierarchy process (AHP) and technique for order preference by similarity to ideal solution (TOPSIS) under fuzzy atmosphere. Walailak J. Sci. & Tech. 2013. https://doi.org/10.2004/wjst.v10i1.357
18. S. Bal and S. Samal. Carbon nanotube reinforced polymer composites—a state of the art. Bull. Mater. Sci. 2007, https://doi.org/10.1007/s12034-007-0061-2.
19. P. J. Harris. Carbon nanotube composites. Int. Mater. Rev. 2004, https://doi.org/10.1179/095066004225010505.
20. O. E Ige, F. L Inambao, and G. A Adewumi. Synthesis of Natural Carbon Nanospheres From Palm Kernel Fiber. Int. J. Mech. Eng. Technol. 2019; **10**, 625-641.
21. K.-J. Lee et al.. Tribological and mechanical behavior of carbon nanotube containing brake lining materials prepared through sol–gel catalyst dispersion and CVD process. J. Alloys Compd. 2009, https://doi.org/10.1016/j.jallcom.2008.08.107
22. S. J. Kim, M. H. Cho, K. H. Cho, and H. Jang. Complementary effects of solid lubricants in the automotive brake lining. Tribol. Internat. 2007, https://doi.org/10.1016/j.triboint.2006.01.022.
23. . Han, L. Huang, J. Zhang, and Y. Lu. Optimization of ceramic friction materials. Compos. Sci. Technol. 2006, https://doi.org/10.1016/j.compscitech.2006.02.027.
24. M. H. Cho, J. Ju, S. J. Kim, and H. Jang. Tribological properties of solid lubricants (graphite, Sb2S3, MoS2) for automotive brake friction materials. Wear. vol. 260, no. 7, pp. 855-860, 2006/04/07/ 2006, doi: https://doi.org/10.1016/j.wear.2005.04.003.

25. *H. Jang and S. J. Kim. The effects of antimony trisulfide (Sb2S3) and zirconium silicate (ZrSiO4) in the automotive brake friction material on friction characteristics. Wear. 2000, https://doi.org/10.1016/S0043-1648(00)00314-8.*
26. *T. Singh, A. Patnaik, B. Gangil, and R. Chauhan. Optimization of tribo-performance of brake friction materials: effect of nano filler. Wear. 2015 https://doi.org/10.1016/j.wear.2014.11.020.*
27. *O. Gbadeyan, K. Kanny, and M. T. Pandurangan. Tribological, mechanical, and microstructural of multiwalled carbon nanotubes/short carbon fiber epoxy composites. J. Tribol. 2018; **140**, 022002.*
28. *F. Gojny, M. Wichmann, U. Köpke, B. Fiedler, and K. Schulte. Carbon nanotube-reinforced epoxy-composites: enhanced stiffness and fracture toughness at low nanotube content. Compos. Sci. Technol. 2004, https://doi.org/10.1016/j.compscitech.2004.04.002.*
29. *K. Yang, M. Gu, Y. Guo, X. Pan, and G. Mu. Effects of carbon nanotube functionalization on the mechanical and thermal properties of epoxy composites. Carbon. 2009, https://doi.org/10.1016/j.carbon.2009.02.029.*
30. *S.-Y. Yang et al.. Synergetic effects of graphene platelets and carbon nanotubes on the mechanical and thermal properties of epoxy composites. Carbon. 2011, https://doi.org/10.1016/j.carbon.2010.10.014.*
31. *S. Zhou, Q. Zhang, C. Wu, and J. Huang. Effect of carbon fiber reinforcement on the mechanical and tribological properties of polyamide6/polyphenylene sulfide composites. Mater. Des. 2013, https://doi.org/10.1016/j.matdes.2012.08.029.*
32. *N. Burger, A. Laachachi, M. Ferriol, M. Lutz, V. Toniazzo, and D. Ruch. Review of thermal conductivity in composites: mechanisms, parameters and theory. Prog. Polym. Sci. 2016, https://doi.org/10.1016/j.progpolymsci.2016.05.001.*
33. *A. Yasmin, J.-J. Luo, and I. M. Daniel. Processing of expanded graphite reinforced polymer nanocomposites. Compos. Sci. Technol. 2006, https://doi.org/10.1016/j.compscitech.2005.10.014.*
34. *R. Sengupta, M. Bhattacharya, S. Bandyopadhyay, and A. K. Bhowmick. A review on the mechanical and electrical properties of graphite and modified graphite reinforced polymer composites. Prog. Polym. Sci. 2011, https://doi.org/10.1016/j.progpolymsci.2010.11.003*
35. *J. Li and Y. Xia. The reinforcement effect of carbon fiber on the friction and wear properties of carbon fiber reinforced PA6 composites. Fibers Polym. 2009, https://doi.org/10.1007/s12221-009-0519-5*
36. *H. Meng, G. Sui, G. Xie, and R. Yang. Friction and wear behavior of carbon nanotubes reinforced polyamide 6 composites under dry sliding and water lubricated condition. Compos. Sci. Technol. 2009, https://doi.org/10.1016/j.compscitech.2008.12.004*
37. *E. Omrani, P. L. Menezes, and P. K. Rohatgi. State of the art on tribological behavior of polymer matrix composites reinforced with natural fibers in the green materials world. Eng. Sci. Technol. 2016, https://doi.org/10.1016/j.jestch.2015.10.007*
38. *D. ASTM. Standard test method for indentation hardness of rigid plastics by means of a barcol impressor. In American Society for Testing and Materials, ed, 2001. 2001, vol. vol. D 2583-95.*
39. *I. Lawrence and U. A. Paul. Critical evaluation/reassessment of (abfm) automotive brake friction materials. Sci. Res. Essays. 2013; **1**, 275-288.*
40. *D. ASTM. Standard Test Method for Water Absorption of Plastics1. In American Society for Testing and Materials, 1998, vol. D 570-98.*
41. *R. Edokpia, V. Aigbodion, O. Obiorah, and C. Atuanya. Evaluation of the properties of ecofriendly brake pad using egg shell particles–Gum Arabic. Elsevier, 2014.*

42. K. Friedrich, Z. Zhang, and A. K. Schlarb. Effects of various fillers on the sliding wear of polymer composites. Compos. Sci. Technol. 2005, https://doi.org/10.1016/j.compscitech.2005.05.028.

43. K. Ikpambese, D. Gundu, and L. Tuleun. Evaluation of palm kernel fibers (PKFs) for production of asbestos-free automotive brake pads. J. King Saud University Eng. Sci. 2016, https://doi.org/10.1016/J.JKSUES.2014.02.001.

44. S. Pesetskii, S. Bogdanovich, and N. Myshkin. Tribological behavior of nanocomposites produced by the dispersion of nanofillers in polymer melts. J. Frict. Wear. 2007, https://doi.org/10.3103/S1068366607050091.

45. F.-h. Su, Z.-z. Zhang, and W.-m. Liu. Mechanical and tribological properties of carbon fabric composites filled with several nano-particulates. Wear. 2006, https://doi.org/10.1016/j.wear.2005.04.015

46. R. Ertan and N. Yavuz. The effects of graphite, coke and ZnS on the tribological and surface characteristics of automotive brake friction materials. Ind. Lubr. Technol Tribol. 2011, https://doi.org/10.1108/00368791111140468.

47. I. M. Dagwa and A. Ibhadode. Some physical and mechanical properties of asbestos–free experimental brake pad. J. Raw Mater. Res. 2015; **3**(2).

48. M. Afolabi, O. Abubakre, S. Lawal, and A. Raji. Experimental investigation of palm kernel shell and cow bone reinforced polymer composites for brake pad production. Int. J. Chem.Mater. Res. 2015, https://doi.org/10.18488/journal.64/2015.3.2/64.2.27.40.

49. S. W. Kim, S. J. Lee, B. K. Park, and S. K. Rhee. A comprehensive study of humidity effects on friction, pad wear, disc wear, DTV, brake noise and physical properties of pads. SAE Technical Paper, 0148-7191, 2011.

50. M. H. Cho, S. J. Kim, D. Kim, and H. Jang. Effects of ingredients on tribological characteristics of a brake lining: an experimental case study. Wear. 2005, https://doi.org/10.1016/j.wear.2004.11.021

51. D.-S. Lim, J.-W. An, and H. J. Lee. Effect of carbon nanotube addition on the tribological behavior of carbon/carbon composites. Wear. 2002, https://doi.org/10.1016/S0043-1648(02)00012-1.

52. A. O. A. Ibhadode and I. M. Dagwa. Development of asbestos-free friction lining material from palm kernel shell. J. Braz. Soc. Mech. Sci. Eng. 2008, https://doi.org/10.1590/S1678-58782008000200010.

53. P. J. Blau. Compositions, functions, and testing of friction brake materials and their additives. Oak Ridge National Lab., TN (US), 2001.

54. 54] C. Menapace, M. Leonardi, G. Perricone, M. Bortolotti, G. Straffelini, and S. Gialanella. Pin-on-disc study of brake friction materials with ball-milled nanostructured components. Mater. Des. 2017, https://doi.org/10.1016/j.matdes.2016.11.065.

55. M. Eriksson and S. Jacobson. Tribological surfaces of organic brake pads. Tribol. Int. 2000, https://doi.org/10.1016/S0301-679X(00)00127-4

56. J. Bijwe, N. Aranganathan, S. Sharma, N. Dureja, and R. Kumar. Nano-abrasives in friction materials-influence on tribological properties. Wear. 2012, https://doi.org/10.1016/j.wear.2012.07.023.

57. W. Österle et al. A comprehensive microscopic study of third body formation at the interface between a brake pad and brake disc during the final stage of a pin-on-disc test. Wear. 2009, https://doi.org/10.1016/j.wear.2008.11.023

CHAPTER 7: THERMO-MECHANICAL ANALYSIS OF BIO-BASED HYBRID NANOCOMPOSITES FOR BRAKE PAD APPLICATION

To cite this article: O. E. Ige, F. L. Inambao, and O. J. Gbadeyan, "Thermo-Mechanical Analysis of Bio-Based Hybrid Nanocomposites for Brake Pad Application," *International Journal of Mechanical and Production Engineering Research and Development* (IJMPERD). ISSN (P): 2249-6890; ISSN (E): 2249-8001. Vol. 11, Issue 2, Apr 2021, 155-170

The link to this article

www.tjprc.org

International Journal of Mechanical and Production Engineering Research and Development (IJMPERD)
ISSN (P): 2249–6890; ISSN (E): 2249–8001
Vol. 11, Issue 2, Apr 2021, 155–170

TRANS STELLAR
•Journal Publications •Research Consultancy

Original Article

THERMO-MECHANICAL ANALYSIS OF BIO-BASED HYBRID NANOCOMPOSITES FOR BRAKE PAD APPLICATION

OLUWAFEMI E. IGE*, FREDDIE L. INAMBAO, OLUWATOYIN J. GBADEYAN

Department of Mechanical Engineering, University of KwaZulu-Natal, Durban, South Africa

ABSTRACT

In this study, a friction material filled with carbon nanospheres (CNSs) was developed and tested. The CNSs were produced by simple physical activation under a nitrogen atmosphere. Bio-based hybrid nanocomposite (BHN) brake pads were produced and their thermo-mechanical properties were assessed. In this work, friction nanocomposite materials that were varied with carbon nanospheres were developed with different parameters. Thermo-mechanical properties of the BHN brake pads developed were assessed, such as compressive strength, impact strength, dynamic mechanical analysis (DMA) and thermo-gravimetric analysis (TGA). The BHN brake pad samples were compared with control (CONTR). Subsequently, a scanning electron microscopy (SEM) study was performed on the brake pads fracture surfaces. From the SEM images, micro-cracks were noticed on BHN 4 and BHN 5 fractured surfaces while surface degradation was observed on BHN 1 and an interlocking structure observed on BNH 3 and BHN 6. The results showed a uniform distribution of carbon nanospheres that supported impact stress resistance results. This structural formation improved the inner hardness of BHN brake pads, thus improving the breaking fracture resistance. TGA showed the loading of CNS improved thermal stability of friction nanocomposites. The CONTR and BHN brake pads had similar thermal stability and degradation temperatures. The results showed that the BHN exhibited excellent mechanical properties compared to CONTR.

KEYWORDS: CNS, Mechanical Analysis, Friction Materials, TGA, DMA.

Received: Jan 03, 2021; **Accepted**: Jan 23, 2021; **Published**: Mar 08, 2021; **Paper Id.**: IJMPERDAPR202113

INTRODUCTION

In the last two decades the formulation of brake pad materials has undergone significant changes due to health problems related to the asbestos brake pad, and a meaningful effort has been made to develop high-performance non-asbestos brake pad materials from agricultural waste [1-4] and composite materials [5-7]. Automobile brake pads are ubiquitous, so the materials used in the development of such products need to be carefully selected to reduce their impact on health and the environment [8-13]. Globally, material researchers and formulation designers are involved in developing multi-phased friction composite material, i.e., combinations of filler, fibers, binders and friction modifiers that meet quality requirements, as automotive braking technology continues to improve [14, 15]. The primary use of a binder is to hold the various components of the brake pad together and to prevent the decomposition of its components [16-18]. In essence, fillers are used to reduce the total cost of the material and effectively improve the brake pad properties [19]. Composite materials help researchers modify the existing materials, making them more suitable and consistent, thereby developing a suitable substitute for the existing materials. According to reports by [20], [21], [22], and [23], the use of various decision-making techniques and models to optimize the friction composite materials can be used to improve the design of friction formulations for standard performance objectives. Today, hybrid polymer composites material are being studied globally and

becoming potential alternative materials in producing different components, products, and parts in industrial applications [24, 25].

The manufacturing of friction materials need to meet specific thermo-mechanical requirements [9, 26-31]. Braking friction materials must have good wear resistance, stable friction, low noise, and damping over a wide range of temperature, pressure, and speed [15, 32]. Maintaining stable performance in terms of friction, wear, fade, and recovery under a wide variety of operating conditions is the main attribute of the friction composite materials [15].

Thermo-gravimetric analysis and differential scanning calorimetric (TGA, DSC) have been used to study the thermal behavior of materials [33]. The thermal analyser machine is used to calculate the heat flow (differential scanning calorimetry) and the weight loss (thermo-gravimetric) in the material with respect to temperature and time. The data obtained from TGA is used to distinguish between endothermic measurements that are not associated with weight loss and exothermic measurements that are associated with weight loss [34]. When assessing the thermal behavior of the brake pad, the methodology described above is applicable to this study. The determination of thermal properties, compressive strength, impact strength and dynamic mechanical analysis (DMA) are suitable for this study, especially to determine the performance of braking and stopping force of the hybrid brake pads.

A new BHN brake pad has been developed which is a mixture of nanoscale carbon-based materials and has been employed to produce brake pads. The work investigates the thermo-mechanical properties of BHN friction materials.

EXPERIMENT

Materials

ATM Composite in Durban, South Africa, supplied the BHN materials based on a neat epoxy resin of LR 20 type without modification which was used as a binder. The carbon nanospheres (CNSs) were produced by simple physical activation under nitrogen atmosphere (catalyst-free) at the Department of Chemistry, University of Zululand, South Africa. Stainless steel nanoparticles and graphite nanoparticles were purchased from Capital Lab supplies, Durban, South Africa. These materials were added together to make 100% by weight to the produced BHN brake pads as shown in Table 1. Each nanosphere was about 10 nm to 60 nm in diameter [35].

Prior to the production of the BHN brake pad, epoxy resin was weighed and heated to a temperature of 70 °C in a beaker to reduce the viscosity and facilitate the dispersion of other components. The components were mixed using a mechanical stirrer for one hour at 500 rpm to attain a homogenous mixture.

Table 1: Bio-Based Hybrid Nanocomposite Formulation

Samples	Composite in Weight Percentage (wt. %)				
	Binder	Graphite Nanoparticles	Carbon Nano-Spheres	Stainless Steel Nanoparticles	Total (%)
BHN 1	98.1	1	0.1	0.8	100
BHN 2	98.6	0.3	0.3	0.8	100
BHN 3	98	1	0.2	0.8	100
BHN 4	98.6	0.5	0.1	0.8	100
BHN 5	97.9	1	0.3	0.8	100
BHN 6	98.7	0.3	0.2	0.8	100

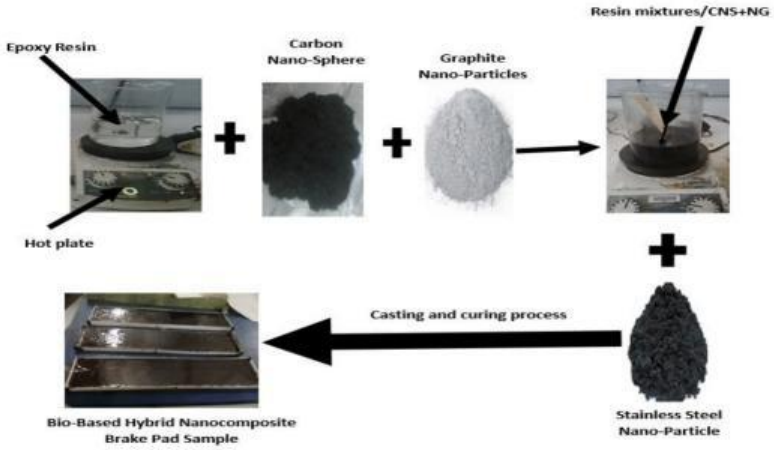

Figure 1: Bio-based Hybrid Nanocomposite Brake Pad Process Overview

The BHN material was achieved at room temperature and mixed with 100 vol.% to 30 vol.% of catalyst to improve the curing process. Stainless steel nanoparticles (8.0 wt.%) were added to the different compositions, as shown in Figure 1. The plastic mold was waxed before the material was poured into the mold for easy removal of the BHN sample after two days. After curing for 14 days, the samples were tested.

MECHANICAL PROPERTIES

Compressive Strength

The compressive strength of a material is the ability of the material to resist fracture under compression. The compressive properties of the BHN brake pads were calculated according to a standard specification of the ASTM D 695 tests [36]. A Lloyd Universal Testing Machine equipped with a 30 kN load cell was used to test the samples as shown in Figure 2. A rectangular test sample with width, thickness, and dimensional length of 12.7 mm x 12.7 mm x 57.0 mm was cut from the developed biobased hybrid nanocomposite using a diamond-cutting machine. Before testing, sandpaper was used to smooth any sharp edges of the samples left by the diamond-cutting machine.

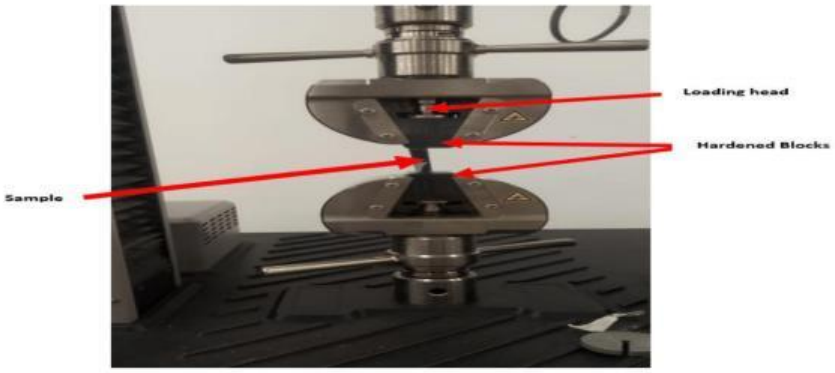

Figure 2: Compressive Test with Hardened Blocks on Lloyd Testing Machine

The test sample was gripped directly between the compression plates prepared in the moveable crosshead, and the bottom crosshead blocks were compressed before gauge failure. After proper positioning and tightening of the sample between the compression plates, the load was applied, and the compressive strain was examined from the display output. The load was applied slowly to the sample, and at regular intervals the corresponding strain was recorded. The six samples were tested at ambient temperature with a test speed of 1.3 mm ± 0.3 mm (0.050 inches ± 0.010 inches) / min. The average value was used for graphical representation, and a discussion of the six samples was reported. The following equation was used to calculate compressive strength, strain, and modulus.

$$\sigma_e = \frac{F^*}{A^\circ} \quad (1)$$

$$\varepsilon_e = \frac{(l_\circ - l^*)}{l_\circ} \quad (2)$$

$$E = \frac{\sigma_2 - \sigma_1}{\varepsilon_2 - \varepsilon_1} \quad (3)$$

$l_\circ$: Original gauge length (mm)

A° : Original cross-sectional area of the sample in the gauge length (mm^2)

F^*: Maximum load applied before crushing (N)

σ_e Compressive strength

l^*: Specimen length after crushing (mm)

σ_1, σ_2 : Corresponding stress at the specific strain (MPa)

ε_1,ε_2: Corresponding stress at the specific stress (MPa)

E: Compressive modulus (MPa)

Impact Strength

The impact resistance of developed bio-based hybrid nanocomposite and conventional brake pads was determined by conducting a Charpy test at room temperature using the Hounsfield Balance Impact Tester produced by Tensometer Ltd. Croydon, United Kingdom. The Hounsfield Balance Impact Machine is made according to the ASTM D6110-10 standard with a three-point to Charpy device [121]. The geometric size of the sample cut from the brake pad was 50 mm^3× 10 mm^3× 5 mm^3 i.e., length, width, and thickness. This method allowed the samples' width to vary according to the different materials (either brittle or ductile). All samples had a 4 mm deep mark at the center part opposite the impact part, and the impact width area was 6 mm. The six samples were examined for brake pad formation, and the impact speed was about 6.7 m / s. The average collected value was used to determine the energy absorption using the following formula:

$$IS = \frac{AE}{WT} \quad (4)$$

IS: Impact strength (KJ/m2)

AE: Absorbed energy (Joule)

W: Remaining width at the notch (m)

T: Specimen thickness (m)

Scanning Electron Microscopy (SEM)

After the impact test, the BHN brake pad fracture surfaces were examined with scanning electron microscopy (SEM) using EVO HD 15 model produced by Carl Zeiss Environmental SEM operating 1000 times zoom under atmospherically controlled conditions at 20 kV [19, 37, 38]. The samples were coated with an ultra-thin gold film before microstructure analysis.

THERMAL ANALYSIS

The thermo-mechanical properties of the BHN samples were investigated using dynamic mechanical analysis (DMA), while the BHN samples' thermal behavior was studied using a (TGA). The TGA test aimed to determine the thermal stability, temperature degradation, and heat energy absorption of each brake pad.

Thermo-Gravimetric Analysis (TGA)

The TGA testing was conducted under a dry nitrogen gas flow rate of 100 mL/min from 20 °C to 600 °C and a 100 °C/min heating rate. The thermal stability and degradation of the BHN samples were measured using the thermal analyser instrument SDT Q600 V20.9 Build 20. TGA is a widely used thermal analytical technique for determining thermal stability, ash content, etc., related to composite materials. TGA calculates the weight loss of the sample in relation to the temperature.

Dynamic Mechanical Analysis (DMA)

The thermo-mechanical properties of the BHN brake pads were investigated using DMA to determine the storage modulus (E'), loss modulus (E"), and tan-delta ($Tan\ \delta$) in relation to temperature scanned. The DMA of each BHN sample was examined using TA instrument DMA (model Q800 V21.2 Build 88) following the ASTM E1867 standard at the frequency of 10 Hz under three-point bending mode from 20 °C to 190 °C under atmospheric conditions with the temperature scan [39]. The sample size of 5.5 cm × 1.2 mm × 0.35 cm was examined [40].

RESULTS AND DISCUSSION

Compressive Properties

The compressive strength of BHN and the control (CONTR) brake pads are presented in Table 2. It can be seen that BHN 1, BHN 2 BHN 3, BHN 5, and BHN 6 brake pads had a higher compressive strength compared to CONTR, while sample BHN 4 did not. Sample BHN 2 exhibited 43.7 % higher compressive strength than CONTR; this improvement could be due to nanoparticles and nanosphere in the composition.

Table 2: Compressive Strength of BHN and Control Brake Pads

Bio-Based Hybrid Nanocomposite	Compressive Strength (MPa)	Remarks (%)
CONTR	3000,1	
BHN 1	3410,3	13,7
BHN 2	4311,4	43,7
BHN 3	3896,3	29,9
BHN 4	1772,6	-40,9
BHN 5	3771,4	25,7
BHN 6	3557,3	18,6

As shown in Figure 3, it was noticed that there was a different compressive strength for each brake pad formulation. The bond between the quantity and the constituent type affects the composite strength and influences the final properties [41]. Given this aspect, in the formulation of each brake pad, the inconsistent compressive strength shown in Figure 3 can be attributed to the different content of the additives.

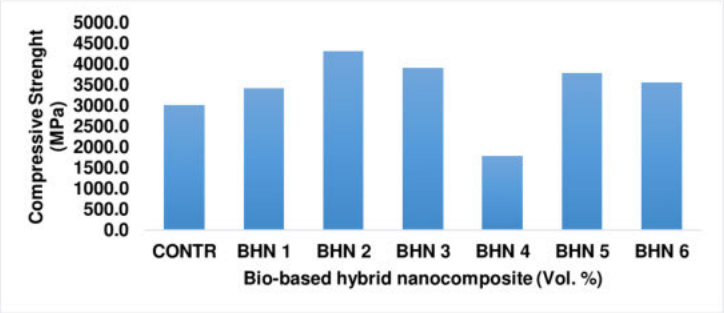

Figure 3: Compressive Strength of the BHN and CONTR Brake Pads

The higher loading of graphite nanoparticles, therefore, resulted in lower compressive strength of the BHN 4 sample. In conclusion, strength was affected by better bonding of brake pad additives. The compressive strength of the BHN brake pads sample filled with 0.3 % CNSs improved with an increase in CNS content. Although the CNS content of BHN 3, BHN 5, and BHN6 brake pads increased, BHN 2 showed the highest strength.

This improved strength meant that BHN 2 had a greater resistance to force than other BHN and CONTR brake pads. The damage caused by compressive stress and the failure that accompanied this manifested as delamination and fracture of brake pad additives.

Impact Properties

Table 3 indicates the impact strength of the BHN and CONTR brake pads computed on the Charpy impact tester. Figure 4 shows the impact fractures of both developed BHN and CONTR brake pads. It was noted that, except for BHN 1, BHN 2, and BHN 5, the BHN brake pads had better impact resistance than the CONTR brake pad. The reduction in the impact strength of BHN 1, BHN 2, and BHN 5 may be due to the agglomeration produced by high loading graphite nanoparticle. The impact resistance of BHN brake pads varied with their composition. The impact resistance of BHN 4 was highest at 4.1 KJ/m^2, which was 35.1 % higher than the CONTR brake pad impact value of 3.0 KJ/m^2. The improvement in impact strength can be credited to the interlocking bond produced by the additives, which ultimately improved the energy absorption capacity.

Table 3: Impact Strength of BHN and CONTR Brake Pads

	Impact Strength (KJ/M^2)	Remarks (%)
CONTR	3,0	
BHN 1	2,9	-2,5
BHN 2	2,9	-4,6
BHN 3	3,4	11,7
BHN 4	4,1	35,1
BHN 5	2,8	-8,0
BHN 6	3,3	8,7

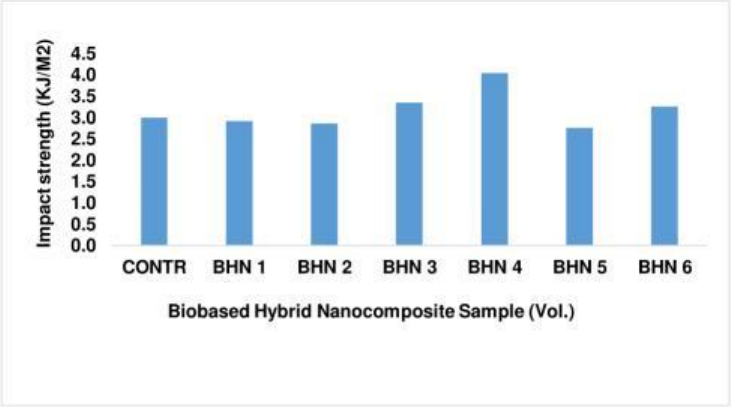

Figure 4: The Impact Fracture Resistance of CONTR and BHN

Subsequently, SEM testing was carried out to determine the brake pad impact failure. Figures 5a to 5g present the SEM micrographs captured for the BHN and CONTR brake pads fracture surfaces at 2500X magnification. The CONTR brake pad fracture surface exhibits disintegration of the composition, porosity, and surface degradation, causing cracks on the CONTR impact surface. These structures indicated a brittle failure and were consistent with the impact value presented in Table 3. However, the trend of BHN brake pads is the opposite, as the fractured surface were together with the hard fracture surface. A uniform distribution of carbon nanosphere was observed, supporting the impact stress resistance results. This structure improved the inner hardness of BHN brake pads, thus improving the breaking fracture resistance.

As shown in Figures 5a to 5g, micro-cracks were noticed on BHN 4 and BHN 5. Surface degradation was observed on BHN 1 and interlocking structure on BNH 3 and BHN 6. These may be due to fiber matrix or additive accumulation at a certain point in the matrix, leading to delamination and reduction in the strength of the BHN brake pads. As the fiber loading increased, the fiber interface reduced. Therefore, it reduced the impact strength, as shown in Table 3.

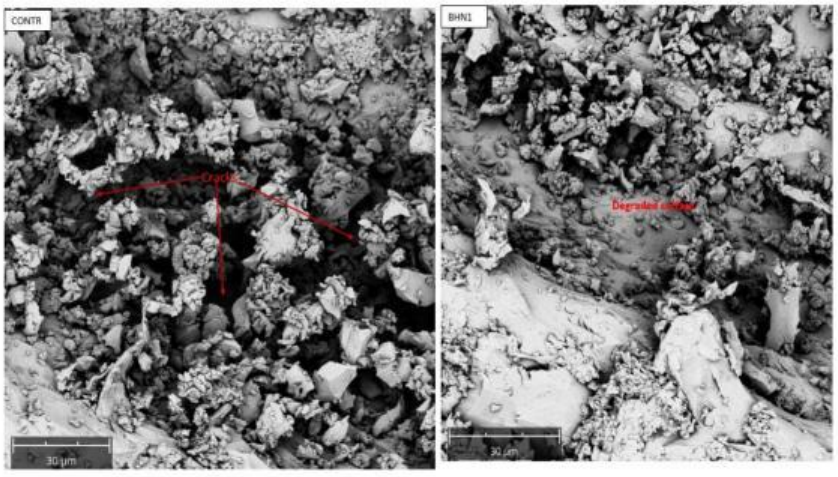

a **b**

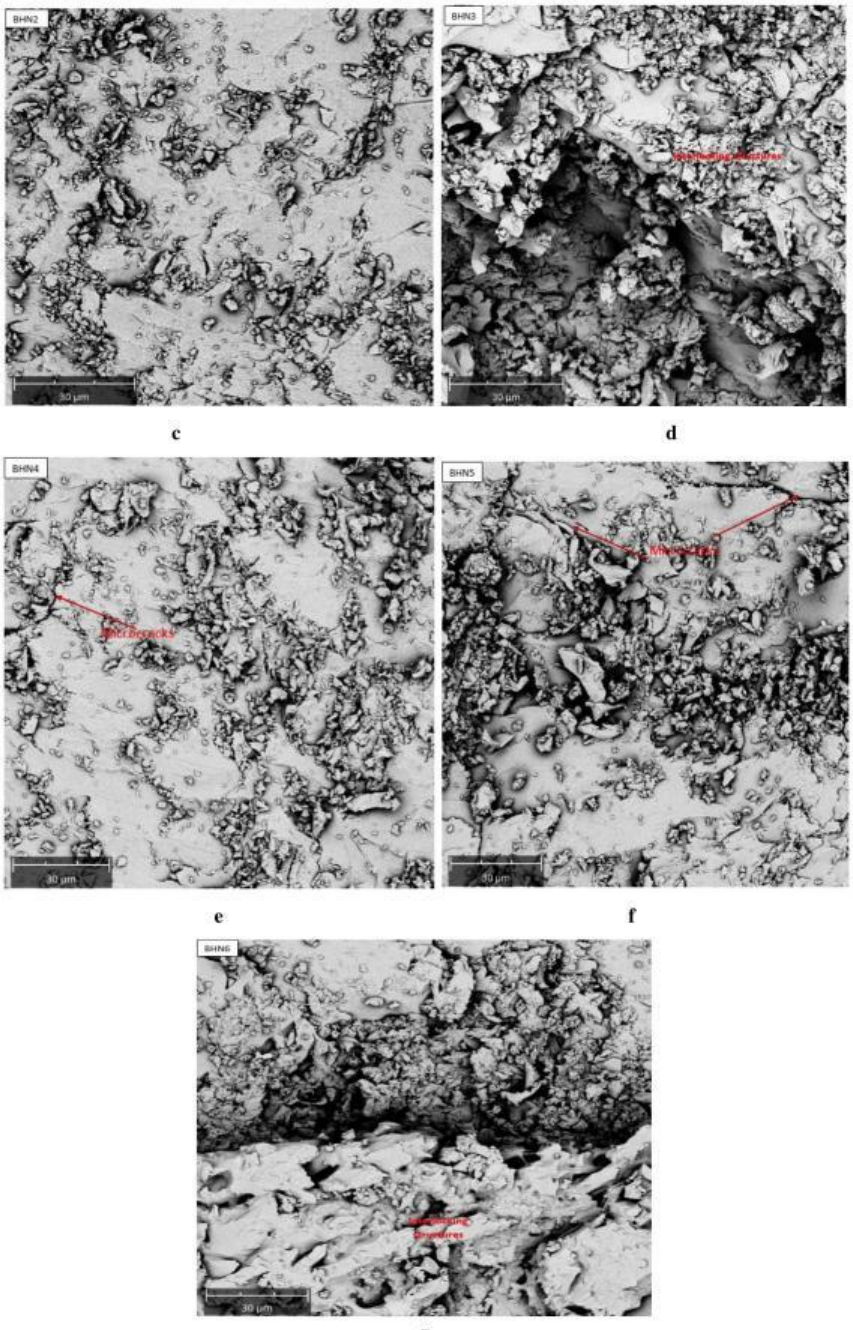

c d e f g

Figure 5 a to g: The SEM Micrograph of the BHN and CONTR brake Pads Impact Fracture Surfaces

BHN 2 shows a tough fractured surface with a uniform mixture of ingredients filled together. This structure forms an interface bond with increased carbon content, which is in line with the excellent impact resistance recorded in Table 3. Therefore, the total energy needed to break the BHN brake pad resulted from the interfacial bond present between the binder and other additives. Hence, the improvement of fracture resistance at which the BHN brake pad broke can be credited to the carbon-based filler loading properties, the binder adhesive qualities, and interactive functions of the carbon-based ingredients.

Thermo-Gravimetric Analysis (TGA)

In respect to the time and temperature, the thermo-gravimeter was used to calculate the weight loss, while differential scanning calorimetry was used to measure the differential heat flow in the material. The thermal stability and degradation of BHN brake pads were studied using TGA, as shown in Figure 6. The results show that the CONTR and BHN brake pads had similar thermal stability and degradation temperatures. This output could be due to the characteristics of the thermal properties in the CNS and graphite nanoparticles in the formulations of the brake pads.

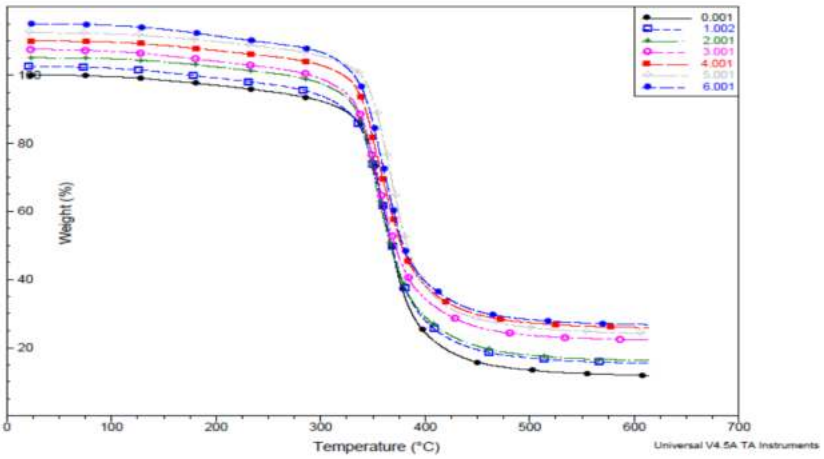

Figure 6: TGA curve of the BHN as a Function of Temperature

0.001 (CONTR), 1.002 (BHN 1), 2.001 (BHN 2), 3.001 (BHN 3), 4.001(BHN 4), 5.001 (BHN 5), 6.001 (BHN 6)

It is also evident from Figure 6 that the weight loss increased with an increase in temperature. It can be understood from the figure that the decomposition temperatures varied according to the different brake pad formulations. These results show that the graphite nanoparticle loading in the formulations impacted the BHN brake pads' decomposition temperature. The BHN brake pad sample with 0.3 % of graphite nanoparticle had a better degradation compared to others. However, the loading of CNS content positively impacted the BHN brake pads with 0.3 vol.% and 0.3 vol.% graphite nanoparticles. The BHN samples had better thermal stability as the CNS content increased accordingly.

The weight loss appeared in three phases. The thermal image of the BHN and CONTR formulation presented in Figure 6 shows that all nanocomposite materials had a gradual decomposition rate at the first stage, and the thermal stability was approximately 98 %. The first weight loss in all friction nanocomposites was very low. About 2 % weight loss occurred at 50 °C to 350 °C related to the sample water and gas. After that, the decomposition rate accelerated as the

vertical negative slope curve at the second stage became sharper and sharper, and the thermal stability was approximately 74 %. The second weight loss was around 20 % to 30 % at about 350 °C to 400 °C due to hemicellulose thermal depolymerization and resin degradation, and the rate of degradation/decomposition was much faster. The decomposition rate changed more gradually at the third stage with an average of 78 % thermal stability.

The third weight loss was about 3 % and happened in the range 400 °C to 600 °C and was due to more decomposition. At temperatures above 400 °C, due to the intersection of degradation curves, an increase in thermal stability of BHN 2 and BHN 5 was observed with a greater quantity of carbon-carbon additives becoming more dominant in thermal stability. The TGA curve showed that adding CNS to the resin matrix greatly improved the materials' thermal stability, but CONTR also showed excellent thermal stability. This thermal stability improvement can be due to the thermal properties of carbon-based additives, which have impeded the distribution of volatile decomposition from the matrix. This output is consistent with the studies by Krump et al. and Duquesne et al. [42-44], where volatile degradation products adsorbed from the surface of the material improved thermal stability.

Table 4: TGA of the BHN Brake Pad Friction Material

Bio-Based Hybrid Nanocomposite	Thermal Stability (%) with Respect to Temperature (°C)		
	50 °C to 350 °C	350 °C to 400 °C	400 °C to 600 °C
CONTR	95,35	44,81	14,73
BHN1	94,99	43,66	15,81
BHN2	95,51	40,58	14,22
BHN3	94,79	42,57	17,55
BHN4	95,68	45,54	18,66
BHN5	96,16	49,79	14,84
BHN6	94,99	42,86	14,66

Table 4 shows the average thermal stability (%) of the BHN brake pad and CONTR at three different temperature zones (50 °C to 350 °C, 350 °C to 400 °C, and 400 °C to 600 °C), illustrated in Figure 6. The BHN brake pads and CONTR brake pad exhibit similar thermal degradation in all three temperature zones.

Dynamic Mechanical Analysis

The dynamic mechanical properties such as storage modulus (E'), loss modulus (E"), and damping factor or tan-delta ($Tan\ \delta$) of the bio-based hybrid nanocomposite materials were investigated as a function of temperature as shown in Figures 7 to 9. This function makes it possible to understand the loss in mechanical, physical, and tribological properties with increased temperature, which can be due to modulus loss [45, 46]. Figure 7 shows the characteristics of the BHN storage modulus. All the BHN samples remained high in the temperature range 20 °C to 55 °C and followed E' magnitude, BHN 6, BHN 5, BHN 4, BHN 3, BHN 2, BHN 1, and CONTR.

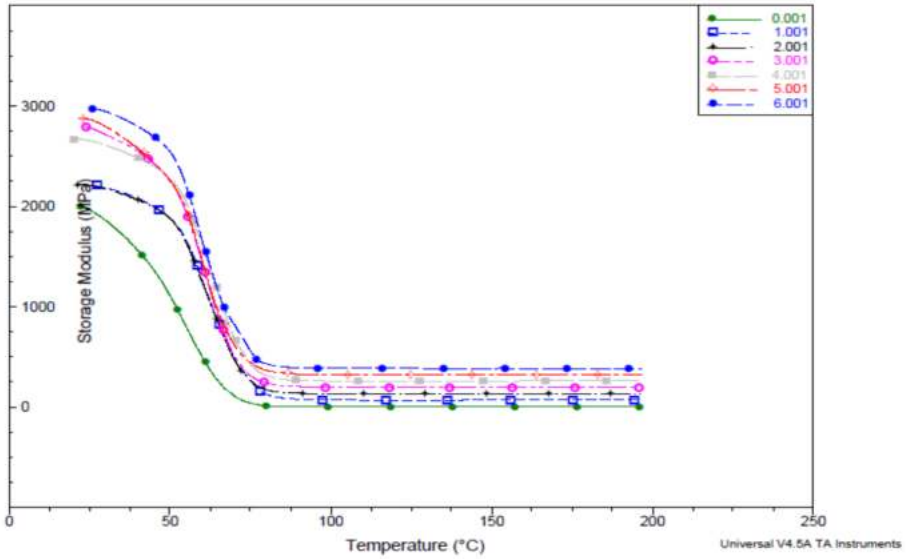

Figure 7: Storage Modulus of the BHN as a Function of Temperature

0.001 (CONTR), 1.001 (BHN 1), 2.001 (BHN 2), 3.001 (BHN 3), 4.001(BHN 4), 5.001 (BHN 5), 6.001 (BHN 6)

There was a steady storage modulus loss at an estimated comparable rate as temperature increased. This outcome could be because of the breaking or weakening of the molecular bonds between various polymeric chains, resulting in weakening of the structure. The material appears to exhibit viscous performance in the temperature range 50 °C to 70 °C, as established by loss modulus curves shown in Figure 8. Thus, the variation of graphite nanoparticles in the samples improved the modulus throughout the formulation. The BHN samples appear to lose their functional properties at a higher temperature. The functionality of the samples nearly finished at the temperature range 80 °C to 190 °C. It can be seen that the loss modulus remained low within the temperature range of about 20 °C to 55 °C as the storage modulus is still in the dominant position throughout the formulation, as shown in Figure 7.

The characteristics of the loss modulus of the BHN material studied are illustrated in Figure 8. At temperatures between 50 °C to 70°C, the loss modulus increased exponentially compared to the sharp fall in the storage modulus. The increase was in BHN 6, BHN 5, BHN 4, BHN 3, BHN 1, BHN 2, and CONTR. It was also observed that the viscous zone temperature moved marginally towards the low-temperature side with a rise in the variation of graphite nanoparticles reinforcement.

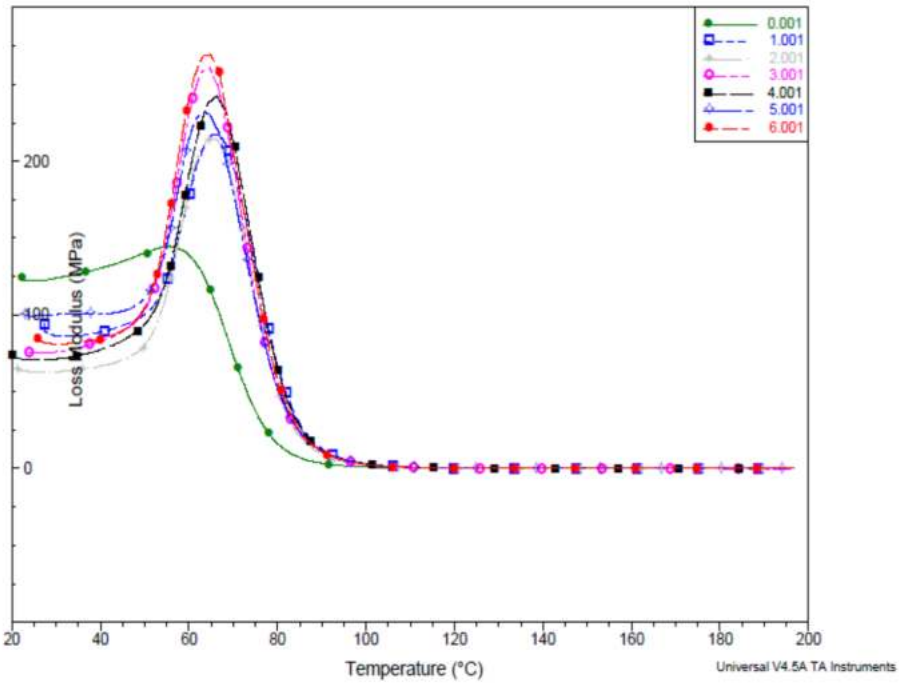

Figure 8: Loss Modulus of the BHN as a Function of Temperature

0.001(CONTR), 1.001 (BHN1), 2.001 (BHN2), 3.001 (BHN3), 4.001(BHN4), 5.001 (BHN5), 6.001 (BHN6)

At a temperature of between 90 °C and 190 °C, all the material failed and resulted to zero loss modulus. The $Tan\ \delta$ loss evaluates the energy lost within the material during the damping process. The characteristics of damping or $Tan\ \delta$ of the BHN materials studied are illustrated in Figure 9. The higher the value of $Tan\ \delta$, the better the damping capacity of the friction materials. Figure 9 showed similar temperatures between 20°C to 55 °C and a similar plot, i.e., CONTR, BHN 6, BHN 5, BHN 4, BHN 3, BHN 2, and BHN 1 storage modulus and loss modulus. It was observed that within the temperature range 20°C to 55 °C, $Tan\ \delta$ had a lower magnitude throughout the formulation, which was due to the supremacy of the storage modulus over the loss modulus. At a temperature range between 55°C and 105 °C, the $Tan\ \delta$ magnitude of BHN was higher due to the supremacy of the loss modulus over the storage modulus.

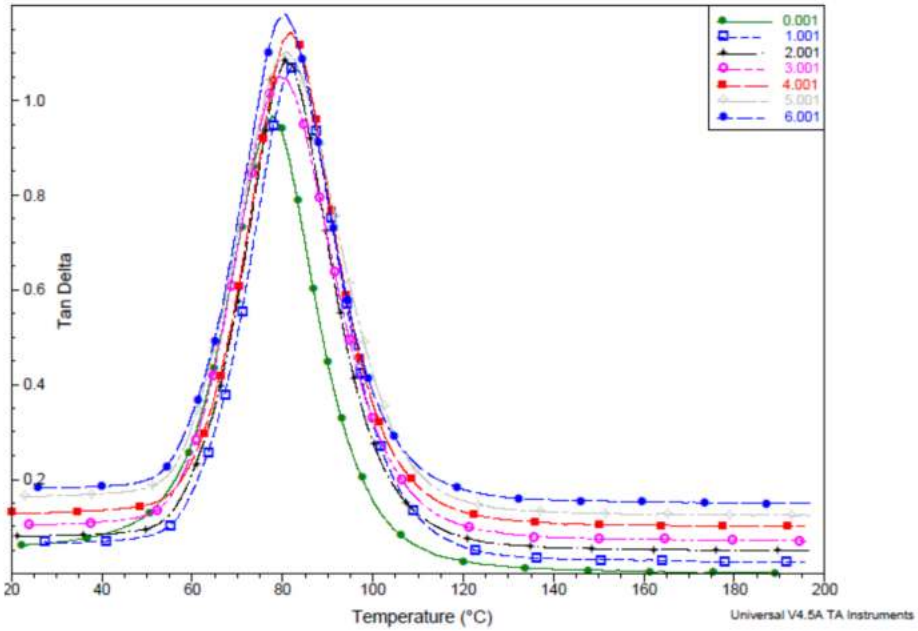

Figure 9: $Tan\ \delta$ of the BHN Friction Materials as a Function of Temperature

0.001 (CONTR), 1.001 (BHN 1), 2.001 (BHN 2), 3.001 (BHN 3), 4.001(BHN 4), 5.001 (BHN 5), 6.001 (BHN 6)

In this area, the BHN materials have outstanding damping characteristics. It was also noted that the peak moved towards the lower temperature side with an increase in graphite nanoparticle reinforcement. Besides, at the temperatures between 105°C and 190 °C, the storage/loss modulus became as low as CONTR, and the BHN $Tan\ \delta$ magnitude became minimal.

CONCLUSIONS

BHN brake pads containing CNS were produced, and their thermo-mechanical properties were evaluated. The thermomechanical analysis of BHN brake pad materials yielded the following important results. The mechanical properties of the BHN brake pad materials investigated were within the industry-standard range. The compressive strength of the BHN brake pads were higher than CONTR by 43.7%. The CONTR brake pad's impact resistance was 17.6 KJ / m^2, while the BHN brake pads' impact strength varied with the formulation. The SEM results revealed micro-cracks on BHN 4 and BHN 5 fractured surfaces, while surface degradation was observed on BHN 1 and interlocking structure observed on BNH 3 and BHN 6.

The TGA curve showed that adding CNS to the resin matrix greatly improved the materials' thermal stability, but CONTR also showed excellent thermal stability. The BHN brake pads' thermal stability increased as the CNS content increased with a corresponding decrease in graphite nanoparticle content. From the DMA result, the integration of CNS into nanocomposite friction material led to improved storage modulus, loss modulus, and damping factor when sufficient graphite nanoparticles were added. The modulus and damping properties of the BHN brake pad materials showed a significant increase in graphite nanoparticle reinforcement and temperature variation. The storage modulus plots showed

the heterogeneity present in the BHN brake pads. At a temperature range between 90°C and 190 °C, all the material failed and resulted to zero loss modulus. $Tan\ \delta$ has a lower magnitude throughout the formulation at the temperature range 20 °C to 55 °C, which was due to the supremacy of the storage modulus over the loss modulus.

REFERENCES

1. *A. O. A. Ibhadode and I. M. Dagwa, "Development of asbestos-free friction lining material from palm kernel shell," J. Braz. Soc. Mech. Sci. Eng., vol. 1, no. 1, pp. 1-2, 2008.*
2. *D. Shinde and K. Mistry, "Asbestos base and asbestos free brake lining materials: Comparative study," World Scientific News, vol. 61, no. 2, pp. 192-198, 2017.*
3. *V. Mahale, J. Bijwe, and S. Sinha, "Influence of nano-potassium titanate particles on the performance of NAO brake-pads," Wear, vol. 376, pp. 727-737, 2017.*
4. *M. Polajnar, M. Kalin, I. Thorbjornsson, J. T. Thorgrimsson, N. Valle, and A. Botor-Probierz, "Friction and wear performance of functionally graded ductile iron for brake pads," Wear, vol. 382, pp. 85-94, 2017.*
5. *O. J. Gbadeyan and K. Kanny, "Tribological behaviors of polymer-based hybrid nanocomposite brake pad," Journal of Tribology, vol. 140, no. 3, 2018.*
6. *J. O. Agunsoye, S. A. Bello, A. A. Bamigbaiye, K. A. Odunmosu, and I. O. Akinboye, "Recycled ceramic composite for automobile brake pad application," Journal of Research in Physics, vol. 39, no. 1, p. 35, 2018.*
7. *C. Menapace, M. Leonardi, G. Perricone, M. Bortolotti, G. Straffelini, and S. Gialanella, "Pin-on-disc study of brake friction materials with ball-milled nanostructured components," Materials & Design, vol. 115, pp. 287-298, 2017.*
8. *A. Ganguly and R. George, "Asbestos free friction composition for brake linings," Bulletin of Materials Science, vol. 31, no. 1, pp. 19-22, 2008.*
9. *K. H. Cho, M. H. Cho, S. J. Kim, and H. Jang, "Tribological properties of potassium titanate in the brake friction material; morphological effects," Tribology letters, vol. 32, no. 1, pp. 59-66, 2008.*
10. *[D. Chan and G. Stachowiak, "Review of automotive brake friction materials," Proceeding of the Institution of Mechanical Engineers, Part D: J. Auto. Eng. , vol. 218, pp. 953-966, 2004.*
11. *M. Cho, S. Kim, R. Basch, J. Fash, and H. Jang, "Tribological study of gray cast iron with automotive brake linings: The effect of rotor microstructure," Tribology International, vol. 36, no. 7, pp. 537-545, 2003.*
12. *S. S. Bernard and L. Jayakumari, "Pressure and temperature sensitivity analysis of palm fiber as a biobased reinforcement material in brake pad," Journal of the Brazilian Society of Mechanical Sciences and Engineering, vol. 40, no. 3, p. 152, 2018.*
13. *R. Yun, P. Filip, and Y. Lu, "Performance and evaluation of eco-friendly brake friction materials," Tribology International, vol. 43, no. 11, 2010.*
14. *K. N. Kumar and K. Suman, "Review of brake friction materials for future development," J Mech Mech Eng, vol. 3, pp. 1-29, 2017.*
15. *J. Bijwe, "Composites as friction materials: Recent developments in non-asbestos fiber reinforced friction materials—a review," Polymer composites, vol. 18, no. 3, pp. 378-396, 1997.*
16. *J. Bijwe and M. Kumar, "Optimization of steel wool contents in non-asbestos organic (NAO) friction composites for best*

combination of thermal conductivity and tribo-performance," Wear, vol. 263, no. 7-12, pp. 1243-1248, 2007.

17. *G. Ingo, M. D'uffizi, G. Falso, G. Bultrini, and G. Padeletti, "Thermal and microchemical investigation of automotive brake pad wear residues," Thermochimica acta, vol. 418, no. 1-2, pp. 61-68, 2004.*
18. *V. Malhotra, P. Valimbe, and M. Wright, "Effects of fly ash and bottom ash on the frictional behavior of composites," Fuel, vol. 81, no. 2, pp. 235-244, 2002.*
19. *K. Ikpambese, D. Gundu, and L. Tuleun, "Evaluation of palm kernel fibers (PKFs) for production of asbestos-free automotive brake pads," Journal of King Saud University-Engineering Sciences, vol. 28, no. 1, pp. 110-118, 2016.*
20. *Y. Lu, "A combinatorial approach for automotive friction materials: combined effects of ingredients on friction performance," Polymer composites, vol. 23, no. 5, pp. 814-823, 2002.*
21. *T. Singh, A. Patnaik, B. K. Satapathy, and M. Kumar, "Performance analysis of organic friction composite materials based on carbon nanotubes-organic-inorganic fibrous reinforcement using hybrid AHP-FTOPSIS approach," Composites: Mechanics, Computations, Applications: An International Journal, vol. 3, no. 3, 2012.*
22. *T. SINGH, A. PATNAIK, B. SATAPATHY, and B. TOMAR, "Development and optimization of hybrid friction materials consisting of nanoclay and carbon nanotubes by using analytical hierarchy process (AHP) and technique for order preference by similarity to ideal solution (TOPSIS) under fuzzy atmosphere," Walailak Journal of Science and Technology (WJST), vol. 10, no. 4, pp. 343-362, 2013.*
23. *T. Singh, A. Patnaik, B. Gangil, and R. Chauhan, "Optimization of tribo-performance of brake friction materials: effect of nano filler," Wear, vol. 324, pp. 10-16, 2015.*
24. *J. S. Raj, T. Christy, S. D. Gnanaraj, and B. Sugozu, "Influence of calcium sulfate whiskers on the tribological characteristics of automotive brake friction materials," Engineering Science and Technology, an International Journal, vol. 23, no. 2, pp. 445-451, 2020.*
25. *S. Jeganmohan, B. Sugozu, M. Kumar, and D. R. Selvam, "Experimental investigation on the friction and wear characteristics of palm seed powder reinforced brake pad friction composites," Journal of The Institution of Engineers (India): Series D, vol. 101, no. 1, pp. 61-69, 2020.*
26. *A. Patnaik, M. Kumar, B. K. Satapathy, and B. S. Tomar, "Performance sensitivity of hybrid phenolic composites in friction braking: effect of ceramic and aramid fibre combination," Wear, vol. 269, no. 11-12, pp. 891-899, 2010.*
27. *N. Dadkar, B. S. Tomar, B. K. Satapathy, and A. Patnaik, "Performance assessment of hybrid composite friction materials based on flyash–rock fibre combination," Materials & Design, vol. 31, no. 2, pp. 723-731, 2010.*
28. *J. Bijwe, N. Majumdar, and B. Satapathy, "Influence of modified phenolic resins on the fade and recovery behavior of friction materials," Wear, vol. 259, no. 7-12, pp. 1068-1078, 2005.*
29. *B. Satapathy and J. Bijwe, "Performance of friction materials based on variation in nature of organic fibres: Part I. Fade and recovery behaviour," Wear, vol. 257, no. 5-6, pp. 573-584, 2004.*
30. *B. Satapathy and J. Bijwe, "Fade and recovery behavior of non-asbestos organic (NAO) composite friction materials based on combinations of rock fibers and organic fibers," Journal of reinforced plastics and composites, vol. 24, no. 6, pp. 563-577, 2005.*
31. *M. H. Cho, J. Ju, S. J. Kim, and H. Jang, "Tribological properties of solid lubricants (graphite, Sb2S3, MoS2) for automotive brake friction materials," Wear, vol. 260, no. 7-8, pp. 855-860, 2006.*
32. *D. Chan and G. Stachowiak, "Review of automotive brake friction materials," Proceedings of the Institution of Mechanical*

Engineers, Part D: Journal of Automobile Engineering, vol. 218, no. 9, pp. 953-966, 2004.

33. *B. Wielage, T. Lampke, G. Marx, K. Nestler, and D. Starke, "Thermogravimetric and differential scanning calorimetric analysis of natural fibres and polypropylene," Thermochimica Acta, vol. 337, no. 1-2, pp. 169-177, 1999.*
34. *O. J. Gbadeyan, "Low friction hybrid nanocomposite material for brake pad application," 2017.*
35. *O. E Ige, F. L Inambao, and G. A Adewumi, "Synthesis of Natural Carbon Nanospheres From Palm Kernel Fiber," International Journal of Mechanical Engineering and Technology, vol. 10, no. 12, pp. 625-641, 2019.*
36. *D. ASTM, "Standard Test Method for Rigid Plastics," in American Society for Testing and Materials, 2006, vol. D 695-2a,, ed, 2006 ed.*
37. *S. Pesetskii, S. Bogdanovich, and N. Myshkin, "Tribological behavior of nanocomposites produced by the dispersion of nanofillers in polymer melts," Journal of Friction and Wear, vol. 28, no. 5, pp. 457-475, 2007.*
38. *F.-h. Su, Z.-z. Zhang, and W.-m. Liu, "Mechanical and tribological properties of carbon fabric composites filled with several nano-particulates," Wear, vol. 260, no. 7-8, pp. 861-868, 2006.*
39. *S. Bhaskar, M. Kumar, and A. Patnaik, "Microstructure, Thermal, Thermo-mechanical and Fracture Analyses of Hybrid AA2024-SiC Alloy Composites," Transactions of the Indian Institute of Metals, vol. 73, no. 1, pp. 181-190, 2020.*
40. *J. Olusanya, K. Kanny, and S. Singh, "Bulk cure study of nanoclay filled epoxy glass fiber reinforced composite material," Journal of Polymer Engineering, vol. 37, no. 3, pp. 247-259, 2017.*
41. *I. Lawrence and U. Paul, "Critical evaluation/reassessment of (abfm) automotive brake friction materials," Standard Research Journal, 2013.*
42. *O. J. Gbadeyan, K. Kanny, and T. Mohan, "Influence of the multi-walled carbon nanotube and short carbon fibre composition on tribological properties of epoxy composites," Tribology-Materials, Surfaces & Interfaces, vol. 11, no. 2, pp. 59-65, 2017.*
43. *S. Parveen, S. Rana, and R. Fangueiro, "A review on nanomaterial dispersion, microstructure, and mechanical properties of carbon nanotube and nanofiber reinforced cementitious composites," Journal of Nanomaterials, vol. 2013, 2013.*
44. *A. A. Koval'chuk, V. G. Shevchenko, A. N. Shchegolikhin, P. M. Nedorezova, A. N. Klyamkina, and A. M. Aladyshev, "Effect of carbon nanotube functionalization on the structural and mechanical properties of polypropylene/MWCNT composites," Macromolecules, vol. 41, no. 20, pp. 7536-7542, 2008.*
45. *D. Matykiewicz, M. Barczewski, D. Knapski, and K. Skórczewska, "Hybrid effects of basalt fibers and basalt powder on thermomechanical properties of epoxy composites," Composites Part B: Engineering, vol. 125, pp. 157-164, 2017.*
46. *M. Kumar and A. Kumar, "Thermomechanical analysis of hybrid friction composite material and its correlation with friction braking performance," International Journal of Polymer Analysis and Characterization, vol. 25, no. 2, pp. 65-81, 2020.*

CHAPTER 8: CONCLUSION AND FUTURE WORK

8.1 Conclusion

This study aimed to develop an efficient BHN brake pad material prepared from PKF agricultural waste to investigate the brake pads' functional properties such as mechanical, thermal stability, and tribological, compared with conventional brake pads. A mixture of carbon nanosphere synthesized from PKF, graphite nanoparticles, steel nanoparticles, and epoxy resin was used to produce the BHN brake pads. The following are conclusions drawn from this work.

The review of various biomass-based waste materials as an alternative to asbestos brake pads material showed that the biomass materials performance was similar to the asbestos brake pads with no negative health issues or environmental impacts. The studies hitherto have found that loading of fillers has a significant effect on the final material properties. The advantage of these materials is that they are biomass residues and have good mechanical properties. In the case of PKF (biomass) as a filler material, both materials and binders affected the mechanical, tribological, and physical properties of the brake pad sample developed. The wear rate improved with the addition of bio-based filler into the developed brake pad material. The combination of the binder and fillers at a smaller quantity offered composite material with improved wear resistance and stable coefficient of friction.

The process of synthesis of CNSs from PKF involved carbonization at 600 °C for 2 hours, followed by physical activation under CO_2 gas at 850 °C for 1 hour, then treatment for 30 minutes using ethanol vapour at temperatures of 700 °C, 850 °C, and 1000 °C. The synthesis results of CNSs prepared from PKF carbon activated without catalysts or toxic materials revealed that the synthesized CNSs could be used as filler or reinforcement materials in brake pad production applications due to their simple production process, non-toxicity, and cost-effectiveness. The SEM studies confirmed that carbon nanospheres with diameters between 10 nm, and 60 nm were formed at 1000 °C. The EDX showed high carbon contents of 89.33 %, 87.59 %, and 89.40 %, respectively, in all CNSs synthesized. The elemental analysis of the CNSs showed that the highest carbon content of 89.40 % after ethanol vapor treatment occurred at 1000 °C. The results also showed that the CNSs were spheres with smooth surfaces.

The temperature effect of the synthesis on the growth of CNSs from PKF activated charcoal using ethanol vapor treatment at a temperature of 700 °C, 850 °C, and 1000 °C at 150 °C intervals was recorded. The low synthesis temperature at 700 °C was not sufficient to form CNSs, while a small

sphere morphology was formed at a temperature of 850 °C. Several CNSs with little quantities of amorphous carbon were formed at 850 °C. At a temperature of 1000 °C, clean CNSs were produced with a uniform diameter size. The SEM images revealed that the temperature growth affected the growth rate of the CNSs, the diameter and the density. In addition, temperature played a significant role in the production of high quality and high yield CNSs.

The experiment and analysis of results of brake pad properties developed from BHN materials showed that the brake pad performance changed with each pad formulation. The BHN brake pad material showed better performance than the CON brake pad in most tests. Loading of CNSs improved the tribological and mechanical properties of the BHN brake pad. The CON brake pad hardness was 27.3, which was slightly higher than the hardness found in the BHN brake pads except for BHN 2 and BHN 6 that were 13 % and 16 % tougher. The water absorption value of BHN and CON recorded a lower rate ranging from 0.18 % to 2.02 %, which was better than the water absorption value recorded in some literature [3, 75], while the oil absorption rate of both BHN and CON brake pad varied with several formations. In the same conditions, most of the BHN brake pads absorbed less oil compared to CON brake pads.

The COF of both brake pad samples was within SAE J661 CODE standard value (0.3 to 0.6) as recommended for vehicle brake pad applications. The SEM image of the CON brake pad worn surface revealed inconsistent and stress yielding surface textures, while homogenous dispersion, wear debris, flakes, and plateaus were observed in the BHN brake pad surfaces. Furthermore, the BHN brake pads had better tribological properties than the CON brake pad.

Thermo-mechanical properties such as compressive strength, thermal stability and impact strength of the developed BHN brake pad were compared with the CONTR brake pad. The compressive strength of the BHN brake pad was higher than CONTR by 43.7%. The higher compressive strength can be credited to the interconnected C-C bonds of CNS and graphite nanoparticles, which produced a covalent bond between the carbon and the binder. The CONTR impact resistance was 17.6 KJ / m^2, while the BHN brake pad impact strength varied with the formulation. The impact strength of BHN 3, BHN 4, and BHN 6 were higher compared to CONTR. The improvement in impact strength can be credited to the additives' interlocking bonds thereby improving the energy absorption capacity. SEM showed micro-cracks on BHN 4 and BHN 5 fractured surfaces, while surface degradation was observed on BHN 1 and interlocking structure observed on BNH 3 and BHN 6.

The results of the thermal stability and degradation temperature of the BHN brake pad material showed a constant increase in temperature. Both BHNs and CONTR brake pads had similar (approximately 98%) thermal stability and weight at the three-temperature zone as they had a gradual decomposition

rate at the first stage of 50 °C to 350 °C. At the second stage of 350 °C to 400 °C, the thermal stability was approximately 74 % due to hemicellulose thermal depolymerization and resin degradation. The weight lost at 400 °C to 600 °C, the third stage, was due to more decomposition. However, the final weight loss of the BHN brake pads after 400 °C, which was higher than the brake pad average operating temperature (300 °C to 400 °C), can be attributed to the addition of carbon-based additives.

From the DMA result, at a temperature between 55 °C to 105 °C, the $Tan\ \delta$ magnitude of BHN was higher due to the loss modulus supremacy over the storage modulus. At a temperature between 55 ° to 105 °C, the $Tan\ \delta$ magnitude of BHN was higher due to the loss modulus supremacy over the storage modulus. In addition, at the temperature between 105 °C to 190 °C, both the storage modulus and loss modulus became as low as CONTR, and BHN $Tan\ \delta$ magnitude reduced. There was a steady loss of storage modulus at an estimated comparable rate as temperature increased.

8.2 Future work

Some limitations were encountered on completing this study, pointing the way to future studies using other bio-based precursors to synthesize nanoparticles for brake pad production.

1) A longer curing time will influence the brake pad mass production; therefore, it is recommended to fast cure the resin.

2) For future work, it is recommended that a high percentage of the resin should be present in the brake pad formulation in order to have good consolidation and integration of the components and thus to achieve better properties. The results of this work confirmed this.

3) The results of strength and wear rate are improved by the presence of a good weight percentage of resin. Likewise, the use of a suitable percentage of lubricant and reinforcement can improve the material properties.

4) A new possible area for future research is the thermal stability and degradation of the BHN brake pad; improving these properties will enable researchers to produce a more efficient brake pad.

5) Another area that needs attention in the future is the interfacial adhesion and bonding strength between the nanocomposite and the matrix to improve tribological and mechanical properties.

6) The nanoparticle materials used to make brake pads were tested at room temperature. In the future the properties of different nanoparticle materials should also be investigated at high temperatures and below room temperature.

APPENDICES

Appendix I: Pictures of the equipment

Picture 1: Thermo-Gravimetric Analyser (TGA) / Differential Scanning Calorimeter (DSC)

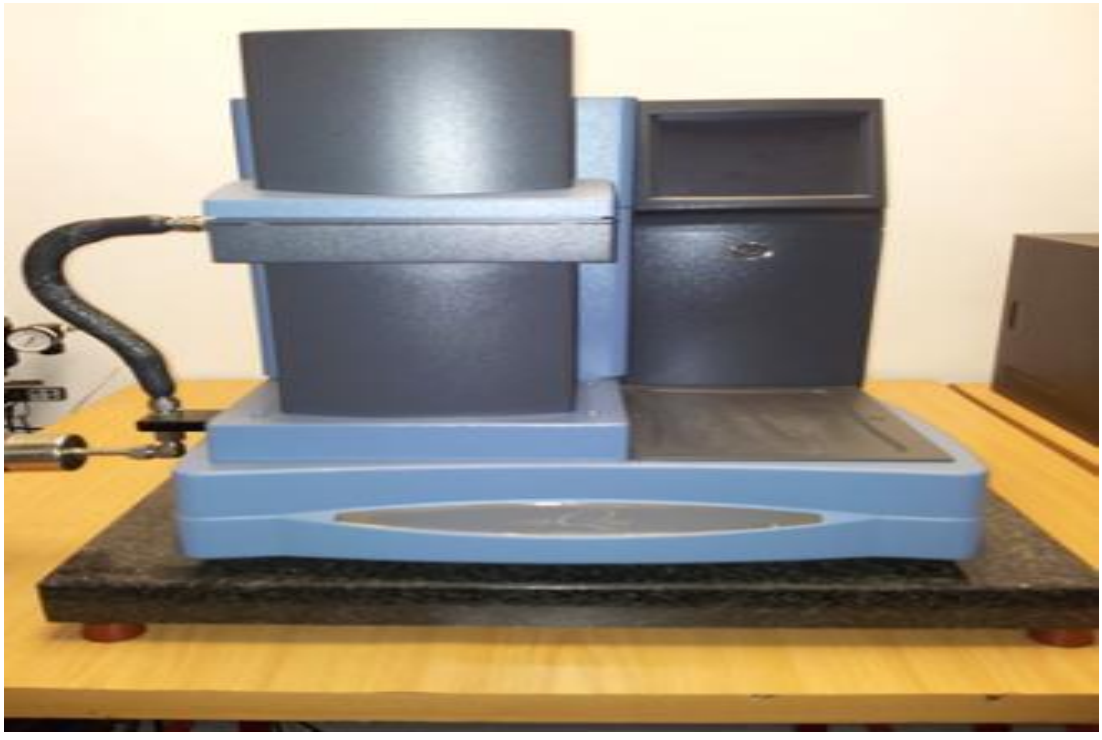

Picture 2: Dynamic Mechanical Analyser (DMA)

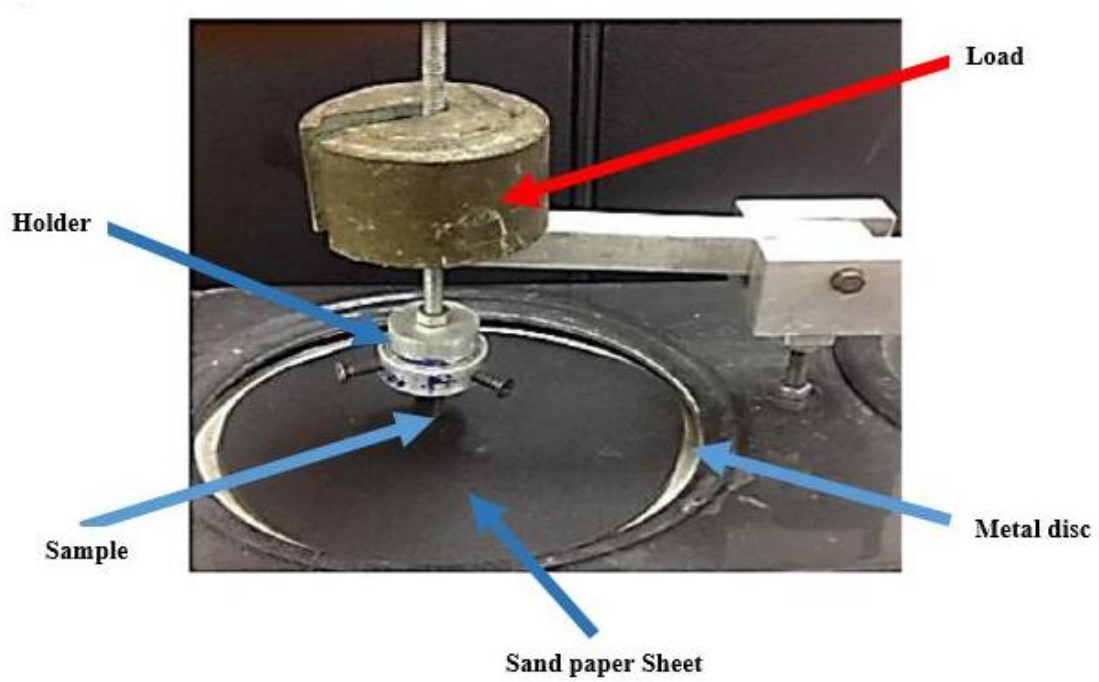

Picture 3: Tribometer (In-house built pin-on-disc)

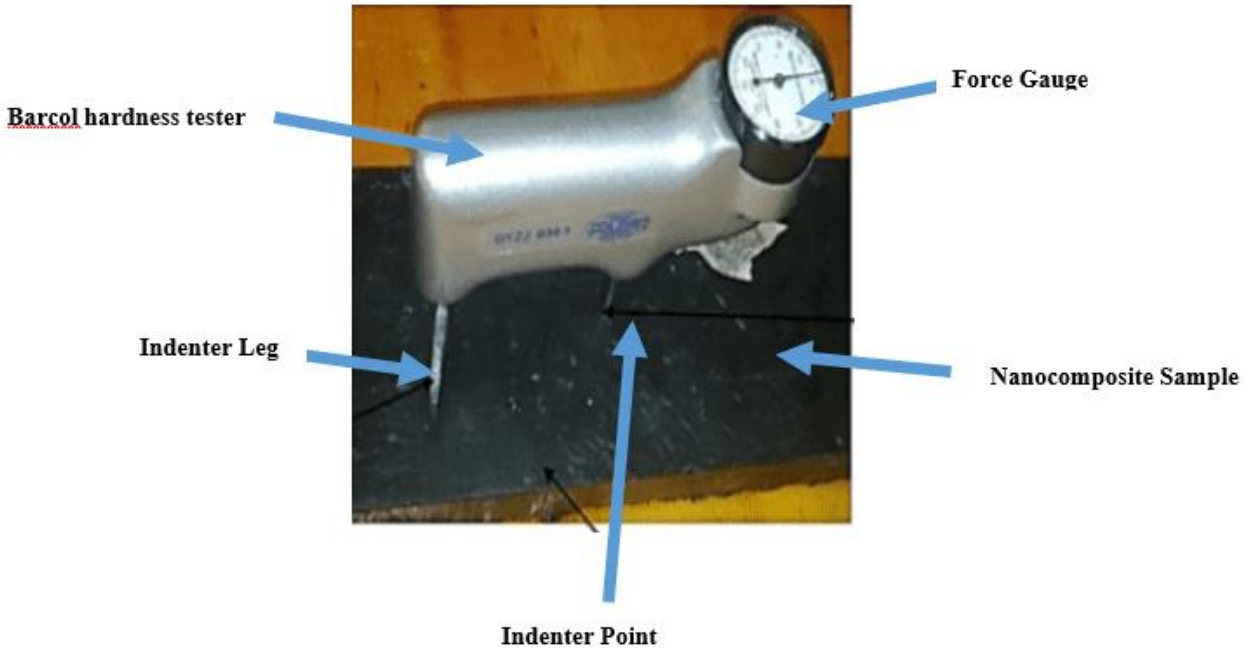

Picture 4: Barber Colman Barcol impressor hardness tester

Picture 5: Pendulum Type Impact Tester

Picture 6: FEG-SEM

Picture 7: FT-IR Spectrometer

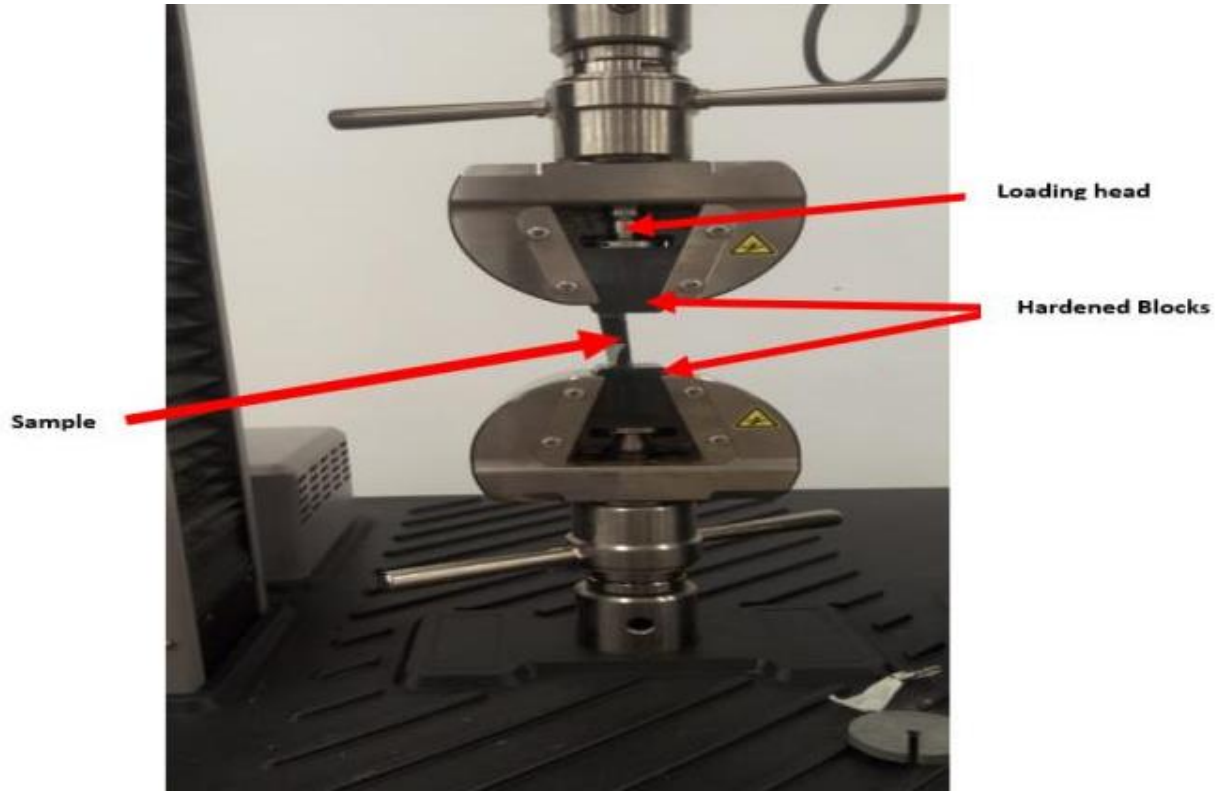

Picture 8: Lloyd testing machine

Appendix II: Editing Certificates

Appendix A: Introduction and Conclusion

DR RICHARD STEELE
BA, HDE, MTech(Hom)
HOMEOPATH
Registration No. A07309 HM
Practice No. 0807524
Freelance academic editor
Associate member: Professional Editors' Guild, South Africa

110 Cato Road
Glenwood, Durban 4001
031-201-6508/082-928-6208
Postal: P.O. Box 30043, Mayville 4058
Email: rsteele@vodamail.co.za

EDITING CERTIFICATE

Re: **Oluwafemi E. Ige**
PhD thesis: **RESEARCH, DEVELOPMENT AND TESTING OF BRAKE PAD MATERIALS FROM BIOMASS-BASED NANOCOMPOSITES**

I confirm that I have edited Chapter 1 and Chapter 7 of this thesis for clarity, language and layout. I returned the document to the author with track changes so correct implementation of the changes and clarifications requested in the text and references is the responsibility of the author. I am a freelance editor specialising in proofreading and editing academic documents. My original tertiary degree which I obtained at the University of Cape Town was a B.A. with English as a major and I went on to complete an H.D.E. (P.G.) Sec. with English as my teaching subject. I obtained a distinction for my M.Tech. dissertation in the Department of Homoeopathy at Technikon Natal in 1999 (now the Durban University of Technology). I was a part-time lecturer in the Department of Homoeopathy at the Durban University of Technology for 13 years and supervised many Master's degree dissertations during that period.

Dr Richard Steele
21 January 2021
per email

Appendix B: Chapter 2

DR RICHARD STEELE
BA, HDE, MTech(Hom)
HOMEOPATH
Registration No. A07309 HM
Practice No. 0807524
Freelance academic editor
Associate member: Professional Editors' Guild, South Africa

110 Cato Road
Glenwood, Durban 4001
031-201-6508/082-928-6208
Fax 031-201-4989
Postal: P.O. Box 30043, Mayville 4058
Email: rsteele@telkomsa.net

EDITING CERTIFICATE

Re: **Oluwafemi E. Ige**
Journal article: **Biomass-Based Composites for Brake Pads: A Review**

I confirm that I have edited this article and the references for clarity, language and layout. I am a freelance editor specialising in proofreading and editing academic documents. I returned the document to the author with track changes so correct implementation of the changes in the text and references is the responsibility of the author. My original tertiary degree which I obtained at the University of Cape Town was a B.A. with English as a major and I went on to complete an H.D.E. (P.G.) Sec. with English as my teaching subject. I obtained a distinction for my M.Tech. dissertation in the Department of Homeopathy at Technikon Natal in 1999 (now the Durban University of Technology). During my 13 years as a part-time lecturer in the Department of Homoeopathy at the Durban University of Technology I supervised numerous Master's degree dissertations.

Dr Richard Steele
08 January 2019
per email

Appendix C: Chapter 3

DR RICHARD STEELE
BA, HDE, MTech(Hom)
HOMEOPATH
Registration No. A07309 HM
Practice No. 0807524
Freelance academic editor
Associate member: Professional Editors' Guild, South Africa

110 Cato Road
Glenwood, Durban 4001
031-201-6508/082-928-6208
Fax 031-201-4989
Postal: P.O. Box 30043, Mayville 4058
Email: rsteele@telkomsa.net

EDITING CERTIFICATE

To: **Oluwafemi E. Ige**
For editing journal article: **EFFECTS OF FIBER, FILLERS AND BINDERS ON AUTOMOBILE BRAKE PAD**

I confirm that I have edited this article and the references for clarity, language and layout. I returned the document to the author with track changes so correct implementation of the changes and clarifications requested in the text and references is the responsibility of the author. I am a freelance editor specialising in proofreading and editing academic documents. My original tertiary degree which I obtained at the University of Cape Town was a B.A. with English as a major and I went on to complete an H.D.E. (P.G.) Sec. with English as my teaching subject. I obtained a distinction for my M.Tech. dissertation in the Department of Homeopathy at Technikon Natal in 1999 (now the Durban University of Technology). During my 13 years as a part-time lecturer in the Department of Homoeopathy at the Durban University of Technology I supervised numerous Master's degree dissertations.

Dr Richard Steele
07 April 2019
per email

Appendix D: Chapter 4

DR RICHARD STEELE
BA, HDE, MTech(Hom)
HOMEOPATH
Registration No. A07309 HM
Practice No. 0807524
Freelance academic editor
Associate member: Professional Editors' Guild, South Africa

110 Cato Road
Glenwood, Durban 4001
031-201-6508/082-928-6208
Fax 031-201-4989
Postal: P.O. Box 30043, Mayville 4058
Email: rsteele@vodamail.co.za

EDITING CERTIFICATE

Re: **Oluwafemi E. Ige**
Journal article: **Synthesis of Natural Carbon Nano-spheres from Palm Kernel Fiber**

I confirm that I have edited this article and the references for clarity, language and layout. I returned the document to the author with track changes so correct implementation of the changes and clarifications requested in the text and references is the responsibility of the author. I am a freelance editor specialising in proofreading and editing academic documents. My original tertiary degree which I obtained at the University of Cape Town was a B.A. with English as a major and I went on to complete an H.D.E. (P.G.) Sec. with English as my teaching subject. I obtained a distinction for my M.Tech. dissertation in the Department of Homeopathy at Technikon Natal in 1999 (now the Durban University of Technology). I was a part-time lecturer in the Department of Homoeopathy at the Durban University of Technology for 13 years.

Dr Richard Steele
23 December 2019
per email

Appendix E: Chapter 5

DR RICHARD STEELE
BA, HDE, MTech(Hom)
HOMEOPATH
Registration No. A07309 HM
Practice No. 0807524
Freelance academic editor
Associate member: Professional Editors' Guild, South Africa

110 Cato Road
Glenwood, Durban 4001
031-201-6508/082-928-6208
Postal: P.O. Box 30043, Mayville 4058
Email: rsteele@vodamail.co.za

EDITING CERTIFICATE

Re: **Oluwafemi E. Ige**
For editing journal article: **The Effect of Synthesis Temperature on Carbon Nanospheres from Palm Kernel Fiber**

I confirm that I have edited this article and the references for clarity, language and layout. I returned the document to the author with track changes so correct implementation of the changes and clarifications requested in the text and references is the responsibility of the author. I am a freelance editor specialising in proofreading and editing academic documents. My original tertiary degree which I obtained at the University of Cape Town was a B.A. with English as a major and I went on to complete an H.D.E. (P.G.) Sec. with English as my teaching subject. I obtained a distinction for my M.Tech. dissertation in the Department of Homeopathy at Technikon Natal in 1999 (now the Durban University of Technology). I was a part-time lecturer in the Department of Homoeopathy at the Durban University of Technology for 13 years.

Dr Richard Steele
12 April 2020
per email

Appendix F: Chapter 6

DR RICHARD STEELE
BA, HDE, MTech(Hom)
HOMEOPATH
Registration No. A07309 HM
Practice No. 0807524
Freelance academic editor
Associate member: Professional Editors' Guild, South Africa

110 Cato Road
Glenwood, Durban 4001
031-201-6508/082-928-6208
Postal: P.O. Box 30043, Mayville 4058
Email: rsteele@vodamail.co.za

EDITING CERTIFICATE

To: **Oluwafemi E. Ige**
Journal article: **Development and study of tribological performance of bio-based hybrid nanocomposites for brake pad application**

I confirm that I have edited this article and the references for clarity, language and layout. I returned the document to the author with track changes so correct implementation of the changes and clarifications requested in the text and references is the responsibility of the author. I am a freelance editor specialising in proofreading and editing academic documents. My original tertiary degree which I obtained at the University of Cape Town was a B.A. with English as a major and I went on to complete an H.D.E. (P.G.) Sec. with English as my teaching subject. I obtained a distinction for my M.Tech. dissertation in the Department of Homoeopathy at Technikon Natal in 1999 (now the Durban University of Technology). I was a part-time lecturer in the Department of Homoeopathy at the Durban University of Technology for 13 years and supervised many Master's degree dissertations during that period.

Dr Richard Steele
13 December 2020
per email

Appendix G: Chapter 7

DR RICHARD STEELE
BA, HDE, MTech(Hom)
HOMEOPATH
Registration No. A07309 HM
Practice No. 0807524
Freelance academic editor
Associate member: Professional Editors' Guild, South Africa

110 Cato Road
Glenwood, Durban 4001
031-201-6508/082-928-6208
Postal: P.O. Box 30043, Mayville 4058
Email: rsteele@vodamail.co.za

EDITING CERTIFICATE

Re: **Oluwafemi E. Ige**
Journal article: **Thermo-mechanical analysis of bio-based hybrid nanocomposites for brake pad application**

I confirm that I have edited this article and the references for clarity, language and layout. I returned the document to the author with track changes so correct implementation of the changes and clarifications requested in the text and references is the responsibility of the author. I am a freelance editor specialising in proofreading and editing academic documents. My original tertiary degree which I obtained at the University of Cape Town was a B.A. with English as a major and I went on to complete an H.D.E. (P.G.) Sec. with English as my teaching subject. I obtained a distinction for my M.Tech. dissertation in the Department of Homoeopathy at Technikon Natal in 1999 (now the Durban University of Technology). I was a part-time lecturer in the Department of Homoeopathy at the Durban University of Technology for 13 years and supervised many Master's degree dissertations during that period.

Dr Richard Steele
10 January 2021
per email

Appendix III: Publications Certificates

Appendix A: Chapter 6

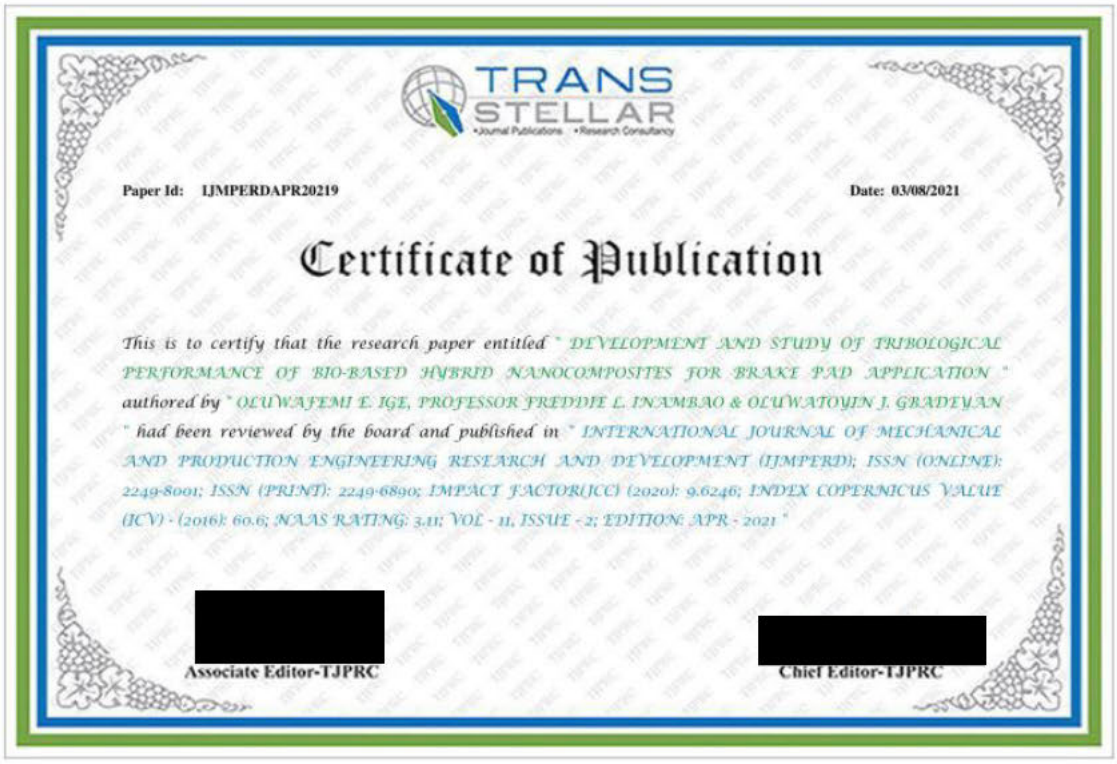

TRANS STELLAR
•Journal Publications •Research Consultancy

Paper Id: IJMPERDAPR20219 Date: 03/08/2021

Certificate of Publication

This is to certify that the research paper entitled " DEVELOPMENT AND STUDY OF TRIBOLOGICAL PERFORMANCE OF BIO-BASED HYBRID NANOCOMPOSITES FOR BRAKE PAD APPLICATION " authored by " OLUWAFEMI E. IGE, PROFESSOR FREDDIE L. INAMBAO & OLUWATOYIN J. GBADEYAN " had been reviewed by the board and published in " INTERNATIONAL JOURNAL OF MECHANICAL AND PRODUCTION ENGINEERING RESEARCH AND DEVELOPMENT (IJMPERD); ISSN (ONLINE): 2249-8001; ISSN (PRINT): 2249-6890; IMPACT FACTOR(JCC) (2020): 9.6246; INDEX COPERNICUS VALUE (ICV) - (2016): 60.6; NAAS RATING: 3.11; VOL - 11, ISSUE - 2; EDITION: APR - 2021 "

[redacted]
Associate Editor-TJPRC

[redacted]
Chief Editor-TJPRC

Appendix B: Chapter 7

TRANS STELLAR
•Journal Publications •Research Consultancy

Paper Id: IJMPERDAPR202113 Date: 03/08/2021

Certificate of Publication

This is to certify that the research paper entitled " THERMO-MECHANICAL ANALYSIS OF BIO-BASED HYBRID NANOCOMPOSITES FOR BRAKE PAD APPLICATION " authored by " OLUWAFEMI E. IGE*, FREDDIE L. INAMBAO, OLUWATOYIN J. GBADEYAN " had been reviewed by the board and published in " INTERNATIONAL JOURNAL OF MECHANICAL AND PRODUCTION ENGINEERING RESEARCH AND DEVELOPMENT (IJMPERD); ISSN (ONLINE): 2249-8001; ISSN (PRINT): 2249-6890; IMPACT FACTOR(JCC) (2020): 9.6246; INDEX COPERNICUS VALUE (ICV) - (2016): 60.6; NAAS RATING: 3.11; VOL - 11, ISSUE - 2; EDITION: APR - 2021 "

[redacted]
Associate Editor-TJPRC

[redacted]
Chief Editor-TJPRC